UNRECOGNIZED DIVERSITY OF MICROBES LINKING METHANOTROPHY TO NITROGEN LOSS IN MARINE OXYGEN MINIMUM ZONES

A Dissertation
Presented to
The Academic Faculty

by

Cory Cruz Padilla

In Partial Fulfillment
of the Requirements for the Degree
Doctor of Philosophy in the
School of Biological Sciences

Georgia Institute of Technology
December 2017

UNRECOGNIZED DIVERSITY OF MICROBES LINKING METHANOTROPHY TO NITROGEN LOSS IN MARINE OXYGEN MINIMUM ZONES

Approved by:

Dr. Frank J Stewart, Advisor
School of Biological Sciences
Georgia Institute of Technology

Dr. Jennifer B Glass
School of Earth and Atmospheric Science
Georgia Institute of Technology

Dr. Thomas J DiChristina
School of Biological Sciences
Georgia Institute of Technology

Dr. Bo Thamdrup
Department of Biology and Nordic Center for Earth Evolution
University of Southern Denmark

Dr. Kostas T. Konstantinidis
School of Biological Sciences
Georgia Institute of Technology

Date Approved: November 1, 2017

This work is dedicated to my Grandparents, Ofelio and Regina Padilla, and to my Uncle Charles Padilla.

ACKNOWLEDGEMENTS

I would like to thank Kate O'Neill for her constant love and support throughout the entire process from temporary lab positions to oceanographic cruises and finally the Ph.D. proceess, I look forward to our next steps in life. I would also like to thank my parents, James and Dwan Padilla, for their encouragement to follow my curiosities, wherever they may lead.

I would also like to thank my advisor, Dr. Frank Stewart for his guidance and for offering me uncountable opportunities to get involved with amazing projects and people. Along those lines, I would like to express my sincerest gratitude toward the members of the Stewart Lab, past and present. It has been an honor working along side all of you.

I am grateful to have such a large number of talented collaborators. In particular, I would like to recognize Laura Bristow and Bo Thamdrup, for their guidance and support both with generating exciting research and for offering much-needed comic relief and commiseration on cruises. Science is rarely a solo effort, and I have been more than fortunate work with and learn from all of you.

Lastly, I would like to thank all my former labs, the Zehr lab, Repeta Lab, and Karl lab. The support from everyone in these labs helped to motivate me and gave me a vast background and experieance in oceanography, which allowed me to start graduate school running at full speed.

TABLE OF CONTENTS

LIST OF TABLES

LIST OF FIGURES

LIST OF SYMBOLS AND ABBREVIATIONS

CH_4	Methane
CO_2	Carbon dioxide
DO	Dissolved Oxygen
EDTA	Ethylene diamine tetraacetic acid
H_2S	Hydrogen sulfide
N	Nitrogen
N_2	Dinitrogen gas
N_2O	Nitrous oxide
NED	N-(1-Naphthyl)ethylenediamine
NH_4^+/NH_3	Ammonium
NO	Nitric oxide
NO_2^-	Nitrite
NO_3^-	Nitrate
O_2	Oxygen gas
pH	Hydrogen ion concentration
SDS	Sodium Dodecyl Sulfate
SO_4^{2-}	Sulfate
Tris-HCl	2-Amino-2-hydroxymethyl1-1,3-propanediol hydrochloride
AOA	Ammonia oxidizing archaea
AOB	Ammonia oxidizing bacteria
NOB	Nitrite oxidizing bacteria
OPU	Operationial PMO unit
amo	Ammonia monooxygenase
fdh	Fomate dehydrogenase
hao	Hydroxyalamine oxidoreductase
HATO	High-affinity terminal oxidases
LATO	Low-affinity terminal oxidases
mdh	Methanol dehydrogenase
MMO	Methane monooxygenase
nap	Periplasmic nitrate/nitrite oxidoreductase
nar	Nitrate reductase
nas	Assimilatory nitrate reductase
nir	Nitrite reductase
nod	Nitric oxide dismutase
nor	Nitric oxide reductase
nos	Nitrous oxide reductase
nxr	Nitrite oxidoreductase
pmo	Particulate methane monooxygenase
qnor	Quinol-dependent nitric oxide reductase
xox	Methanol dehydrogenase - rare earth element

Ek	Light intensities
kDA	Kilodalton
Km	Michaelis-Menten constant
L	Litre
m	Meter
nM	Nanomolar
µM	Micromolar
µm	Micrometer
BLAST	Basic Local Alignment Search Tool
CTD	Conductivity, Temperature, and Depth
HMM	Hidden Markov Model
KAAS	KEGG Automatic Annotation Server
LCA	Lowest Common Ancestor
PCR	Polymerase chain reaction
PF	Prefilter
qPCR	Quantitative polymerase chain reaction
STOX	Switchable trace amount oxygen sensor
cDNA	Complementary DNA
DNA	Deoxyribonucleic Acid
dsDNA	Double stranded DNA
gDNA	Genomic DNA
KEGG	Kyoto Encylopedia of Genes and Genomes
mRNA	Messenger RNA
ORF	Open Reading Frame
OTU	Operational taxonomic unit
RNA	Ribonucleic Acid
rRNA	Ribosomal RNA
Ca.	*Candidatus*
FL	Free Living
NCBI	National Center for Biotechnology Information
PA	Partical Associated
sp.	Species
Anammox	Anaerobic ammonium oxidation
AOM	Anaerobic oxidation of methane
DNRA	Dissimilatory nitrate reduction to ammonium
EMC	Ethylmalonyl-CoA pathway
GCP	Gross community production
N-DAMO	Nitrite-Dependent anaerobic methane oxidation
S-DAMO	Sulfate-Dependent anaerobic methane oxidation
NCP	Net community production
R*	Potential respiration rates
RuMP	Ribulose monophosphate cycle
AMZ	Anoxic marine zone

ETNP	Eastern Tropical North Pacific
ETSP	Eastern Tropical South Pacific
GD	Golfo Dulce
OMZ	Oxygen minimum zones
OMZoMBiE	Oxygen Minimum Zone Microbial Biogeochemstry Expedition
R/V	Research Vessel
SCM	Secondary chlorophyll maximum

SUMMARY

Methane (CH_4) is a potent greenhouse gas with 25 times the warming potential of carbon dioxide (CO_2) on a per mol basis. Marine oxygen minimum zones (OMZs) are enriched in CH_4 compared to oxygenated water columns and are predicted to expand under global warming. OMZs are also key sites for microbially-mediated nitrogen (N) loss, which has been shown in other systems to be linked to CH_4 consumption. Diverse groups of microorganisms mediate the global cycling of both CH_4 and N. Microbial genes encoding the enzyme used in CH_4 oxidation, particulate methane monooxygenase (*pmo*), have previously been detected in OMZs. However, the genomic diversity and ecological importance of the OMZ CH_4-cycling community are unclear, as is the mechanism by which CH_4 consumption is carried out by these microbes. This thesis uses a combination of metagenomics, metatranscriptomics, and biogeochemical measurements to explore the activity and diversity of methanotrophic microbes in OMZs. OMZs were found to harbor at least two metabolic strategies for CH_4 consumption. First, we found evidence that bacteria belonging to the recently discovered NC10 phylum are present and transcriptionally active at the functionally anoxic core of the OMZ. NC10 bacteria link anaerobic CH_4 oxidation to nitrite (NO_2^-)-driven denitrification through a unique O_2-producing intra-aerobic methanotrophy pathway. rRNA and mRNA transcripts assignable to NC10 peaked within the OMZ and included genes mediating this unique methanotrophic pathway. Second, metagenomic binning uncovered a separate and distinct methanotrophic strategy that is present and active within and just below the oxycline. In this strategy, gammaproteobacteria, designated phylogenetically as belonging to the OPU3 clade, were found to carry and express genes for methanotrophy

and partial denitrification, thereby supporting respiration under low O_2 concentrations and allowing for available O_2 to be used directly for CH_4 oxidation. These findings confirm OMZs as a niche for diverse and previously overlooked forms of denitrification-linked methanotrophy. Further characterization of these niches and the environmental constraints on OMZ CH_4 consumption is critical for predicting the effects of OMZ expansion on global C cycling, greenhouse gas consumption, and N loss.

CHAPTER 1

INTRODUCTION

Methane (CH_4) is a potent greenhouse gas with 25 times more warming potential than carbon dioxide (CO_2) on a per-mol basis. Since the industrial revolution, atmospheric concentrations of CH_4 have increased from ~600 ppb to ~1300 ppb since the industrial revolution (Kirschke et al., 2013; Stocker et al., 2013). Microbes are critical components of the global CH_4 cycle as crucial drivers of CH_4 production (Cicerone et al., 1988) and consumption. Microbial CH_4 destruction is second only to tropospheric oxidation with hydroxyl radicals as a route for CH_4 removal (Fischer et al., 2011; Kirschke et al., 2013), making microbially-mediated CH_4 an important mechanism for CH_4 loss. The oceans contribute roughly 10% of natural atmospheric CH_4. The marine CH_4 cycle is governed by microbial CH_4 creation (methanogenesis) and methane consumption (methanotrophy). Pelagic marine CH_4 cycling has been vastly understudied as most oceanic research has focused on hydrothermal vents, hydrate systems, and sediments (Reeburgh, 2007; Valentine, 2010). Oxygen-depleted pelagic regions, known as oxygen minimum zones (OMZs), contain elevated concentrations of CH_4 and oxidized nitrogen compounds compared to oxygenated pelagic zones (Sansone et al., 2001; Navqi et al., 2010). Functionally anoxic OMZs are key sites for linking dissimilatory nitrogen (N) loss to other chemical cycles through microbial metabolisms (Codsipoti et al., 2001; Thamdrup, 2012). Cultures of non-OMZ microbes have been shown to use denitrification pathways to facilitate methanotrophy when oxygen (O_2) is either limiting or absent (Raghoebarsing et al., 2006; Ettiwg et al., 2010; Kits et al., 2015). It is unclear if OMZ microbes contain

the metabolic potential to carry out these coupled N-CH_4 reactions, as genomic information from OMZs is sparse. The co-occurrence of CH_4 and oxidized N compounds in OMZs suggest a pelagic niche for methanotrophs conducting reductive N transformations. This thesis utilizes metagenomic, transcriptomic, and biogeochemical measurements to characterize the microbial abundance and activity in OMZs that participate in CH_4 oxidation and N loss.

1.1 Microbial methane metabolisms

1.1.1 Methanogenesis

CH_4 sources can be partitioned into three categories: thermogenic, pyrogenic, and biogenic (Cicerone et al. 1988; Bousquet et al., 2006; Kirschke et al., 2013). All three processes for CH_4 production involve natural and anthropogenic components. Thermogenic CH_4 is derived from geological processes, which take millions of years, where organic matter in deep sediments (>1,000 m below sea) is converted to hydrocarbon gas through high pressure and temperature. In this route, CH_4 is released through natural venting from seeps and mud volcanoes, or through burning coal, oil, and natural gas energy sources. Pyrogenic production involves the burning of biomass in forest fires (Cicerone et al. 1988; Bousquet et al., 2006). Biogenic sources are primarily made up of CH_4 -generating microbes known as methanogens (Liu, 2010), and contribute ~70% of the global production of CH_4 annually based on isotopic composition (Bousquet et al., 2006; Kirschke et al., 2013). The focus of the CH_4 production discussion will be on the biogenic process as it is a key source of CH_4 in natural environments.

Methanogenesis is the last step in organic matter remineralization. This anaerobic process follows two main biochemical pathways that require either hydrogen (H_2) for CO_2 reduction or acetate for acetate fermentation. These reactions produce low energy yields and generally require the absence of more favorable electron acceptors such as O_2, nitrate (NO_3^-), manganese IV (MnIV), iron III (FeIII), or sulfate (SO_4^{2-}) (Thauer et al., 1977). To date, microbes implicated in the anaerobic production of CH_4 fall exclusively in the domain Archaea. Originally, methanogens were thought to fall within the Phylum of Euryarchaeota (Liu, 2010; Luo et al., 2009), however, recent metagenomic assemblies from aquifers recovered a Bathyarchaeota encoding the methanogenesis pathway (Evans et al., 2015). This finding suggests that methanogensis is contained in much wider array of microbes and that full extent of microbial diversity participating in methanogenesis is not fully characterized.

Methanogens are found in a wide range of anaerobic habitats such as wetlands, meromictic lakes, tundra soils, rice paddies, and the guts of ruminants and termites (Thauer et al., 2008). Increased agricultural practices such as rice farming and livestock production have been a growing niche for methanogens. Such anthropogenic practices have been a key component in increased atmospheric CH_4 concentrations (Kirschke et al., 2013). A recent concern for methanogenic derived-CH_4 release is from thawing tundra soils. As global temperatures increase, the permafrost on tundra melts and releases a flood of CH_4 to the atmosphere which creates a positive feedback loop where warming causes the release of more potent greenhouse gases (Zimov et al., 2006).

Microbial methane production has long been viewed as a strictly anaerobic process. However, an indirect pathway for aerobic methane generation in oceanic systems was proposed (Karl et al., 2008) and has been confirmed (Repeta et al, 2016; Carini et al., 2014). This pathway involves the breakdown of methylated organic phosphorus compounds in phosphate depleted oceanic systems. This process will be further described in section 1.2. This, again, points to the incomplete picture we currently have on methane related biochemical pathways and how they are distributed across the tree of life.

1.1.2 Methanotrophy

CH_4 consumption involves abiotic and biotic processes. CH_4 sinks predominantly consist of chemical reactions with hydroxyl, atomic oxygen, and chlorine radicals in the atmosphere. CH_4-consuming microbes (methanotrophs) account for ~4% of the CH_4 loss annually (Kirschke et al., 2013; Curry, 2007; Zhuang et al, 2004; Cicerone, 1988). In some environments, such as aerobic interfaces overlying anoxic environments, methanotrophy plays an important role in mediating the net flux of CH_4 to the atmosphere from soils and sediments (De Visschet et al., 2007; Reeburgh, 2007; Conrad, 2009). Canonical methanotrophy is considered to be an aerobic process where O_2 is used as an electron acceptor for the oxidation of CH_4 to CO_2. However, in the past two decades, a biological mechanism for anaerobic oxidation of methane (AOM) has been discovered in microbial enrichments using SO_4^{2-} combined with a reversal of the methanogensis pathway (Boutieus et al., 2000). More recently, AOM has been linked to the oxidized N

compounds NO_3^- (Raghoebarsing et al., 2006; Haroon et al., 2013) and NO_2^- (Ettwig et al., 2010). These AOM processes are further discussed in section 1.1.3. CH_4 consuming microbes are incredibly diverse and prosper in a wide range of environments (Kneif, 2015). Current methanotrophic diversity is spread across several Classes of bacteria, including Alphaproteobacteria, Gammaproteobacteria, Verrucomicrobia, and recently the proposed phylum NC10 (Bowman, 2006; Kneif, 2015). Two Classes of Archaea known as ANaerobic MEthanotrophs (ANME) carry out the AOM process (Knittle and Boetius, 2009)

Aerobic methanotrophic bacteria are typically found near anoxic and oxic interfaces where O_2 is available for rapid oxidation of CH_4 escaping the anoxic systems (Reeburgh, 2007; Kneif, 2015). This includes terrestrial sediments, lakes, and marine environments (Bowman, 2014). The current classification system for aerobic methanotrophs is primarily based on carbon (C) fixation pathways; Type I use the ribulose monophosphate pathway (RuMP), consisting of gammaproteobacteria, and Type II use the serine cycle, primarily made up of alphaproteobacteria. Additional differences between Type I and II methanotrophs include the length of fatty acids produced and the arrangement of internal membranes (Hanson and Hanson, 1996; Trotsenko and Murrell, 2008). Phylogenetic analysis of the alpha subunit of the particulate methane monooxygenase enzyme (*pmoA*) and of the 16S rRNA gene supports the evolutionary divergence between Type I and II methanotrophs (Kneif, 2015). However, there are deviations from this categorization, notably regarding to placement of the Verrucomicrobia (Type III or Type X); the efficacy of this classification scheme therefore has been questioned (Op den Camp et al., 2009; Semrau et al., 2010). Recent

advances in metagenomic and single cell DNA sequencing demonstrate methanotrophy occurs in a wider range of organisms than previously thought. These results suggest that CH_4 consumption could be distributed more broadly across the tree of life. Moreover, biochemical pathways involved in methanotrophy have not been comprehensively described. Methanotrophic metabolisms and diversity under O_2 limiting conditions is an area that remains poorly characterized.

1.1.3 Anoxic and Hypoxic methane oxidation

The hypothesis that methanotrophs could use other oxidized substrates, such as SO_4^{2-}, NO_3^-, NO_2^-, and oxidized metals, as terminal electron acceptors in place of O_2 was proposed decades ago. Thermodynamic calculations supported AOM hypotheses despite the lack of clear biological mechanisms for the reactions (Feely and Kulp, 1957; Davis and Yarbrough, 1966; Reeburgh, 2007). Geochemical data in aquatic sediments further supported this hypothesis as steep declines in CH_4 concentrations are observed under functionally anoxic conditions; suggesting AOM as a CH_4 sink preventing CH_4 escaping sediments (Reeburgh, 1976; Reeburgh, 1980; Reeburgh, 2007; Valentine 2010). However, recent biological mechanisms for SO_4^{2-}, NO_3^-, and NO_2^- dependent AOM have been described, intimating that the full extend of biochemical pathways for methane consumption have not been reported (Boetius et al., 2000; Raghoebarsing et al, 2006; Ettwig et al. 2010; Haroon et al., 2013). These AOM processes are recognized as environmentally important, but the extent of which AOM is distributed in the

environment and across microbial taxa is still not well understood. Furthermore, it remains possible that other undiscovered metabolic processes may contribute to AOM.

The first described AOM metabolism was sulfate dependent anaerobic methane oxidation (S-DAMO), which is carried out by a microbial consortium. In this symbiosis, sulfate-reducing bacteria (SRB) and archaeal anaerobic methanotrophs (ANME), where ANME archaeal cells shuttle electrons generated from reverse methanogenesis to SRB. SRB use the elections to reduce SO_4^{2-} to hydrogen sulfide (H_2S) (Knittel and Boetius, 2009). This process can play an important role in structuring co-occurring microbial communities. For example, S-DAMO-derived H_2S in marine sediments can support microbial communities and populations of chemosynthetic symbiotic organisms in oceanic sediments (Reeburgh, 2007; Valentine 2010). Additionally, there are other oxidized compounds that provide thermodynamically favorable redox reactions including oxidized N. NO_3^- and NO_2^- are two components have also been long proposed to facilitate AOM.

Microbes using nitrogen-dependent anaerobic methane oxidation (N-DAMO) were initially characterized in enrichments seeded from wastewater treatment sludge (Raghoebarsing et al, 2006). Subsequently, pure cultures of N-DAMO microbes have been isolated (Ettwig et al., 2010; Haroon et al., 2013). NO_3^- driven N-DAMO operates similarly to S-DAMO where microbes couple reverse methanogenesis with NO_3^- reduction as an electron acceptor. The ANME implicated in NO_3^- - N-DAMO is *Methanoperedens nitroreducens*. This ANME is phylogenetically related to the S-DAMO AMNE archaea, its genome contains the genes encoding nitrate reductase (*nar*) thereby removing the need to a symbiotic electron sink (Haroon et al., 2013).

Bacteria of the candidate phylum NC10 perform NO_2^- driven N-DAMO. NC10 are distinct from the ANME-based processes in two fundamental ways. First, NC10 are not archaea and second, reverse methanogenesis is not the mechanism by which CH_4 is oxidized (Ettwig et al., 2010). NC10 reduce NO_2^- to nitric oxide (NO). Next, NC10 reportedly use a unique form of the quniol-based nitric oxide reductase (qNor) to facilitate a dismutation reaction with two NO molecules, producing intracellular N_2 and O_2 (Ettwig et al, 2010; Ettwig et al., 2012). At this point, NC10 bacteria use the aerobic methanotroph pathway involving the enzyme *pmo* to oxidize CH_4 using the NO derived O_2 as the electron acceptor (Ettwig et al, 2010).

Additionally, bacterial groups canonically associated with aerobic methanotrophy play a role in N loss through the use of NO_3^- or NO_2^- as terminal oxidants to support respiration demands when O_2 is limited. This allows any available O_2 to oxidize CH_4 by *pmo*. Studies with isolates of two Methylococcales genera, *Methylomonas* and *Methylomicrobium*, demonstrate that hypoxic conditions stimulate partial denitrification to produce nitrous oxide (N_2O) accompanied by increased energy production (Kits et al., 2015a, b). Thus, low O_2-adapted methanotrophs may act as both a source of N_2O and a sink for CH_4, depending on O_2 availability.

1.2 Oceanic methane cycling

The majority of the marine water column is at saturation with respect to atmospheric CH_4 concentrations (Reeburgh, 2007; Valentine, 2011). The marine CH_4 cycle is governed by the microbial production and consumption of CH_4. Most of the CH_4 is

generated in sediments by methanogensis, dissolving CH_4 hydrates, or through volcanic activity. CH_4 is oxidized in sediment by AOM processes or aerobically by the well-oxygenated water column (Reeburgh, 2007; Valentine, 2011). However, there are areas of the ocean where CH_4 does accumulate to super-saturated levels in the water column. These regions include the CH_4 maxima occurring in the pycnocline (Karl et al., 2008) and OMZs (Sansone et al., 2001; 2004; Pack et al., 2015). Information regarding the distribution and cycling of pelagic CH_4 is relatively scarce since the key focus of marine CH_4 has historically focused on gas hydrates, cold seeps, and sediments.

Methanogenesis is a crucial source of marine CH_4. Current estimates suggest that methanogensis produces between 0.7 – 1.4 Tg of CH_4 annually in marine sediments (Reeburgh, 2007; Valentine, 2011). This reaction has been observed globally in marine sediments (Reeburgh, 2007; Valentine, 2011). Small quantities of sediment-derived CH_4 escapes the sediments. Observations implicate S-DAMO as an integral CH_4 sink mediating ebullition into the water column (Reeburgh, 2007). The overlaying water column acts as an oxidative net preventing CH_4 from reaching the atmosphere. While most of the oceans contain ~4 nM CH_4, which is equal to atmospheric saturation, there are regions of the oceans where CH_4 can reach concentrations exceeding 10 μM (Reeburgh, 2007). One such region is a mid-water CH_4 maxima, containing 5-8 nM CH_4, at the pycnocline in the large oceanographic gyres. It was long thought that methanogenesis in sinking particles was the source of this mid-water CH_4 (Karl and Tillbrook, 1994). Recently, it was found that in phosphate-limited oligotrophic gyres bacteria catabolize methylated organophosphates generating orthophosphate and CH_4 (Karl et al., 2008; Reeburgh, 2007).

OMZs have also been noted as regions were CH_4 accumulates in the water column. Marine OMZs, such as those in the Eastern Tropical Pacific, the Black Sea and the Cariaco Basin, exhibit elevated CH_4 concentrations. CH_4 ranges from 80-100 nM in the Eastern Tropical Pacific and > 10 μM in the closed anoxic basins of the Black Sea and Cariaco Basin (Sansone et al., 2001; 2004; Reeburgh, 1976, Reeburgh et al., 1991). The lack of O_2 in OMZs prevents the rapid oxidation of CH_4 allowing CH_4 to accumulate. These OMZ regions constitute the largest pool of pelagic CH_4 (Sansone et al., 2004) and could be key CH_4 sites for hypoxic and anoxic CH_4 consumption.

1.3 Oxygen minimum zones as sites of CH_4 and N linkages

OMZs are a prominent feature of the marine water column. Aerobic respiration of organic matter in OMZs occurs at a faster rate than O_2 production (Wyrtki, 1962; Helly and Levin, 2004; Wright et al., 2012). In some areas such as the Eastern Tropical Pacific and the Arabian Sea, up-welling induces high rates of primary production in surface water. As this surface biomass dies and sinks, microbial communities rapidly consume the organic matter using O_2 as an oxidant. This rapid O_2 consumption is coupled with poor ventilation at these sites, which causes extreme O_2 depletion. In these regions, O_2 falls below the detection of modern sensors (Thamdrup et al., 2012; Tiano et al., 2014) and is accompanied by step gradients in biogeochemical parameters (Wright et al., 2012). These functionally anoxic conditions select for microbes that use anaerobic metabolisms. These metabolisms rely on alternative oxidized compounds such as NO_3^-, NO_2^-, SO_4^{2-}, and metal oxides as terminal electron acceptors. NO_3^- and NO_2^- are present in high concentrations below the oxycline, and offer reasonably high thermodynamic redox

energy yields and are therefore used to oxidize a wide range of reduced compounds. These pathways result in the production of biologically unavailable N_2 gas. Thus OMZs link N loss to numerous biochemical transformations (Stewart et al., 2012; Ulloa et al., 2012, Canfeild et al., 2010).

Microbial activities in OMZs contribute up to half of oceanic N loss (Gruber et al., 2004). N is removed from OMZs through denitrification or anaerobic ammonia oxidation (anammox) by diverse microbial taxa (Codispoti et al., 2001; Thamdrup et al., 2012; Ulloa et al., 2012). Anoxic OMZs, sometimes referred as anoxic marine zones (AMZs), are characterized by high concentrations of NO_2^- relative to oxic water column environments (Kamykowski and Zentara, 1991; Wright et al., 2012). This NO_2^- accumulation is presumably caused by modularity in the denitrification process. NO_3^- is reduced to NO_2^- and released to the water column for other microbes to carry out the next steps in denitrification (Hawley et al., 2014; Wright et al., 2012). The lack of O_2 prevents nitrification from occurring, thus inhibiting NO_2^- oxidation back to NO_3^-. OMZs provide a unique oceanic niche for microorganisms containing the enzymes nitrate reductase (*nar*) and nitrite oxidoreductase (*nir*) (Stewart et al., 2012; Ulloa et al., 2012; Tsementzi et al., 2016). Genes encoding this enzyme, along with other key catalytic enzymes for denitrification and anammox, are among the most abundant in OMZs (Stewart et al., 2012; Ulloa et al., 2012; Wright et al., 2012). Modern sequence technology has increased the ability to recover and assemble these genes from OMZ systems and link them to other enzymes involved biochemical reactions in poorly described microbes. This ability has enabled descriptions of uncultivated microbial species using unique metabolic strategies (Tsementzi et al., 2016).

OMZs may be important sites for pelagic CH_4 cycling as they are the largest pool of water column CH_4 in the global ocean (Sansone et al., 2001, Sansome et al, 2004), and represent potentially important sources of CH_4 to the atmosphere (Naqvi et al., 2010). Diverse microbes may be responsible for linking CH_4 oxidation to pathways of N loss under anoxia. This linkage might include microbes carrying the N-DAMO process such as bacteria of the NC10 Phylum. Another group that could facilitate methanotrophy driven N loss are the bacterial groups canonically associated with aerobic methanotrophy These bacteria use partial denitrification to support respiration while using O_2 to directly oxidize CH_4 (Kits et al., 2015). Evidence for aerobic methanotroph populations persisting in low-to-no O_2 environments have been reported in both culture-dependent and -independent studies (Kalyuzhnaya et al., 2013; Chistoserdova, 2015; Kits et al., 2015a,b; Danilova et al., 2016). While a partial denitrification process has been linked to aerobic methanotrophs in cultures it has not been described in natural environments.

The physiological mechanisms used by planktonic methanotrophs remain unclear in natural OMZ communities. Indeed, PCR-based surveys of the methanotroph marker gene *pmo* have identified diverse marine clades of methanotrophs as being widely distributed through pelagic and sediment low oxygen environments (Tavormina et al., 2008, 2010), including OMZs (Hayaski et al., 2007; Tavormina et al., 2013). Metagenomic studies of OMZs have recovered NC10-like sequences involved in N reduction (Ganesh et al., 2015). Given the enrichment of oxidized N compounds and CH_4 in OMZs and know methanotrophy driven N loss pathways, linkages between N loss and CH_4 oxidation may be prevalent throughout OMZs. This would represent an overlooked route of N loss in OMZs.

1.4 Objectives

Overlapping zones of elevated CH_4 and oxidized N concentrations in OMZs suggest a pelagic niche for methanotrophs conducting reductive N transformations. Since OMZs are predicted to expand with global warming (Stramma et al., 2008; Long et al., 2016), characterizing CH_4-consuming microbial populations in OMZs is critical for understanding greenhouse gas and nutrient budgets. ***The main objective of this work is to characterize the microbial abundance and activity in OMZs that participate in CH_4 oxidation and N loss.***

1.4.1 Objective 1 (Chapter 2)

A crucial first step in marine microbial studies is to isolate planktonic cells from the water column. Typically, this is achieved by filtering suspended biomass through a series of filters separating large particles and eukaryotic cells (1.0 – 30 μm) from the free-living cells suspended in the water (0.1 – 0.2 μm). This step lacks standardization across studies as researchers use filters of differing pore size, and this is often compounded with a wide range (< 1 L to >100 L) of seawater volume passed through the filters. Particle retention and clogging of these filters has been well documented, as has taxa bias. The impact that the volume of seawater filtered has on microbial community diversity estimates has not been quantitatively assessed. We utilized 16S rRNA gene amplicon sequencing to describe community structure in two microbial biomass size fractions (0.2 – 1.6 μm, > 1.6 μm) over a gradient of filtered water volumes (0.05 to 5 L). This work

establishes best practices for characterizing microbial diversity from seawater without introducing sampling biases. This is a critical component of subsequent chapters because each question addressed depends on successful, unbiased, collection of biomass in order to link patterns in the proportional representation of genes/taxa to chemical measurements.

1.4.2 Objective 2 (Chapter 3)

Sequences from the candidate phylum NC10 have been detected under the anoxic conditions of the world's largest OMZs in the Eastern Tropical Pacific. This group of recently described bacteria has the ability to generate intracellular O_2 from NO to oxidize CH_4. This process allows for anaerobic CH_4 oxidation while generating N_2 gas, thus contributing to N loss while oxidizing a potent greenhouse gas. OMZs in the Eastern Tropical Pacific contain relatively high concentrations of both CH_4 and NO_2^-, compared to more oxygenated pelagic regions. Given the functionally anoxic conditions in these regions combined with the availability of the NC10 N-DAMO reactants (CH_4 and NO_2^-), we hypothesize that these anoxic OMZs are a suitable niche for NC10 that link CH_4 oxidation to N loss. While NC10-like sequences have been recovered from OMZs in previous work, OMZs as a niche for N-DAMO had yet to be confirmed. We used a combination of (q)PCR, phylogenetics, and transcriptomic analyses coupled to chemical rate experiments to investigate this hypothesis.

1.4.3 Objective 3 (Chapter 4)

Genomic characterizations of oceanic methanotrophs are sparse. Descriptions of marine methanotrophic populations have relied on the detection of copper-monooxygenase phylotypes known as operational *pmo* units (OPUs). While OPU sequences have been shown to be enriched in OMZs it remains unknown what mechanism these aerobic methanotrophs use to function in this low O_2 niche. Cultured methanotrophs *Methylomicrobium album* BG8 and *Methylomonas dentrificans* FJG1 have been shown to use nitrate as an electron acceptor to relieve respiratory stresses under hypoxic culture conditions. This processes has not been detected in natural environments. In Chapter 3, high rates of CH_4 oxidation were detected in the Golfo Dulce (GD), Costa Rica in the NO_2^- maxima, just beneath the oxycline. However, NC10 transcripts were an order of magnitude lower in the GD compared to the ETNP, raising the possibility that other microbes may be contributing to OMZ methanotrophy. In exploring this hypothesis, we detected a high abundance of 16S rRNA gene and transcript sequences affiliated with a gammaproteobacteria OPU population, known as OPU3. This population of gammaproteobacteria could be responsible for the unexplained CH_4 oxidation rates. We therefore conducted a genomic study to test for a link between methanotrophy and denitrification, as observed in other cultured representatives. In this analysis, involving the assembly of metagenomic bins and metatranscriptome mapping to the OPU3 genome in the anoxic GD, we aim to describe the mechanisms allowing these "aerobic" methanotrophs to thrive in anoxic conditions.

1.5 References

Boetius, A., Ravenschlag, K., Schubert, C. J., Rickert, D., Widdel, F., Gieseke, A., et al. (2000). A marine microbial consortium apparently mediating anaerobic oxidation of methane. Nature, 407(6804), 623-626. doi:10.1038/35036572

Bousquet, P., Ciais, P., Miller, J. B., Dlugokencky, E. J., Hauglustaine, D. A., Prigent, C., et al. (2006). Contribution of anthropogenic and natural sources to atmospheric methane variability. Nature, 443(7110), 439-443. doi:10.1038/nature05132

Bowman, J. (2006). The methanotrophs—the families methylococcaceae and methylocystaceae. In The prokaryotes (pp. 266-289): Springer.

Bowman, J. P. (2014). The family methylococcaceae. In The prokaryotes (pp. 411-440): Springer.

Canfield, D. E., Stewart, F. J., Thamdrup, B., De Brabandere, L., Dalsgaard, T., Delong, E. F., et al. (2010). A cryptic sulfur cycle in oxygen-minimum-zone waters off the chilean coast. Science, 330(6009), 1375-1378. doi:10.1126/science.1196889

Carini, P., White, A. E., Campbell, E. O., & Giovannoni, S. J. (2014). Methane production by phosphate-starved sar11 chemoheterotrophic marine bacteria. Nature Communications, 5. doi:10.1038/ncomms5346

Chistoserdova, L. (2015). Methylotrophs in natural habitats: Current insights through metagenomics. Applied Microbiology and Biotechnology, 99(14), 5763-5779. doi:10.1007/s00253-015-6713-z

Cicerone, R. J., & Oremland, R. S. (1988). Biogeochemical aspects of atmospheric methane. Global Biogeochemical Cycles, 2(4), 299-327. doi:10.1029/GB002i004p00299

Codispoti, L. A., Brandes, J. A., Christensen, J. P., Devol, A. H., Naqvi, S. W. A., Paerl, H. W., & Yoshinari, T. (2001). The oceanic fixed nitrogen and nitrous oxide budgets: Moving targets as we enter the anthropocene? Scientia Marina, 65, 85-105.

Conrad, R. (2009). The global methane cycle: Recent advances in understanding the microbial processes involved. Environmental Microbiology Reports, 1(5), 285-292. doi:10.1111/j.1758-2229.2009.00038.x

Curry, C. L. (2007). Modeling the soil consumption of atmospheric methane at the global scale. Global Biogeochemical Cycles, 21(4). doi:10.1029/2006gb002818

Danilova, O. V., Suzina, N. E., Van De Kamp, J., Svenning, M. M., Bodrossy, L., & Dedysh, S. N. (2016). A new cell morphotype among methane oxidizers: A spiral-shaped obligately microaerophilic methanotroph from northern low-oxygen environments. ISME J. doi:10.1038/ismej.2016.48

Davis, J. B., & Yarbroug.Hf. (1965). Anaerobic oxidation of hydrocarbons by desulfovibrio desulfuricans. Texas Reports on Biology and Medicine, 23(3), 632-&.

De Visscher, A., Boeckx, P., & Van Cleemput, O. (2007). 12 artificial methane sinks. Greenhouse gas sinks, 184.

Ettwig, K. F., Butler, M. K., Le Paslier, D., Pelletier, E., Mangenot, S., Kuypers, M. M. M., et al. (2010). Nitrite-driven anaerobic methane oxidation by oxygenic bacteria. Nature, 464(7288), 543-+. doi:10.1038/nature08883

Ettwig, K. F., Speth, D. R., Reimann, J., Wu, M. L., Jetten, M. S. M., & Keltjens, J. T. (2012). Bacterial oxygen production in the dark. Biochimica Et Biophysica Acta-Bioenergetics, 1817, S155-S155. doi:10.1016/j.bbabio.2012.06.406

Evans, P. N., Parks, D. H., Chadwick, G. L., Robbins, S. J., Orphan, V. J., Golding, S. D., & Tyson, G. W. (2015). Methane metabolism in the archaeal phylum bathyarchaeota revealed by genome-centric metagenomics. Science, 350(6259), 434-438. doi:10.1126/science.aac7745

Feely, H. W., & Kulp, J. L. (1957). Origin of gulf coast salt-dome sulphur deposits. AAPG Bulletin, 41(8), 1802-1853.

Fisher, R. E., Sriskantharajah, S., Lowry, D., Lanoiselle, M., Fowler, C. M. R., James, R. H., et al. (2011). Arctic methane sources: Isotopic evidence for atmospheric inputs. Geophysical Research Letters, 38. doi:10.1029/2011gl049319

Ganesh, S., Bristow, L. A., Larsen, M., Sarode, N., Thamdrup, B., & Stewart, F. J. (2015). Size-fraction partitioning of community gene transcription and nitrogen metabolism in a marine oxygen minimum zone. ISME J, in Press

Hanson, R. S., & Hanson, T. E. (1996). Methanotrophic bacteria. Microbiological Reviews, 60(2), 439-+.

Haroon, M. F., Hu, S. H., Shi, Y., Imelfort, M., Keller, J., Hugenholtz, P., et al. (2013). Anaerobic oxidation of methane coupled to nitrate reduction in a novel archaeal lineage. Nature, 500(7464), 567-+. doi:10.1038/nature12375

Hawley, A. K., Brewer, H. M., Norbeck, A. D., Pasa-Tolic, L., & Hallam, S. J. (2014). Metaproteomics reveals differential modes of metabolic coupling among ubiquitous oxygen minimum zone microbes. Proceedings of the National Academy of Sciences of the United States of America, 111(31), 11395-11400. doi:10.1073/pnas.1322132111

Hayashi, T., Obata, H., Gamo, T., Sano, Y., & Naganuma, T. (2007). Distribution and phylogenetic characteristics of the genes encoding enzymes relevant to methane oxidation in oxygen minimum zones of the eastern pacific ocean. Res J Environ Sci, 1, 275-284.

Helly, J. J., & Levin, L. A. (2004). Global distribution of naturally occurring marine hypoxia on continental margins. Deep-Sea Research Part I-Oceanographic Research Papers, 51(9), 1159-1168. doi:10.1016/j.dsr.2004.03.009

Kalyuzhnaya, M. G., Yang, S., Rozova, O. N., Smalley, N. E., Clubb, J., Lamb, A., et al. (2013). Highly efficient methane biocatalysis revealed in a methanotrophic bacterium. Nature Communications, 4. doi:10.1038/ncomms3785

Kamykowski, D., & Zentara, S. J. (1991). Spatiotemporal and process-oriented views of nitrite in the world ocean as recorded in the historical data set. Deep-Sea Research Part a-Oceanographic Research Papers, 38(4), 445-464. doi:10.1016/0198-0149(91)90046-i

Karl, D. M., Beversdorf, L., Bjorkman, K. M., Church, M. J., Martinez, A., & DeLong, E. F. (2008). Aerobic production of methane in the sea. Nature Geoscience, 1(7), 473-478. doi:10.1038/ngeo234

Karl, D. M., & Tilbrook, B. D. (1994). Production and transport of methane in oceanic particulate organic-matter. Nature, 368(6473), 732-734. doi:10.1038/368732a0

Kirschke, S., Bousquet, P., Ciais, P., Saunois, M., Canadell, J. G., Dlugokencky, E. J., et al. (2013). Three decades of global methane sources and sinks. Nature Geoscience, 6(10), 813-823. doi:10.1038/ngeo1955

Kits, K. D., Campbell, D. J., Rosana, A. R., & Stein, L. Y. (2015). Diverse electron sources support denitrification under hypoxia in the obligate methanotroph methylomicrobium album strain bg8. Frontiers in Microbiology, 6. doi:10.3389/fmicb.2015.01072

Kits, K. D., Klotz, M. G., & Stein, L. Y. (2015). Methane oxidation coupled to nitrate reduction under hypoxia by the gammaproteobacterium methylomonas denitrificans, sp nov type strain fjg1. Environmental Microbiology, 17(9), 3219-3232. doi:10.1111/1462-2920.12772

Knief, C. (2015). Diversity and habitat preferences of cultivated and uncultivated aerobic methanotrophic bacteria evaluated based on pmoa as molecular marker. Frontiers in Microbiology, 6. doi:10.3389/fmicb.2015.01346

Knittel, K., & Boetius, A. (2009). Anaerobic oxidation of methane: Progress with an unknown process. Annual Review of Microbiology, 63, 311-334. doi:10.1146/annurev.micro.61.080706.093130

Liu, Y. (2010). Taxonomy of methanogens. In Handbook of hydrocarbon and lipid microbiology (pp. 547-558): Springer.

Long, M. C., Deutsch, C., & Ito, T. (2016). Finding forced trends in oceanic oxygen. Global Biogeochemical Cycles, 30(2), 381-397. doi:10.1002/2015gb005310

Luo, H. W., Sun, Z. Y., Arndt, W., Shi, J., Friedman, R., & Tang, J. J. (2009). Gene order phylogeny and the evolution of methanogens. Plos One, 4(6). doi:10.1371/journal.pone.0006069

Naqvi, S. W. A., Bange, H. W., Farias, L., Monteiro, P. M. S., Scranton, M. I., & Zhang, J. (2010). Marine hypoxia/anoxia as a source of ch4 and n2o. Biogeosciences, 7(7), 2159-2190. doi:10.5194/bg-7-2159-2010

Op den Camp, H. J. M., Islam, T., Stott, M. B., Harhangi, H. R., Hynes, A., Schouten, S., et al. (2009). Environmental, genomic and taxonomic perspectives on methanotrophic verrucomicrobia. Environmental Microbiology Reports, 1(5), 293-306. doi:10.1111/j.1758-2229.2009.00022.x

Pack, M. A., Heintz, M. B., Reeburgh, W. S., Trumbore, S. E., Valentine, D. L., Xu, X. M., & Druffel, E. R. M. (2015). Methane oxidation in the eastern tropical north pacific ocean water column. Journal of Geophysical Research-Biogeosciences, 120(6), 1078-1092. doi:10.1002/2014jg002900

Raghoebarsing, A. A., Pol, A., van de Pas-Schoonen, K. T., Smolders, A. J. P., Ettwig, K. F., Rijpstra, W. I. C., et al. (2006). A microbial consortium couples anaerobic methane oxidation to denitrification. Nature, 440(7086), 918-921. doi:10.1038/nature04617

Reeburgh, W. S. (1976). Methane consumption in cariaco trench waters and sediments. Earth and Planetary Science Letters, 28(3), 337-344. doi:10.1016/0012-821x(76)90195-3

Reeburgh, W. S. (1980). Anaerobic methane oxidation - rate depth distributions in skan bay sediments. Earth and Planetary Science Letters, 47(3), 345-352. doi:10.1016/0012-821x(80)90021-7

Reeburgh, W. S. (2007). Oceanic methane biogeochemistry. Chemical Reviews, 107(2), 486-513. doi:10.1021/cr050362v

Reeburgh, W. S., Ward, B. B., Whalen, S. C., Sandbeck, K. A., Kilpatrick, K. A., & Kerkhof, L. J. (1991). Black-sea methane geochemistry. Deep-Sea Research Part a-Oceanographic Research Papers, 38, S1189-S1210.

Repeta, D. J., Ferron, S., Sosa, O. A., Johnson, C. G., Repeta, L. D., Acker, M., et al. (2016). Marine methane paradox explained by bacterial degradation of dissolved organic matter. Nature Geoscience, 9(12), 884-+. doi:10.1038/ngeo2837

Sansone, F. J., Graham, A. W., & Berelson, W. M. (2004). Methane along the western mexican margin. Limnology and Oceanography, 49(6), 2242-2255.

Sansone, F. J., Popp, B. N., Gasc, A., Graham, A. W., & Rust, T. M. (2001). Highly elevated methane in the eastern tropical north pacific and associated isotopically enriched fluxes to the atmosphere. Geophysical Research Letters, 28(24), 4567-4570. doi:10.1029/2001gl013460

Semrau, J. D., DiSpirito, A. A., & Yoon, S. (2010). Methanotrophs and copper. Fems Microbiology Reviews, 34(4), 496-531. doi:10.1111/j.1574-6976.2010.00212.x

Stewart, F. J., Ulloa, O., & DeLong, E. F. (2012). Microbial metatranscriptomics in a permanent marine oxygen minimum zone. Environmental Microbiology, 14(1), 23-40. doi:10.1111/j.1462-2920.2010.02400.x

Stocker, T., Qin, D., Plattner, G., Tignor, M., Allen, S., Boschung, J., et al. (2013). Ipcc, 2013: Climate change 2013: The physical science basis. contribution of working group i to the fifth assessment report of the intergovernmental panel on climate change. Retrieved from Cambridge, United Kingdom and New York, NY USA:

Stramma, L., Johnson, G. C., Sprintall, J., & Mohrholz, V. (2008). Expanding oxygen-minimum zones in the tropical oceans. Science, 320(5876), 655-658. doi:10.1126/science.1153847

Tavormina, P. L., Ussler, W., Joye, S. B., Harrison, B. K., & Orphan, V. J. (2010). Distributions of putative aerobic methanotrophs in diverse pelagic marine environments. Isme Journal, 4(5), 700-710. doi:10.1038/ismej.2009.155

Tavormina, P. L., Ussler, W., & Orphan, V. J. (2008). Planktonic and sediment-associated aerobic methanotrophs in two seep systems along the north american margin. Applied and Environmental Microbiology, 74(13), 3985-3995. doi:10.1128/aem.00069-08

Tavormina, P. L., Ussler, W., Steele, J. A., Connon, S. A., Klotz, M. G., & Orphan, V. J. (2013). Abundance and distribution of diverse membrane-bound monooxygenase (cu-mmo) genes within the costa rica oxygen minimum zone. Environmental Microbiology Reports, 5(3), 414-423. doi:10.1111/1758-2229.12025

Thamdrup, B. (2012). New pathways and processes in the global nitrogen cycle. In D. J. Futuyma (Ed.), Annual review of ecology, evolution, and systematics, vol 43 (Vol. 43, pp. 407-428). Palo Alto: Annual Reviews.

Thamdrup, B., Dalsgaard, T., & Revsbech, N. P. (2012). Widespread functional anoxia in the oxygen minimum zone of the eastern south pacific. Deep-Sea Research Part I-Oceanographic Research Papers, 65, 36-45. doi:10.1016/j.dsr.2012.03.001

Thauer, R. K., Jungermann, K., & Decker, K. (1977). Energy conservation in chemotrophic anaerobic bacteria. Bacteriological reviews, 41(1), 100.

Tiano, L., Garcia-Robledo, E., Dalsgaard, T., Devol, A. H., Ward, B. B., Ulloa, O., et al. (2014). Oxygen distribution and aerobic respiration in the north and south eastern tropical pacific oxygen minimum zones. Deep-Sea Research Part I-Oceanographic Research Papers, 94, 173-183. doi:10.1016/j.dsr.2014.10.001

Trotsenko, Y. A., & Murrell, J. C. (2008). Metabolic aspects of aerobic obligate methanotrophy. Advances in Applied Microbiology, Vol 63, 63, 183-229. doi:10.1016/s0065-2164(07)00005-6

Tsementzi, D., Wu, J. Y., Deutsch, S., Nath, S., Rodriguez, L. M., Burns, A. S., et al. (2016). Sar11 bacteria linked to ocean anoxia and nitrogen loss. Nature, 536(7615), 179-+. doi:10.1038/nature19068

Ulloa, O., Canfield, D. E., DeLong, E. F., Letelier, R. M., & Stewart, F. J. (2012). Microbial oceanography of anoxic oxygen minimum zones. Proceedings of the National Academy of Sciences of the United States of America, 109(40), 15996-16003. doi:10.1073/pnas.1205009109

Valentine, D. L. (2011). Emerging topics in marine methane biogeochemistry. Annual Review of Marine Science, Vol 3, 3, 147-171. doi:10.1146/annurev-marine-120709-142734

Wright, J. J., Konwar, K. M., & Hallam, S. J. (2012). Microbial ecology of expanding oxygen minimum zones. Nature Reviews Microbiology, 10(6), 381-394. doi:10.1038/nrmicro2778

Wyrtki, K. (1962). The oxygen minima in relation to ocean circulation. Deep-Sea Research, 9(1), 11-23. doi:10.1016/0011-7471(62)90243-7

Zhuang, Q., Melillo, J. M., Kicklighter, D. W., Prinn, R. G., McGuire, A. D., Steudler, P. A., et al. (2004). Methane fluxes between terrestrial ecosystems and the atmosphere at northern high latitudes during the past century: A retrospective analysis with a process-based biogeochemistry model. Global Biogeochemical Cycles, 18(3). doi:10.1029/2004gb002239

Zimov, S. A., Schuur, E. A. G., & Chapin, F. S. (2006). Permafrost and the global carbon budget. Science, 312(5780), 1612-1613. doi:10.1126/science.1128908

CHAPTER 2.

STANDARD FILTRATION PRACTICES MAY SIGNIFICANTLY DISTORT PLANKTONIC MICROBIAL DIVERSITY ESTIMATES

Disclaimer: This chapter was published with the same title, along with the supplementary material in Appendix C, in the journal Frontiers in Microbiology on 2 June 2015.

Citation: **Padilla, C. C., Ganesh, S., Gantt, S., Huhman, A., Parris, D. J., Sarode, N., Stewart, F. J.** (2015). Standard filtration practices may significantly distort planktonic microbial diversity estimates. *Front Microbiol*, *6*, 547-547

2.1 Abstract

Fractionation of biomass by filtration is a standard method for sampling planktonic microbes. It is unclear how the taxonomic composition of filtered biomass changes depending on sample volume. Using seawater from a marine oxygen minimum zone, we quantified the 16S rRNA gene composition of biomass on a prefilter (1.6 μm pore-size) and a downstream 0.2 μm filter over sample volumes from 0.05 to 5 L. Significant community shifts occurred in both filter fractions, and were most dramatic in the prefilter community. Sequences matching Vibrionales decreased from ~40-60% of prefilter datasets at low volumes (0.05-0.5 L) to less than 5% at higher volumes, while groups such at the Chromatiales and Thiohalorhabdales followed opposite trends, increasing from minor representation to become the dominant taxa at higher volumes. Groups often associated with marine particles, including members of the Deltaproteobacteria, Planctomycetes and Bacteroidetes, were among those showing the greatest increase with volume (4 to 27-fold). Taxon richness (97% similarity clusters) also varied significantly with volume, and in opposing directions depending on filter fraction, highlighting potential biases in community complexity estimates. These data raise concerns for studies using filter fractionation for quantitative comparisons of aquatic microbial diversity, for example between free-living and particle-associated communities.

2.1 Introduction

Most studies of planktonic microbes begin by isolating organisms from the environment. This task usually involves collection of suspended biomass by passing

water through a filter. For studies of planktonic bacteria and archaea, it is routine to use an inline series of filters during the collection step, often with a prefilter of larger pore size (typically 1.0-30 μm) upstream of a primary collection filter of smaller pore size (0.1-0.2 μm; Fuhrman et al., 1988; Venter et al., 2004; Walsh et al., 2009; Morris and Nunn, 2013; Stewart 2013). Both filters retain microbial biomass, and the larger and smaller biomass size fractions are often used to approximate divisions between particle-associated and free-living microbes, respectively (e.g., Acinas et al., 2009; Crump et al., 1999; Hollibaugh et al., 2000; Moeseneder et al., 2001; LaMontagne and Holden, 2003; Ghiglione et al., 2007, 2009; Rusch et al., 2007; Kellog and Demming, 2009; Smith et al., 2013; D'Ambrosio et al., 2014; Ganesh et al., 2014; Mohit et al., 2014; Orsi et al., 2015, among others). Retained biomass can be used towards a range of analytical goals, including quantitative measurements of community taxonomic and metabolic diversity, based for example on 16S rRNA gene or metagenome sequencing. Such analyses shape our understanding of microbial distributions and functions in the environment.

The effects of filtration method on quantitative measurements of community genetic diversity are poorly understood, and rarely accounted for in study design. Notably, it is unclear how prefiltration and variation in filtered water volume influence the relative abundances of taxa retained in different filter fractions. This is surprising given an extensive literature demonstrating variation in particle retention and clogging rates among filter types and in the size spectra of retained particles due to clogging (Nagata, 1986; Taguchi and Laws, 1988; Knefelkamp et al., 2007), and a smaller number of studies showing differential selection of target taxa based on filter type (Gasol and Moran, 1999), or variation in DNA extraction efficiency depending on filtered water

volume (Boström et al., 2004). Indeed, sample volume varies widely across studies, from less than 1 L for coastal or eutrophic environments (Hollibaugh et al., 2000) to greater than 100 L for open ocean settings (Rusch et al., 2007). Fewer studies sample at very low volumes (microliters), in part to avoid under-sampling community richness, potentially due to microscale heterogeneity in biomass distributions (Long and Azam, 2001). Sample volume is often also variable among samples within a study, differing for instance between samples collected for DNA versus RNA analysis (Frias-Lopez et al., 2008; Hunt et al., 2013). While it has been assumed that the proportion of free-living bacteria retained in the prefilter fraction increases with the volume of filtered water (Lee et al., 1995), the effects of such retention on community composition measurements are unknown. Advances in high-throughput 16S rRNA gene sequencing now enable rapid, low-cost quantification of microbial community structure (Caporaso et al, 2011). These methods can be used to help identify biases associated with common sample collection practices.

We conducted experiments to test whether variation in the volume of filtered seawater biases estimates of marine microbial diversity. Biomass representing two size fractions (0.2-1.6 μm, >1.6 μm) was collected from a marine oxygen minimum zone (OMZ) following a sequential inline filtration protocol used routinely to study planktonic microbes (Fuhrman et al., 1988; Frias-Lopez et al., 2008; Stewart, 2013). Sequencing of community 16S rRNA gene amplicons revealed significant shifts in community structure and richness over volumes ranging from 0.05 to 5 L. We discuss these results as evidence that sample volume should be critically examined as a potentially confounding variable in comparing estimates of aquatic microbial diversity.

2.3 Materials and Methods

2.3.1 Sample collection and filtration

Seawater was collected from the OMZ off Manzanillo, Mexico during the Oxygen Minimum Zone Microbial Biogeochemistry Expedition 2 (OMZoMBiE2) cruise (R/V New Horizon; cruise NH1410; May 10-June 8, 2014). Collections were made using 30 L Niskin bottles attached to a CTD-Rosette. Seawater was emptied into 20 L cubitainers upon retrieval on deck and stored in the dark at 4°C until filtration (<1 hr). Two experiments were conducted to assess the impact of sample volume on microbial diversity. Experiment 1 collected biomass after filtration of 0.1, 1, and 5 L from the sample pool, with 3-5 replicate filtration lines per volume. Experiment 2 examined volumes of 0.05, 0.1, 0.5, 1, 2, and 5 L, with 2-3 replicates per volume. These ranges encompass volumes typical for studies of both coastal and open ocean environments, although fewer studies collect volumes at the lower end of the range. Water for experiment 1 was collected from depth 150 m near the secondary nitrite maximum at a site ~95 km offshore from Manzanillo (18'12"N 104'12"W). Water for experiment 2 was collected from depth 400 m at a site ~300 km offshore from Manzanillo (20'00" N, 107'00" W). Collections depths at both sites were beneath the photic zone. Total water depth at both sites was > 1000 m.

For each experiment, discrete water volumes were measured from the stored sample water, transferred into pre-washed secondary containers (graduated cylinders or glass bottles), and filtered by sequential in-line filtration at room temperature through a

glass fiber disc pre-filter (GF/A, 47 mm, 1.6 µm pore-size, Whatman) and a primary collection filter (Sterivex-GP filter cartridge, polyethersulfone membrane, 0.22 µm pore-size, Millipore) using a peristaltic pump (Masterflex L/S modular drive pump, 1-100 rpm, Cole-Parmer®) at constant speed (60 rpm). Replicate filters were collected in parallel (separate filter lines) for each discrete volume, with a maximum of 5 lines (replicates) running in parallel at once. After filtration, prefilters were transferred to cryovials containing lysis buffer (~1.8 ml; 50 mM Tris-HCl, 40 mM EDTA, and 0.73 M Sucrose), Sterivex cartridges were filled with lysis buffer (~1.8 ml) and capped at both ends, and both filter types were stored at -80°C until DNA extraction. After filtration of one set of replicates, filter lines were rinsed, and clean filters were added. Aliquots representing the next sample in the volume series were then measured from the source water, and the filtration sequence was repeated.

2.3.2 DNA extraction

DNA was extracted from prefilters and Sterivex cartridges using a phenol:chloroform protocol as in Ganesh *et al.* (2014). Cells were lysed by adding lysozyme (2 mg in 40 µl of lysis buffer per filter) directly to the prefilter-containing cryovials and the Sterivex cartridges, sealing the caps/ends, and incubating for 45 min at 37°C. Proteinase K (1 mg in 100 µl lysis buffer, with 100 µl 20% SDS) was added, and cryovials and cartridges were resealed and incubated for 2 hours at 55°C. The lysate was removed, and DNA was extracted once with phenol:chloroform:isoamyl alcohol (25:24:1) and once with Chloroform:Isoamyl Alcohol (24:1) and then concentrated by

spin dialysis using Ultra-4 (100 kDa, Amicon) centrifugal filters. Double stranded DNA was quantified on a Qubit® Fluorometer using the dsDNA BR Assay Kit.

2.3.3 16S rRNA gene quantitative PCR

Quantitative PCR (qPCR) was used to count total bacteria 16S rRNA gene copies in DNA extracted from both prefilter and Sterivex size fractions. Total 16S counts were obtained using SYBR® Green-based qPCR and universal bacterial 16S primers 1055f and 1392r, as in Hatt et al. (2013). Ten-fold serial dilutions of DNA from a plasmid carrying a single copy of the 16S rRNA gene (from *Dehalococcoides mccartyi*) were included on each qPCR plate and used to generate standard curves. Assays were run on a 7500 Fast PCR System and a StepOnePlus™ Real-Time PCR System (Applied Biosystems). All samples were run in triplicate (20 µL each) and included 1X SYBR® Green Supermix (BIO-RAD), 300 nM of primers, and 2 µL of template DNA (diluted 1:100). Thermal cycling involved: incubation at 50°C for 2 min to activate uracil-N-glycosylase, followed by 95 °C for 10 min to inactivate UNG, denature template DNA, and activate the polymerase, followed by 40 cycles of denaturation at 95°C (15 sec) and annealing at 60°C (1 min).

2.3.4 Diversity analyses

High-throughput sequencing of dual-indexed PCR amplicons encompassing the V4 region of the 16S rRNA gene was used to assess microbial community composition.

Briefly, amplicons were synthesized using Platinum® PCR SuperMix (Life Technologies) with primers F515 and R806, encompassing the V4 region of the 16S rRNA gene (Caporaso *et al.,* 2011). These primers are used primarily for bacterial 16S rRNA genes analysis, but also amplify archaeal sequences. Both forward and reverse primers were barcoded and appended with Illumina-specific adapters according to Kozich *et al.* (2013). Equal amounts of starting DNA (0.5 ng) were used for each PCR reaction to avoid potential PCR biases due to variable template concentrations (Kennedy et al., 2014). Thermal cycling involved: denaturation at 94°C (3 min), followed by 30 cycles of denaturation at 94°C (45 sec), primer annealing at 55°C (45 sec) and primer extension at 72°C (90 sec), followed by extension at 72°C for 10 min. Amplicons were analyzed by gel electrophoresis to verify size (~400 bp, including barcodes and adaptor sequences) and purified using the Diffinity RapidTip2 PCR purification tips (Diffinity Genomics, NY). Amplicons from different samples were pooled at equimolar concentrations and sequenced on an Illumina MiSeq using a 500 cycle kit with 5% PhiX to increase read diversity.

Amplicons were analyzed using QIIME (Caporaso *et al*., 2010) following standard protocols. Barcoded sequences were de-multiplexed and trimmed (length cutoff 100 bp) and filtered to remove low quality reads (average Phred score < 25) using Trim Galore! (http://www.bioinformatics.babraham.ac.uk/projects/trim_galore/). Paired-end reads were then merged using FLASH (Magoč and Salzberg, 2011), with criteria of average read length 250, fragment length 300, and fragment standard deviation 30. Chimeric sequences were detected by reference-based searches using USEARCH (Edgar, 2010). Identified chimeras were filtered from the input dataset, and merged non-chimeric

sequences were clustered into Operational Taxonomic Units (OTUs) at 97% sequence similarity using open-reference picking with the UCLUST algorithm (Edgar, 2010) in QIIME. The number of sequences assigned to OTUs averaged 22,693 (range: 2255-182,051) and 20,638 (range: 5152-46,634) per sample for experiments 1 and 2, respectively.

Taxonomy was assigned to representative OTUs from each cluster using the Greengenes database (DeSantis *et al.,* 2006). OTU counts were rarefied (10 iterations) and alpha diversity was quantified at a uniform sequence depth (n=2255 for exp 1 and 5152 for exp 2) using the Chao1 estimator of richness. Significant differences in Chao1 estimates between volume groupings were detected using pairwise two-sample t-tests with a Bonferroni correction for multiple comparisons. To compare community composition between samples, sequences were aligned in QIIME using PyNAST, and beta diversity was calculated using the weighted Unifrac metric (Lozupone and Knight, 2005). Sample relatedness based on Unifrac was visualized with two-dimensional Principal Coordinate Analyses. The statistical significance of sample grouping according to filtered volume was assessed using the nonparametric adonis method in QIIME based on Unifrac distances run with 999 permutations and Bonferroni corrections for multiple tests (Table B.1).

Taxa (Order level) differing significantly in proportional abundance in pairwise comparisons of filter volumes (lowest versus highest volumes) were identified via an empirical Bayesian approach using the program baySeq (Hardcastle and Kelly, 2010), as in Stewart et al. (2012) and Ganesh et al. (2014). The baySeq method assumes a negative binomial distribution with prior distributions derived empirically from the data (100,000

iterations). Dispersion was estimated via a quasi-likelihood method, with the count data normalized by dataset size (total number of identifiable 16S rRNA gene amplicons per dataset). Posterior likelihoods per Order were calculated for models (volume groupings) in which Orders were either predicted to be equivalently abundant between lowest versus highest filter volumes or differentially abundant. A false discovery rate threshold of 0.05 was used for detecting differentially abundant categories.

All sequence data have been submitted to the Sequence Read Archive at NCBI under BioProject ID PRJNA275901.

2.4 Results

Total bacterial 16S rRNA gene counts (prefilter + Sterivex combined), a rough proxy for microbial abundance, averaged 4 x 10^5 and 7 x 10^4 (averaged across all volumes and replicates) for experiment 1 and 2, respectively, and were 10 to 11-fold higher in the Sterivex size fraction (0.2-1.6 μm; Table B.1). These counts are within the range of or slightly lower than prior bacterial 16S gene counts at OMZ and oxycline depths in the study area (~5x10^4 to 1.3x10^6; Ganesh et al., 2015; Stewart, unpublished), values typical of open ocean waters, and consistent with prior reports of elevated microbial biomass in the smallest ("free-living") size fraction compared to particulate size fractions (Cho and Azam, 1988; Ghiglione et al., 2009). DNA yields, representing both prokaryote and eukaryote sources, were ~2 to 4-fold higher in Sterivex filter fractions compared to prefilters (Figure 2.1A). Both DNA yields and bacterial 16S counts increased linearly with volume in both fractions, and were most variable (among

replicates) for the 5 L samples, suggesting differences in extraction efficiency at high volumes (Figures 2.1A and B.1). Similarly, filtration time increased linearly as a function of sample volume ($R^2 = 0.99$; Figure 2.1B), ranging from <40 seconds (0.05 L) to 43 min (5 L). Average flow rate, calculated from filtration times from all samples, was 0.12 L min^{-1}. A minor increase of filtration times per unit volume was observed for the 5 L samples compared to 1 L and 2 L samples, highlighting a very slight decline in flow rate with volume, potentially due to filter clogging. No filters visibly ruptured during the experiments.

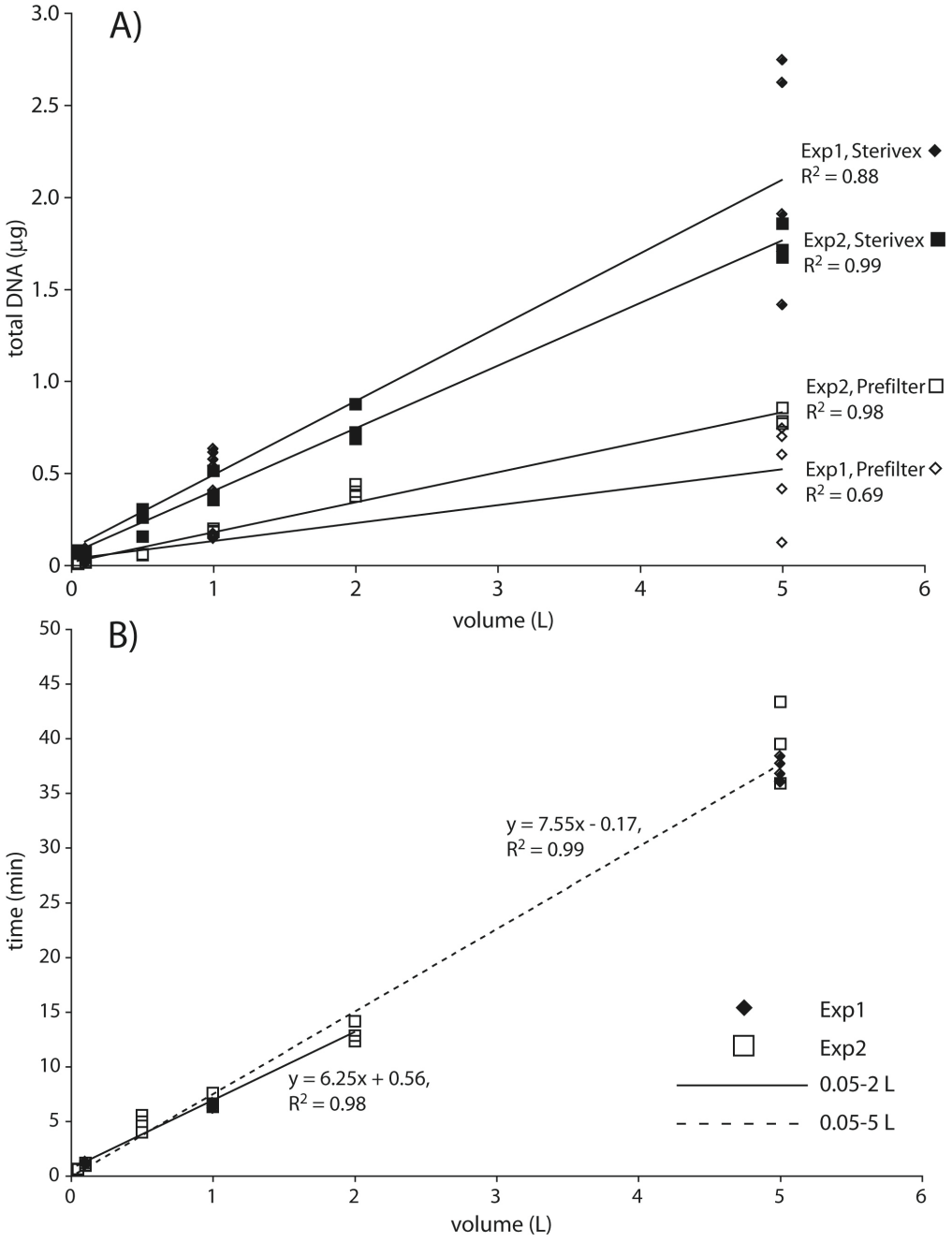

Figure 2.1. Total DNA yield (*A*) and filtration time (*B*) as a function of filtered water volume. The solid regression line in *B* spans the 0.05 L to 2 L range. The dashed regression spans the full dataset, with the increased slope suggesting a slight decrease in flow rate at the highest volumes.

Community structure varied significantly with sample volume in both biomass fractions. Principal coordinates analysis based on the weighted Unifrac metric showed significant differentiation of samples based on filtered volume for both size fractions in both experiments (R^2: 0.50-0.87; $P<0.05$), with the strongest separation occurring between samples of 1 L or more and those of lower volumes (Figure 2.2, 2.3; Table B.2). Chao1 estimates of operational taxonomic unit (OTU; 97% similarity cluster) richness varied with filter volume in both size fractions (Figure 2.4). In both experiments, median richness in the >1.6 μm fraction increased (by up to 68%) with volume, reaching peak values at 1 L, before declining again at the highest volumes (2-5 L). However, differences in prefilter richness between volume groupings were not significant, due partly to limited replication per volume. In contrast, in both experiments richness in the downstream 0.2-1.6 μm 'Sterivex' size fraction declined by ~25-30% over the volume range, with statistically significant declines observed between lower volumes and the 5 L samples in experiment 2 ($P<0.05$).

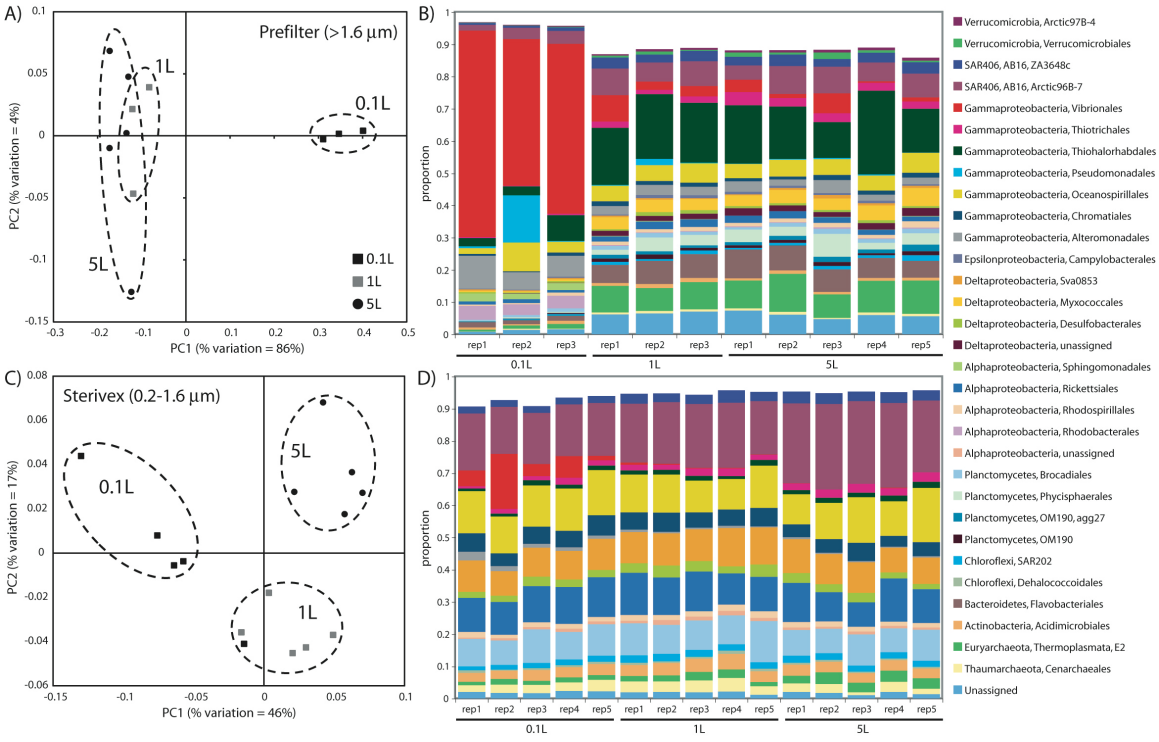

Figure 2.2. Microbial community relatedness (*A,C*) and taxon abundances (*B,D*) in experiment 1 prefilter (>1.6 µm; *A,B*) and Sterivex (0.2-1.6 µm; *C,D*) samples. Relatedness based on 16S rRNA gene amplicon sequencing, as quantified by the weighted Unifrac metric. Samples representing different filtered water volumes are circled. Abundances in *B,D* are percentage abundances of major bacterial Orders. Only Orders with abundance > 0.5% (averaged across all replicates) are shown.

The most dramatic shifts in taxonomic representation with volume occurred in the prefilter fraction (Figure 2.2, 2.3). Of the major Prokaryotic Orders detected in experiment 1, where 'major' here indicates an average percent abundance >0.5% across filter type replicates, 59% (19 of 32) varied significantly in abundance from lowest to highest volumes (0.1 vs. 5 L; $P<0.05$), with 88% (28) undergoing a fold-change of 2 or greater (positive or negative; Table B.3). In experiment 2, 96% of major Orders underwent a fold-change of 2 or greater over the volume range (0.05 vs. 5 L), although fewer (17%) of these changes were statistically significant (likely due to fewer replicates per volume in experiment 2; Table B.4). In both experiments, sequences matching Vibrionales decreased dramatically (21-33 fold) with filter volume, from >50% (average) of the lowest volume datasets, to <3% at 5 L. In contrast, other groups increased to dominate the dataset over the volume range. In experiment 1, sequences related to the gammaproteobacterial Thiohalorhabdales increased nearly 4-fold, becoming the single most abundant Order at 5 L with 17% of total sequences. In experiment 2, the Order Chromatiales increased from an average of 2% at lower volumes (range: 0.2-5.7% over 0.05, 0.1, 0.5 L datasets) to become the most abundant taxon at higher volumes, representing an average of 42% of total sequences at volumes of 1 L or greater (range: 15-77%; Figure 2.3, Table B.4). In both experiments, Euryarchaeota of the Thermoplasmata increased 10 to 20-fold to become the second most abundant Order (7-10%) at 5 L. Diverse members of the Deltaproteobacteria, Planctomycetes, and Bacteroidetes also underwent substantial increases (4 to 27-fold) in the prefilter fraction in both experiments (Tables B.3, B.4).

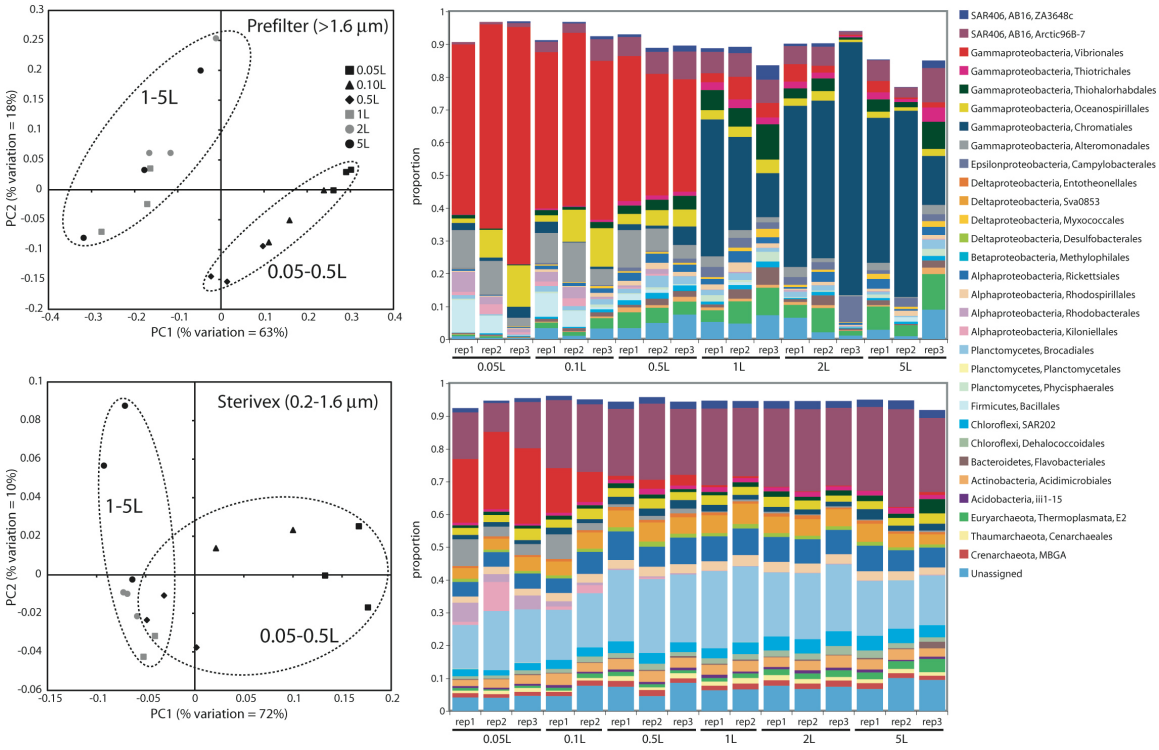

Figure 2.3. Microbial community relatedness (*A,C*) and taxon abundances (*B,D*) in experiment 2 prefilter (>1.6 µm; *A,B*) and Sterivex (0.2-1.6 µm; *C,D*) samples. Relatedness based on 16S rRNA gene amplicon sequencing, as quantified by the weighted Unifrac metric. Samples representing different filtered water volumes are circled. Abundances in *B,D* are percentage abundances of major bacterial Orders. Only Orders with abundance > 0.5% (averaged across all replicates) are shown.

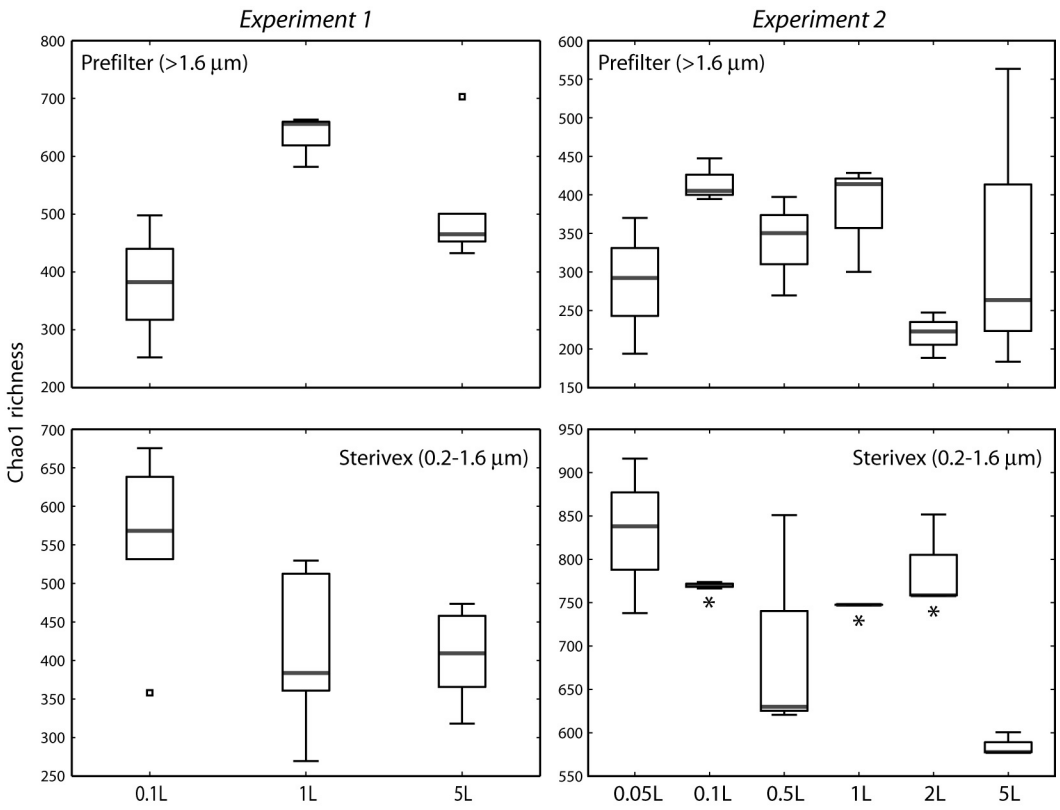

Figure 4. Chao1 estimates of operational taxonomic unit (97% similarity cluster) richness in prefilter (>1.6 µm; *A,B*) and Sterivex (0.2-1.6 µm; *C,D*) samples in experiments 1 and 2. Boxplots show medians within first and third quartiles, with whiskers indicating the lowest and highest values within 1.5 times the interquartile range of the lower and upper quartiles respectively. Note variation in y-axis scales. Asterisks in *D* indicate volume groupings with richness estimates significantly different from those of the 5 L sample ($P<0.05$). All other pairwise differences between volume groupings were not statistically significant.

Large changes in taxon representation also occurred in the Sterivex fraction, but were less dramatic that those in the prefilter community. In both experiments, 14% of the major prokaryotic Orders detected in this fraction changed significantly in representation over the volume range ($P<0.05$, Tables B.3, B.4). As in the prefilter datasets, the most substantial shifts occurred in the Vibrionales, which decreased 51 to 97-fold with volume. Other groups undergoing significant declines included the Alteromonadales, Rhodobacterales, and Kiloniellales, notably with these groups declining 16 to 94-fold in experiment 2. Less dramatic, but still substantial, shifts occurred in the opposite direction, notably with the abundant SAR406 lineage increasing ~2-fold in representation in both experiments to constitute over one quarter of all sequences in the 5 L datasets.

2.5 Discussion

Studies of diverse aquatic habitats consistently show that microbial community composition in the prefilter fraction differs from that of the smaller size fraction (e.g., Simon et al., 2002, 2014, and references therein). These differences have been used to suggest taxonomic, chemical, and metabolic partitioning between particle-associated versus free-living microbial communities (see references in Introduction). While the pore size of the primary collection filter used in such studies is almost always 0.2 μm, the pore size of the prefilter varies, typically from 0.8-1.0 (e.g., Hollibaugh et al., 2000; Allen et al., 2012) to 30 μm (e.g., Fuchsman et al., 2011, 2012), but is most often in the range of 1 to 3 μm, encompassing the 1.6 μm GF/A prefilter used in this study. Here, sample volume had a much stronger effect on prefilter community composition compared to that

of the downstream Sterivex fraction. Taxa such as the Thiohalorhabdales and Chromatiales in experiments 1 and 2, respectively, were evenly distributed between filter fractions at low volumes but dramatically enriched in the prefilter at higher volumes. Furthermore, major taxonomic divisions often described as being enriched in particulate fractions, including the Flavobacteriales (Bacteroidetes), Myxococcales (Deltaproteobacteria), and Planctomycetes (Crump et al., 1999; Simon et al., 2002; Eloe et al., 2011; Allen et al., 2012; Fuchsman et al., 2012), were among those whose proportional abundances in the prefilter fraction increased the most with filter volume, although these groups have also been detected on particles sampled directly by syringe (DeLong et al., 1993; Rath et al., 1998). Such changes were not exclusive to the prefilter fraction. SAR406, an uncultured lineage commonly affiliated with low-oxygen waters (Wright et al., 2012, 2014), increased steadily with volume to become the single most abundant taxonomic group in both experiments. These patterns suggest that differences in sample volume can bias multiple sequential filter fractions, but may be particularly problematic for studies inferring the structure of the particle-associated community, or the association of certain taxa with a particle-attached niche.

Community diversity differences between particle-associated and free-living biomass fractions are often variable across diverse ocean habitats. This has been attributed to environmental variation associated with geographic and vertical zonation, as well as flexibility in microbial lifestyles allowing alternation between particle-associated and free-living lifestyles (Grossart, 2010). Surprisingly, only a small number of studies have evaluated the potential for collection methods to bias community-level diversity measurements (Kirchman et al., 2001; Long and Azam, 2001; Ghiglione et al., 2007).

Focusing on the 0.2-3.0 μm filter fraction, Long and Azam (2001) recovered qualitatively similar community 16S rRNA gene fingerprints (denaturing gradient gel electrophoresis; DGGE) from coastal seawater volumes ranging from 1 μl to 1 L. Similarly, Ghiglione et al. (2007) reported no visible effect of volume (0.1 to 5 L) on fingerprints (capillary electrophoresis-single strand conformation polymorphism) from Mediterranean Sea bacterioplankton on 0.2 and 0.8 μm filters. High throughout 16S amplicon sequencing now provides a cost-competitive alternative to fingerprinting with higher sensitivity for detecting community structural shifts, including those involving rare taxa. Using this method, our results suggest that biases due to variation in filtered volume may also confound comparisons of size-fractionated community structure across habitats and studies.

Our data also suggest that metrics of community (OTU) richness may be sensitive to filtered water volume. In both experiments, richness of the prefilter and Sterivex communities followed opposing trends with volume, increasing in the larger size fraction and decreasing in the smaller. Declines in diversity with filter volume (0.01 vs. 2 L) were previously observed in a study of prefiltered bacterioplankton (0.2-3.0 μm fraction) using DGGE, although determinants of that decline could not be related directly to volume due to variations in the DNA extraction procedure (Kirchman et al., 2001). Here, in experiment 1, richness of the prefilter fraction was lower than that of the Sterivex fraction at 0.1 L, but this pattern was reversed at higher volumes. Enhanced richness in prefilter versus 0.2 μm fractions has been reported from diverse systems (Eloe et al., 2011; Bižić-Ionescu et al., 2014; Ganesh et al., 2014), leading to speculation that the complexity of the microbial community varies differentially between free-living and

particle-associated niches in response to fluctuation in water column conditions or niche-availability on particles. Bulk estimates of community complexity may instead be driven by variation in filtered water volume.

The observed compositional shifts with sample volume are potentially driven by a range of mechanisms. First, the filters may be clogging. A minor increase in filtration time per unit sample volume for the 5 L samples compared to the lower volume samples is consistent with filter clogging, although this trend is not supported by the near linear increase in total DNA yield and bacterial 16S gene counts per volume (Figure 2.1A and B.1). If the filters are indeed clogging, clogging would presumably lead to a progressive increase in the size range and diversity of the retained particles, with smaller (potentially free-living) cells below the size threshold of the unclogged filter increasingly retained as volumes increase. We speculate, for example, that Chromatiales and Thiohalorhabdales cells or cell aggregates are potentially either near the size threshold for passage through the prefilter, or are otherwise easily entrained in the filter matrix, and are therefore preferentially retained if the prefilter clogs.

Clogging could also affect diversity estimates for the downstream Sterivex filter fraction. In this fraction, however, effects due to clogging and increased retention of cells <0.2 μm are presumably minimal, as few planktonic marine microbes likely pass through the 0.2 μm filter to begin with (Fuhrman et al., 1988), although the abundance of very small cells in the open ocean remains an active area of research. Rather, the community shifts in the Sterivex fraction could be driven by clogging of the upstream prefilter, with the decline in OTU richness with filter volume observed in both

experiments potentially reflecting a selective narrowing of the range of taxa making it through the prefilter. Taxa that increase in abundance with volume in the 0.2 μm fraction, such as SAR406, may be relatively small cells, which presumably would be increasingly selected for as the prefilter clogs.

Second, filtration of small volumes, by chance, may fail to capture a representative subset of the particulate fraction, due to microscale patchiness of bacterioplankton and particle distributions (Azam and Hodson, 1981; Azam and Ammerman, 1984; Mitchell and Fuhrman, 1989). Marine particles span gradients of age, size, and source material, and potentially microbial composition (Simon et al., 2002). It is possible that certain particles, due to their low abundance, are unlikely to be captured at low water volumes, but would be sampled at higher volumes, and potentially contribute significantly to bulk microbial counts depending on the local density and richness of microbes on the particle. Changes in taxon representation due to increases in water volume may not be easily distinguished from changes due to filter clogging.

Third, adsorption of free dissolved DNA to filters may contribute disproportionately to diversity estimates at smaller volumes (Turk et al., 1992; Boström et al., 2004). While we cannot rule out this possibility, proportional decreases of filter-bound DNA with volume seems an unlikely explanation for the observed taxonomic shifts, as the dissolved DNA pool would need to be dominated almost exclusively by Vibrionales for this to be true. Also, DNA extraction efficiency has been shown to decrease with filtered water volume (Boström et al., 2004), suggesting that variable extraction efficiencies may affect community composition estimates. A consistent decrease in extraction efficiency with volume was not clearly evident in our samples,

although the range in DNA recovered from 5 L samples indicates that efficiency was variable (Figure 2.1A). Although the potential for extraction efficiency to change with sample volume deserves more attention, and is likely variable among filter types and extraction methods, decreasing efficiencies would only alter composition estimates if the change in efficiency is non-uniform among taxa. It is unknown if this is true.

Finally, it is possible that population turnover (growth or lysis) in the source water during filtering may also have contributed to compositional shifts with volume. We consider this possibility to be unlikely. Growth in the source water was likely negligible given characteristic doubling times of marine microbes (hours to days; Ducklow et al., 2000) and the low temperature of the stored source water (stored at 4°C, but filtered at room temperature). In both experiments, the total processing time of 0.1 and 1 L samples was less than 15 minutes. Growth by even the most active microbes under optimal conditions would be unlikely to result in the dramatic community structural shifts observed between these sample volumes (Figures 2.2, 2.3). Furthermore, the observed taxonomic shifts are inconsistent with changes due to differential turnover of microbial groups. Taxa typically associated with rapid growth during bottle incubations and in response to organic matter enrichment, notably members of the Alteromonadales, Pseudomonadales, and Vibrionales (Pinhassi and Berman, 2003; Allers et al., 2007, 2008; Stewart et al., 2012), decreased in abundance with increasing volume in both experiments (Tables B.3, B.4), inconsistent with results due to rapid growth during filtering. Furthermore, had the observed changes been due to growth, or to differential lysis of cells during sampling, we might predict changes of similar magnitude in both biomass fractions. This was not the

case, as the most dramatic changes were observed in the prefilter biomass, consistent with effects due to filter clogging.

2.6 Conclusion

These results, based on biomass from an open ocean environment and collected following a widely used filtration scheme, highlight a potential for sample volume variation to confound community diversity estimates. However, it is unlikely that our results extrapolate evenly to all systems. The magnitude and exact mechanism of sample volume-based biases likely differ depending on filter type and pore size, pumping rate, community composition, bulk microbial abundance, particle load, and potentially other variables. Such biases may be even greater in waters more eutrophic than those tested here, and may not easily be eliminated by frequent replacement of prefilters. For studies comparing particle-associated versus free-living communities, elimination of the prefiltration step may be necessary, with collection of particle communities based instead on direct sampling of particles without filtration (DeLong et al., 1993), potentially via gravity or flow-cytometric separation. Such alternative methods should be explored. Our data suggest that measurements of community structure for biomass separated by filter fractionation should only be considered accurate and used for quantitative comparisons when effects of sample volume variation are shown to be negligible.

Acknowledgements

We thank the crew of the *R/V New Horizon* for help in sample collection. This work was supported by the National Science Foundation (1151698 to FJS) and the Sloan Foundation (RC944 to FJS). The authors declare that we have no competing commercial interests that conflict with publication of this manuscript.

2.7 References

Acinas, S. G., Anton, J., Rodriguez-Valera, F. (1999). Diversity of free-living and attached bacteria in offshore western Mediterranean waters as depicted by analysis of genes encoding 16S rRNA. Applied and Environmental Microbiology, 65(2), 514-522.

Allen, L. Z., Allen, E. E., Badger, J. H., McCrow, J. P., Paulsen, I. T., Elbourne, L. D. H., et al. (2012). Influence of nutrients and currents on the genomic composition of microbes across an upwelling mosaic. Isme Journal, 6(7), 1403-1414. doi:10.1038/ismej.2011.201

Allers, E., Gomez-Consarnau, L., Pinhassi, J., Gasol, J. M., Simek, K., Pernthaler, J. (2007). Response of Alteromonadaceae and Rhodobacteriaceae to glucose and phosphorus manipulation in marine mesocosms. Environmental Microbiology, 9(10), 2417-2429. doi:10.1111/j.1462-2920.2007.01360.x

Allers, E., Niesner, C., Wild, C., Pernthaler, J. (2008). Microbes enriched in seawater after addition of coral mucus. Applied and Environmental Microbiology, 74(10), 3274-3278. doi:10.1128/aem.01870-07

Azam, F., Ammerman, J. W. (1984). Cycling of organic matter by bacterioplankton in pelagic marine ecosystems: microenvironmental considerations. In Flows of energy and materials in marine ecosystems (pp. 345-360): Springer.

Azam, F., Hodson, R. E. (1981). Multiphasic kinetics for d-glucose uptake by assemblages of natural marine-bacteria. Marine Ecology Progress Series, 6(2), 213-222. doi:10.3354/meps006213

Bizic-Ionescu, M., Zeder, M., Ionescu, D., Orlic, S., Fuchs, B. M., Grossart, H. P., Amann, R. (2015). Comparison of bacterial communities on limnic versus coastal marine particles reveals profound differences in colonization. Environmental Microbiology, 17(10), 3500-3514. doi:10.1111/1462-2920.12466

Bostrom, K. H., Simu, K., Hagstrom, A., Riemann, L. (2004). Optimization of DNA extraction for quantitative marine bacterioplankton community analysis. Limnology and Oceanography-Methods, 2, 365-373.

Caporaso, J. G., Kuczynski, J., Stombaugh, J., Bittinger, K., Bushman, F. D., Costello, E. K., et al. (2010). QIIME allows analysis of high-throughput community sequencing data. Nature Methods, 7(5), 335-336. doi:10.1038/nmeth.f.303

Caporaso, J. G., Lauber, C. L., Walters, W. A., Berg-Lyons, D., Lozupone, C. A., Turnbaugh, P. J., et al. (2011). Global patterns of 16S rRNA diversity at a depth of millions of sequences per sample. Proceedings of the National Academy of Sciences of the United States of America, 108, 4516-4522. doi:10.1073/pnas.1000080107

Cho, B. C., Azam, F. (1988). Major role of bacteria in biogeochemical fluxes in the ocean's interior. Nature, 332(6163), 441-443.

Crump, B. C., Armbrust, E. V., Baross, J. A. (1999). Phylogenetic analysis of particle-attached and free-living bacterial communities in the Columbia river, its estuary, and the adjacent coastal ocean. Applied and Environmental Microbiology, 65(7), 3192-3204.

D'Ambrosio, L., Ziervogel, K., MacGregor, B., Teske, A., Arnosti, C. (2014). Composition and enzymatic function of particle-associated and free-living bacteria: a coastal/offshore comparison. Isme Journal, 8(11), 2167-2179. doi:10.1038/ismej.2014.67

Delong, E. F., Franks, D. G., Alldredge, A. L. (1993). Phylogenetic diversity of aggregate-attached vs free-living marine bacterial assemblages. Limnology and Oceanography, 38(5), 924-934.

DeSantis, T. Z., Hugenholtz, P., Larsen, N., Rojas, M., Brodie, E. L., Keller, K., et al. (2006). Greengenes, a chimera-checked 16S rRNA gene database and workbench compatible with ARB. Applied and Environmental Microbiology, 72(7), 5069-5072. doi:10.1128/aem.03006-05

Ducklow, H. (2000). Bacterial production and biomass in the oceans. Microbial ecology of the oceans, 1, 85-120.

Edgar, R. C. (2010). Search and clustering orders of magnitude faster than BLAST. Bioinformatics, 26(19), 2460-2461. doi:10.1093/bioinformatics/btq461

Eloe, E. A., Shulse, C. N., Fadrosh, D. W., Williamson, S. J., Allen, E. E., Bartlett, D. H. (2011). Compositional differences in particle-associated and free-living microbial assemblages from an extreme deep-ocean environment. Environmental Microbiology Reports, 3(4), 449-458. doi:10.1111/j.1758-2229.2010.00223.x

Frias-Lopez, J., Shi, Y., Tyson, G. W., Coleman, M. L., Schuster, S. C., Chisholm, S. W., DeLong, E. F. (2008). Microbial community gene expression in ocean surface waters. Proceedings of the National Academy of Sciences of the United States of America, 105(10), 3805-3810. doi:10.1073/pnas.0708897105

Fuchsman, C. A., Kirkpatrick, J. B., Brazelton, W. J., Murray, J. W., Staley, J. T. (2011). Metabolic strategies of free-living and aggregate-associated bacterial communities inferred from biologic and chemical profiles in the Black Sea suboxic zone. Fems Microbiology Ecology, 78(3), 586-603. doi:10.1111/j.1574-6941.2011.01189.x

Fuchsman, C. A., Staley, J. T., Oakley, B. B., Kirkpatrick, J. B., Murray, J. W. (2012). Free-living and aggregate-associated Planctomycetes in the Black Sea. Fems Microbiology Ecology, 80(2), 402-416. doi:10.1111/j.1574-6941.2012.01306.x

Fuhrman, J. A., Comeau, D. E., Hagstrom, A., Chan, A. M. (1988). Extraction from natural planktonic microorganisms of dna suitable for molecular biological studies. Applied and Environmental Microbiology, 54(6), 1426-1429.

Ganesh, S., Bristow, L. A., Larsen, M., Sarode, N., Thamdrup, B., Stewart, F. J. (2015). Size-fraction partitioning of community gene transcription and nitrogen metabolism in a marine oxygen minimum zone. ISME J, in Press†

Ganesh, S., Parris, D. J., De Long, E. F., Stewart, F. J. (2014). Metagenomic analysis of size-fractionated picoplankton in a marine oxygen minimum zone. Isme Journal, 8(1), 187-211. doi:10.1038/ismej.2013.144

Gasol, J. M., Moran, X. A. G. (1999). Effects of filtration on bacterial activity and picoplankton community structure as assessed by flow cytometry. Aquatic Microbial Ecology, 16(3), 251-264. doi:10.3354/ame016251

Ghiglione, J., Mevel, G., Pujo-Pay, M., Mousseau, L., Lebaron, P., Goutx, M. (2007). Diel and seasonal variations in abundance, activity, and community structure of particle-attached and free-living bacteria in NW Mediterranean Sea. Microbial ecology, 54(2), 217-231.

Ghiglione, J. F., Conan, P., Pujo-Pay, M. (2009). Diversity of total and active free-living vs. particle-attached bacteria in the euphotic zone of the NW Mediterranean Sea. Fems Microbiology Letters, 299(1), 9-21. doi:10.1111/j.1574-6968.2009.01694.x

Grossart, H. P. (2010). Ecological consequences of bacterioplankton lifestyles: changes in concepts are needed. Environmental Microbiology Reports, 2(6), 706-714. doi:10.1111/j.1758-2229.2010.00179.x

Hardcastle, T. J., Kelly, K. A. (2010). baySeq: Empirical Bayesian methods for identifying differential expression in sequence count data. Bmc Bioinformatics, 11. doi:10.1186/1471-2105-11-422

Hatt, J. K., Ritalahti, K. M., Ogles, D. M., Lebron, C. A., Loffler, F. E. (2013). Design and Application of an Internal Amplification Control to Improve Dehalococcoides mccartyi 165 rRNA Gene Enumeration by qPCR. Environmental Science Technology, 47(19), 11131-11138. doi:10.1021/es4019817

Hollibaugh, J. T., Wong, P. S., Murrell, M. C. (2000). Similarity of particle-associated and free-living bacterial communities in northern San Francisco Bay, California. Aquatic Microbial Ecology, 21(2), 103-114. doi:10.3354/ame021103

Hunt, D. E., David, L. A., Gevers, D., Preheim, S. P., Alm, E. J., Polz, M. F. (2008). Resource partitioning and sympatric differentiation among closely related bacterioplankton. Science, 320(5879), 1081-1085. doi:10.1126/science.1157890

Kellogg, C. T. E., Deming, J. W. (2009). Comparison of free-living, suspended particle, and aggregate-associated bacterial and archaeal communities in the Laptev Sea. Aquatic Microbial Ecology, 57(1), 1-18. doi:10.3354/ame01317

Kennedy, K., Hall, M. W., Lynch, M. D. J., Moreno-Hagelsieb, G., Neufeld, J. D. (2014). Evaluating Bias of Illumina-Based Bacterial 16S rRNA Gene Profiles. Applied and Environmental Microbiology, 80(18), 5717-5722. doi:10.1128/aem.01451-14

Kirchman, D. L., Yu, L. Y., Fuchs, B. M., Amann, R. (2001). Structure of bacterial communities in aquatic systems as revealed by filter PCR. Aquatic Microbial Ecology, 26(1), 13-22. doi:10.3354/ame026013

Knefelkamp, B., Carstens, K., Wiltshire, K. H. (2007). Comparison of different filter types on chlorophyll-a retention and nutrient measurements. Journal of Experimental Marine Biology and Ecology, 345(1), 61-70. doi:10.1016/j.jembe.2007.01.008

Kozich, J. J., Westcott, S. L., Baxter, N. T., Highlander, S. K., Schloss, P. D. (2013). Development of a Dual-Index Sequencing Strategy and Curation Pipeline for Analyzing Amplicon Sequence Data on the MiSeq Illumina Sequencing Platform. Applied and Environmental Microbiology, 79(17), 5112-5120. doi:10.1128/aem.01043-13

LaMontagne, M. G., Holden, P. A. (2003). Comparison of free-living and particle-associated bacterial communities in a coastal lagoon. Microbial Ecology, 46(2), 228-237. doi:10.1007/s00248-001-1072-y

Lee, S., Kang, Y. C., Fuhrman, J. A. (1995). Imperfect retention of natural bacterioplankton cells by glass-fiber filters. Marine Ecology Progress Series, 119(1-3), 285-290. doi:10.3354/meps119285

Long, R. A., Azam, F. (2001). Microscale patchiness of bacterioplankton assemblage richness in seawater. Aquatic Microbial Ecology, 26(2), 103-113. doi:10.3354/ame026103

Lozupone, C., Knight, R. (2005). UniFrac: a new phylogenetic method for comparing microbial communities. Applied and Environmental Microbiology, 71(12), 8228-8235. doi:10.1128/aem.71.12.8228-8235.2005

Magoc, T., Salzberg, S. L. (2011). FLASH: fast length adjustment of short reads to improve genome assemblies. Bioinformatics, 27(21), 2957-2963. doi:10.1093/bioinformatics/btr507

Mitchell, J. G., Fuhrman, J. A. (1989). Centimeter scale vertical heterogeneity in bacteria and chlorophyll-a. Marine Ecology Progress Series, 54(1-2), 141-148. doi:10.3354/meps054141

Moeseneder, M. M., Winter, C., Herndl, G. J. (2001). Horizontal and vertical complexity of attached and free-living bacteria of the eastern Mediterranean Sea, determined by 16S rDNA and 16S rRNA fingerprints. Limnology and Oceanography, 46(1), 95-107.

Mohit, V., Archambault, P., Toupoint, N., Lovejoy, C. (2014). Phylogenetic Differences in Attached and Free-Living Bacterial Communities in a Temperate Coastal Lagoon during Summer, Revealed via High-Throughput 16S rRNA Gene Sequencing. Applied and Environmental Microbiology, 80(7), 2071-2083. doi:10.1128/aem.02916-13

Morris, R. M., Nunn, B. L. (2013). Sample Preparation and Processing for Planktonic Microbial Community Proteomics. Microbial Metagenomics, Metatranscriptomics, and Metaproteomics, 531, 271-287. doi:10.1016/b978-0-12-407863-5.00014-9

Nagata, T. (1986). Carbon and nitrogen-content of natural planktonic bacteria. Applied and Environmental Microbiology, 52(1), 28-32.

Orsi, W. D., Smith, J. M., Wilcox, H. M., Swalwell, J. E., Carini, P., Worden, A. Z., Santoro, A. E. (2015). Ecophysiology of uncultivated marine euryarchaea is linked to particulate organic matter. Isme Journal, 9(8), 1747-1763. doi:10.1038/ismej.2014.260

Pinhassi, J., Berman, T. (2003). Differential growth response of colony-forming alpha- and gamma-proteobacteria in dilution culture and nutrient addition experiments from Lake Kinneret (Israel), the eastern Mediterranean Sea, and the Gulf of Eilat. Applied and Environmental Microbiology, 69(1), 199-211. doi:10.1128/aem.69.1.199-211.2003

Rath, J., Wu, K. Y., Herndl, G. J., DeLong, E. F. (1998). High phylogenetic diversity in a marine-snow-associated bacterial assemblage. Aquatic Microbial Ecology, 14(3), 261-269. doi:10.3354/ame014261

Rusch, D. B., Halpern, A. L., Sutton, G., Heidelberg, K. B., Williamson, S., Yooseph, S., et al. (2007). The Sorcerer II Global Ocean Sampling expedition: Northwest Atlantic through Eastern Tropical Pacific. Plos Biology, 5(3), 398-431. doi:10.1371/journal.pbio.0050077

Simon, H. M., Smith, M. W., Herfort, L. (2014). Metagenomic insights into particles and their associated microbiota in a coastal margin ecosystem. Frontiers in Microbiology, 5. doi:10.3389/fmicb.2014.00466

Simon, M., Grossart, H. P., Schweitzer, B., Ploug, H. (2002). Microbial ecology of organic aggregates in aquatic ecosystems. Aquatic Microbial Ecology, 28(2), 175-211. doi:10.3354/ame028175

Smith, M. W., Allen, L. Z., Allen, A. E., Herfort, L., Simon, H. M. (2013). Contrasting genomic properties of free-living and particle-attached microbial assemblages within a coastal ecosystem. Frontiers in microbiology, 4.

Stewart, F. J. (2013). Preparation of Microbial Community cDNA for Metatranscriptomic Analysis in Marine Plankton. Microbial Metagenomics, Metatranscriptomics, and Metaproteomics, 531, 187-218. doi:10.1016/b978-0-12-407863-5.00010-1

Stewart, F. J., Dalsgaard, T., Young, C. R., Thamdrup, B., Revsbech, N. P., Ulloa, O., et al. (2012). Experimental Incubations Elicit Profound Changes in Community Transcription in OMZ Bacterioplankton. Plos One, 7(5). doi:10.1371/journal.pone.0037118

Taguchi, S., Laws, E. A. (1988). On the microparticles which pass through glass-fiber filter type gf/f in coastal and open waters. Journal of Plankton Research, 10(5), 999-1008. doi:10.1093/plankt/10.5.999

Turk, V., Rehnstam, A. S., Lundberg, E., Hagstrom, A. (1992). Release of bacterial-dna by marine nanoflagellates, an intermediate step in phosphorus regeneration. Applied and Environmental Microbiology, 58(11), 3744-3750.

Venter, J. C., Remington, K., Heidelberg, J. F., Halpern, A. L., Rusch, D., Eisen, J. A., et al. (2004). Environmental genome shotgun sequencing of the Sargasso Sea. Science, 304(5667), 66-74. doi:10.1126/science.1093857

Walsh, D. A., Zaikova, E., Hallam, S. J. (2009). Large volume (20L+) filtration of coastal seawater samples. JoVE (Journal of Visualized Experiments)(28), e1161-e1161.

Wright, J. J., Konwar, K. M., Hallam, S. J. (2012). Microbial ecology of expanding oxygen minimum zones. Nature Reviews Microbiology, 10(6), 381-394. doi:10.1038/nrmicro2778

Wright, J. J., Mewis, K., Hanson, N. W., Konwar, K. M., Maas, K. R., Hallam, S. J. (2014). Genomic properties of Marine Group A bacteria indicate a role in the marine sulfur cycle. Isme Journal, 8(2), 455-468. doi:10.1038/ismej.2013.152

CHAPTER 3.

NC10 BACTERIA IN MARINE OXYGEN MINIMUM ZONES

Disclaimer: This chapter was published in a shortened version with the same title, along with the supplementary material in Appendix C, in the journal ISME J on August 10, 2016.

Citation: **Padilla, C. C., Bristow L.A., Sarode, N., Garcia-Robledo, E., Benson, C.R., Bourbonnais, A., Altabet, M.A., Girguis, P.R., Thamdrup, B., Stewart, F. J.** (2016). NC10 bacteria in marine oxygen minimum zones. *ISME J*, *8*, 2067-71.

3.1 Abstract

Oceanic oxygen minimum zones (OMZs) accumulate large amounts of methane, but their role in the marine methane cycle is poorly explored (Sansone et al., 2001; Naqvi et al., 2010). Aerobic methanotrophy was previously the only known pelagic marine sink for this greenhouse gas, but anaerobic microbial metabolism coupling methane oxidation to denitrification of nitrite (Ettwig et al., 2010) could potentially consume methane in the anoxic, nitrite-rich core of OMZs (Thamdrup et al., 2012). This process, nitrite-dependent anaerobic methane oxidation (n-damo), performed by bacteria of the NC10 phylum, involves nitrite reduction to nitric oxide (NO), followed by dismutation of NO to N_2 and O_2, with the O_2 used in intra-aerobic methanotrophy (Ettwig et al., 2010). Here we show that n-damo bacteria are present and active in OMZs, including a coastal OMZ in Costa Rica and the world's largest OMZ in the Eastern Tropical North Pacific. Particulate methane monooxygenase genes from anoxic depths clustered phylogenetically with those of NC10 bacteria, and NC10 16S rRNA genes and transcripts were detected at all sites, with highest abundances near the nitrite maxima. Metatranscriptomics confirmed transcription of mRNA with top matches to the methane-oxidizing NC10 bacterium '*Candidatus* Methylomirabilis oxyfera'. 'M. oxyfera'-like transcripts peaked within the OMZ and included genes of aerobic methanotrophy and denitrification, with high representation by sequences sharing the unique motif structure of 'M. oxyfera' nitric oxide reductase, hypothesized to participate in O_2-yielding NO dismutation. Anoxic incubations with ^{13}C-labeled methane showed methane oxidation at 2.6 nM d^{-1} at the zone of peak NC10 abundance off Costa Rica. Anaerobic methane oxidation was below our detection limit in other samples, but may nonetheless contribute substantially to OMZ

methane budgets, as estimated from NC10 abundances and cell-specific rates. These findings suggest NC10 bacteria as players in the cycling of methane, nitrogen and oxygen in OMZs. Transcripts from methanogens also peaked within OMZ waters, further suggesting an OMZ methane cycle coupled to a previously overlooked pathway of N_2 production.

3.2 Introduction

Microbes play critical roles in consuming the greenhouse gas methane (CH_4). Aerobic methane oxidation by methanotrophic bacteria accounts for the majority of biological methane removal, primarily in soils and oxic water columns (Reeburgh, 2007; Kirschke et al., 2013). Microbial anaerobic oxidation of methane (AOM) also accounts for a substantial fraction of methane consumption. In marine sediments, this process is catalyzed primarily by Archaea linking reverse methanogenesis to the reduction of sulfate (Boetius et al., 2000). Studies of sulfate-depleted freshwater habitats reveal that AOM can also be coupled to the reduction of oxidized nitrogen compounds, including nitrate or nitrite (Raghoebarsing et al., 2006; Haroon et al., 2013; Nordi et al., 2014). Nitrite-reducing bacteria of the NC10 phylum have been shown to couple methane oxidation to N_2 production through a unique nitrite-dependent anaerobic methane oxidation (n-damo) pathway (Ettwig et al., 2010; Raghoebarsing et al., 2006; Ettwig et al., 2009). In this pathway, characterized in the bacterium *Candidatus* Methylomirabilis oxyfera enriched from freshwater sediments (Ettwig et al., 2010), nitrite is reduced to nitric oxide (NO), which is then dismutated into N_2 and O_2 gas. O_2 then serves as the primary oxidant for an

intra-aerobic methanotrophic metabolism, with initial CH_4 oxidation by particulate methane monooxygenase (pMMO) (Ettwig et al., 2010). The enzymatic basis of the NO-dismutation step remains unclear, although proteins resembling nitric oxide reductases may be involved (Ettwig et al., 2012).

While the discovery of n-damo reveals a direct link between methane metabolism and the loss of fixed nitrogen via denitrification, the ecological significance of this process remains unconstrained. For example, it is unknown if n-damo operates in the major zones of ocean nitrogen loss, notably in the large marine oxygen minimum zones associated with nutrient upwelling. Characterizing the distribution of n-damo in the marine environment is critical for constraining local and global carbon and nitrogen budgets and for predictive models of climate change, as CH_4 is one of the greatest contributors to radiative forcing among long-lived greenhouse gases (Stocker et al., 2013) and marine zones of nitrogen loss are predicted to expand with climate change (Stramma et al., 2008).

To date, biogeochemical evidence for nitrite or nitrate-dependent AOM stems primarily from experimental microcosms or bioreactors seeded with freshwater sludge or sediments (Raghoebarsing et al., 2006; Haroon et al., 2013; Deutzmann et al., 2011). In comparison, genes encoding 16S rRNA or the pMMO enzyme of NC10 bacteria have been detected in diverse anoxic freshwater habitats, including peatlands, rice paddies, and river and lake sediments (Shen et al., 2015, Deutzmann et al., 2014). Recently, NC10-like bacteria were also detected in and enriched from a marine habitat, the nitrite-rich sediments of the South China Sea (Chen et al., 2015; He et al., 2015). N-damo in marine sediments may be a relatively minor process, because methane is consumed by sulfate-

dependent AOM in the subsurface, while nitrate and nitrite are only available near the sediment-water interface (Thamdrup, 2012). However, the potential for n-damo in diverse marine environments remains untested.

In the pelagic ocean, nitrite-dependent n-damo may be favored under the environmental conditions commonly associated with OMZs. In the major upwelling regions of the Arabian Sea and the Eastern Tropical North and South Pacific (ETNP, ETSP), microbial respiration depletes oxygen content at the OMZ core to near anoxia (<10 nM) (Thamdrup et al., 2012; Tiano et al., 2014). Anaerobic microbial processes dominate the OMZ layer, and N_2 production by OMZ bacteria, predominantly through the processes of heterotrophic denitrification and nitrite-dependent anaerobic ammonium oxidation (anammox), contributes up to half of all oceanic nitrogen loss (Codispoti et al., 2001; Gruber, 2004). These processes shape water column chemistry. The reduction of nitrate to nitrite by denitrifiers creates a zone of nitrite accumulation in the OMZ, to levels (1-10 μM) orders of magnitude higher than in oxic layers (Thamdrup et al., 2012). The core of OMZs is further characterized by elevated methane concentrations (Sansone et al., 2001; Naqvi et al., 2010; Sansome et al., 2004). N-damo in OMZs has been hinted at by the presence of NC10-related protein-coding genes in OMZ meta-omic datasets (Ganesh et al., 2015; Dalsgaard et al., 2014), although confirmation of a pelagic niche for these bacteria is lacking. OMZ n-damo would be of potential importance as an alternative route to N_2 loss and in controlling the ocean CH_4 pool, notably as OMZs represent the largest accumulation of open ocean CH_4 in the world (Sansone et al., 2001).

Here, we test the hypothesis that the nitrite-replete waters of OMZs constitute a previously unrecognized niche for denitrification-dependent AOM bacteria. Seawater

samples for molecular and biochemical analyses were collected from sites spanning a nearshore to offshore transition through the ETNP OMZ off Manzanillo, Mexico (May 2014) and in the anoxic, coastal basin of Golfo Dulce (GD), Costa Rica (Dalsgaard et al., 2003) (January 2015) (Extended Data Fig. 1 and Table 1). At both sites, oxygen concentrations decreased by four orders of magnitude from surface levels (~200 μM) to below the detection limit of 20 nM inside the anoxic OMZ core. In the ETNP, the upper boundary of the anoxic core ranged from 70-130 m across sites, shoaling with proximity to land (Fig. 1), with oxygen staying near or below detection until ~800 m depth. Characteristic to anoxic oceanic OMZs, nitrite concentration in the ETNP increased upon depletion of oxygen to a prominent maximum (4-5 μM) within the upper anoxic zone (120-150 m), before declining gradually with depth. In the GD, oxygen was below detection from ~85 m to the seafloor (~200 m) and nitrite also accumulated below the oxic/anoxic interface, peaking at 0.7 μM at 100 m in the anoxic zone and disappearing at 140 m (Fig. 1). This disappearance marked the interface to a sulfidic zone with hydrogen sulfide and ammonium accumulating at 190 m to 6.6 μM and 3.4 μM, respectively.

3.3 Materials and Methods

3.3.1 Sample collection

Samples were collected from four stations (6,8,10,11) in the ETNP OMZ during the Oxygen Minimum Zone Microbial Biogeochemistry Expedition 2 (OMZoMBiE2) cruise (*R/V New Horizon*; cruise NH1410; May 10-June 8, 2014; Figure C.1) and at station #1 in the coastal OMZ of Golfo Dulce (GD) in late January 2015. Molecular data

(metatranscriptome and 16S rRNA amplicon sequences) from samples collected at ETNP stations 6 and 10 in June 2013 are also included in this study; subsets of the 2013 datasets have been published in a prior study (Ganesh et al., 2015). In the ETNP, seawater from discrete depths spanning the oxic zone, lower oxycline, upper OMZ, and OMZ core was collected using Niskin bottles on a rosette or a pump profiling system (PPS; upper 400m only) alongside a Conductivity-Temperature-Depth profiler (Sea-Bird SBE 911plus or Sea-Bird 25 on the PPS) equipped with a Seapoint fluorometer and SBE43 dissolved oxygen sensor. In the GD, samples were collected from discrete depths using a hand-deployed Niskin bottle and dissolved oxygen profiles were measured with a Clark type O_2 electrode (Revsbech, 1989) mounted on a CTD (Sea Sun Technology)

Microbial biomass was collected for RNA analysis by sequential in-line filtration of seawater (~2-4 L) through a glass fiber disc pre-filter (GF/A, 47 mm, 1.6 µm pore-size, Whatman) and a primary collection filter (Sterivex™, 0.22 µm pore-size, Millipore) using a peristaltic pump. Sterivex filters were filled with RNA stabilizing buffer (25 mM Sodium Citrate, 10 mM EDTA, 5.3M Ammonium sulfate, pH 5.2), flash-frozen in liquid nitrogen, and stored at -80°C. Less than 20 min elapsed between sample collection (water on deck) and fixation in buffer. Replicate Sterivex filters for DNA analysis were collected from equivalent water volumes following RNA collection, but were instead filled with lysis buffer (50 mM Tris-HCl, 40 mM EDTA, 0.73 M Sucrose) before freezing.

3.3.2 Oxygen concentrations

In addition to the CTD-mounted SBE43 sensor used in the ETNP and Clark type O_2 electrode used in the GD, a high-resolution Switchable Trace amount OXygen (STOX) sensor was used to measure oxygen concentration at nanomolar levels within both the ETNP and GD OMZs. The STOX sensor was connected to an *in situ* unit (Unisense A/S) and the data acquisition was performed as described by Revsbech et al., 2011. The calibration of the STOX was done using paired values of the SBE sensor or Clark type O_2 electrode and STOX at relatively high oxygen concentrations for the STOX sensor but lower than the maximum values for the *in situ* STOX unit. Changes in sensitivity due to temperature changes were compensated for as described by Tiano et al., 2014. Oxygen concentrations were analyzed during the upcasts, when both SBE and STOX sensors are more stable and the release of oxygen from polymers in the instruments should be minimized.

3.3.3 Nitrite concentrations

Samples for measuring nitrite concentration were collected in acid-washed HDPE bottles and either analyzed within 6 hours of collection (GD) or frozen until analysis (ETNP). Concentrations were determined spectrophotometrically using the Griess method, with a Westco SmartChem 200 (Unity Scientific) or Turner Trilogy (Turner Designs).

3.3.4 Methane quantification

Sample preparation: 20 ml (50 ml in the GD) borosilicate glass crimp top vials (Supelco) were flushed with at least three volumes of sample water. Once filled, 5 ml of sample was carefully withdrawn with a syringe. Then, 2 ml of 1N HCl (or 750 µl of 6N HCl in the case of the 50 ml vials) were added as preservative, and vials were sealed with 1 cm thick blue butyl rubber stoppers and aluminum crimp caps. Blanks were collected in the same manner, except deionized water from the shipboard MilliQ system was used in lieu of seawater. Samples were collected in duplicate from each sampling depth. Post-collection, all samples were stored at room temperature.

Quantification: For quantification, all vials were heated upside down (to prevent gas from escaping the stopper) in a dry sand bath to 99°C. The headspace of each vial was then recovered using a 20 gauge needle connected via PEEK tubing to a vacuum-purged 10 ml autosampler vial (Agilent). A glass gastight syringe with a second 20 gauge needle was filled with 0.2 µm-filter-sterilized and degassed seawater, and used to displace the remaining gas from the original sample vial into the autosampler vial. The methane samples were run on an Agilent 7890A Gas Chromatograph (GC) fitted with an Agilent 25 m x 320 µm x 30 µm Molsieve 5A column (part #CP7536) and coupled to an Agilent 5975C Mass Spectrometer Detector (MSD) modified by the manufacturer for enhanced analyses of lower mass compounds. An Agilent 7697A headspace (HS) sampler was used to deliver gas from the 10 ml vials into the GC-MSD. Each sample was quantified as follows: 1) each sample vial was equilibrated in the HS to 80°C for 1.5 minutes, and then pressurized in the HS to 103 Kpa (15 psi) with ultra-high purity helium, 2) headspace gas was transferred to a 1 mL loop kept at 105°C using the default loop fill mode, 3) the sample in the loop was injected into the GC over 0.5 min through a

transfer line kept at 110 °C, 4) the sample entered the GC injector kept at 100 °C in split 1:1 mode, and then was sent through the Molsieve column at a constant rate of 1 ml min^{-1}, 5) the oven was kept at 35 °C for 10 min and then ramped to 325°C at 60°C min^{-1}, 6) the sample was ionized by electron impact at 70 eV via the MSD source kept at 300 °C, and 7) the ion intensity at m/z 15 (100 ms dwelling time) and m/z 16 (500 ms dwelling time) was acquired using the Selective Ion Mode and an electron amplifier gain of 20 to enhance sensitivity. Post-run, the m/z 16 peak was integrated using Agilent Chemstation™ Software and used for quantification. Calibration curves for each run were calculated using a series of samples prepared every 2-3 days using the following method: 10 mL headspace vials were filled with 5 mL of NaCl solution (3.5 mg/L in deionized water) and crimp-capped. Pure methane or methane dilutions were added to a series of vials to prepare the calibration series. In some cases, methane dilutions were prepared volumetrically in Helium purged serum vials (Chemglass Inc). The calibration samples were allowed to equilibrate for 10 min after vigorous shaking before analysis with the GC-MSD.

3.3.4 RNA/DNA extraction

RNA was extracted from Sterivex filters using a modification of the *mir*Vana™ miRNA Isolation kit (Ambion). Filters were thawed on ice, and RNA stabilizing buffer was expelled via syringe from Sterivex cartridges and discarded. Cells were lysed by adding Lysis buffer and miRNA Homogenate Additive (Ambion) directly to the cartridge. Following vortexing and incubation on ice, lysates were transferred to

RNAase-free tubes and processed via acid-phenol:chloroform extraction according to the kit protocol. The TURBO DNA-free™ kit (Ambion) was used to remove DNA, and the extract was purified using the RNeasy MinElute Cleanup Kit (Qiagen).

DNA was extracted from Sterivex filters using a phenol:chloroform protocol. Cells were lysed by adding lysozyme (2 mg in 40 µl of lysis buffer per filter) directly to the Sterivex cartridge, sealing the caps/ends, and incubating for 45 min at 37°C. Proteinase K (1 mg in 100 µl lysis buffer, with 100 µl 20% SDS) was added, and cartridges were resealed and incubated for 2 hours at 55°C. The lysate was removed, and DNA was extracted once with Phenol:Chloroform:Isoamyl Alcohol (25:24:1) and once with Chloroform:Isoamyl Alcohol (24:1) and then concentrated by spin dialysis using Ultra-4 (100 kDa, Amicon) centrifugal filters.

3.3.5 16S gene quantitative PCR

Quantitative PCR (qPCR) was used to count total bacteria and NC10-like 16S rRNA gene copies in DNA extracted from Sterivex filters. Total 16S counts were obtained using SYBR® Green-based qPCR and universal bacterial 16S primers 1055f and 1392r, as in Ganesh et al., 2015. Ten-fold serial dilutions of DNA from a plasmid carrying a single copy of the 16S rRNA gene (from *Dehalococcoides mccartyi*) were included on each qPCR plate and used to generate standard curves, with a detection limit of ~6 gene copies ml^{-1}. Assays were run on a 7500 Fast PCR System and a StepOnePlus™ Real-Time PCR System (Applied Biosystems). All samples were run in triplicate (20 µL each) and included 1X SYBR® Green Supermix (BIO-RAD), 300 nM of

primers, and 2 μL of template DNA (diluted 1:100). Thermal cycling involved: incubation at 50°C for 2 min to activate uracil-N-glycosylase (UNG), followed by 95 °C for 10 min to inactivate UNG, denature template DNA, and activate the polymerase, followed by 40 cycles of denaturation at 95°C (15 sec) and annealing at 60°C (1 min).

Counts of NC10-like 16S rRNA genes followed the protocol of Ettwig et al., 2009. Prior, to qPCR, DNA from the OMZ core at station 6 in the ETNP was screened using primers qP1F and qP2R, designed based on known NC10 sequences from freshwater habitats and flanking an ~200 bp region of the 16S rRNA gene, under the following thermal cycler conditions: initial melting for 3 min at 94°C, followed by 25 cycles of denaturation at 92°C for 1 min, annealing at 55 °C for 1.5 min, and elongation at 72°C for 1.5 min, with a final elongation step at 72°C for 10 min. Amplicons of the expected product size were detected via gel electrophoresis, purified, and cloned using the TOPO TA cloning kit (Life Technologies) according to manufacturer instructions. Sanger sequencing of a subset of clones revealed consistent sequences with top BLASTN matches to environmental NC10 clones in the GenBank database. DNA from these clones was used as template for generating standard curves for qPCR screens of all samples. NC10-specific 16S rRNA gene counts were obtained using SYBR® Green-based qPCR and primers qP1F and qP2R, as in Ettwig et al., 2009. Assays were run on a 7500 Fast PCR System and a StepOnePlus™ Real-Time PCR System (Applied Biosystems). All samples were run in triplicate (20 μL each) and included 1X SYBR® Green Supermix (BIO-RAD), 300 nM of primers, and 2 μL of template DNA. Thermal cycling involved an initial denaturing step of 95°C for 3 min followed by 40 cycles of

95°C for 1 min, 63°C for 1 min, and 72°C for 1 min. After a final extension for 5 min at 72°C, melting curve analysis was carried out at temperatures from 60°C to 95°C.

3.3.6 pmoA PCR, cloning, sequencing, and phylogenetic analysis

The *pmoA* gene encoding subunit A of particulate methane monooxygenase has been used extensively for phylogenetic characterization of methanotrophs. To confirm the presence of and to describe the diversity of the OMZ NC10-like community, *pmoA* was PCR-amplified from a subset of samples, cloned and sequenced, and used for phylogenetic analysis. PmoA genes were amplified using nested PCR. The first round of PCR used the primers A189b and cmo682 targeting anaerobic methanotroph *pmoA,* and was followed by a second PCR with primers cmo182 and cmo568 (see Luesken et al., 2011 for primer sequences). Thermal cycler conditions for both rounds of amplification were: 4 min at 94°C, followed by 35 cycles of denaturation at 94°C for 1 min, annealing at 52 °C for 1 min, and elongation at 72°C for 1.5 min, with a final elongation step at 72°C for 10 min. All PCR reactions were run with 45 µL Platinum® PCR SuperMix (Life Technologies), 1 µL of 10 µM forward primer, 1 µL of 10 µM reverse primer, 1 µL DNA template, and 2 µL sterile nuclease-free water. PCR products were visualized on agarose gels to confirm the expected size range, and then purified and concentrated using the QIAquick PCR purification kit (Qiagen).

Clone libraries of *pmoA* amplicons were constructed using the TOPO TA cloning kit (Life Technologies). Purified PCR products were inserted into the pCR 2.1 TOPO Vector and transformed into One Shot TOP10 chemically competent *E. coli* cells. Cells

were grown overnight at 37°C on LB plates containing 50 μg/mL ampicillin and spread with 40 μL of 50 mg/ml X-gaL. White colonies were selected and grown overnight in LB broth at 37°C. Plasmids were then extracted from cultured cells using the PureLink Quick Plasmid Miniprep Kit (Life Technologies). PCR with M13 Forward and M13 Reverse primers was used to confirm the presence and correct length of inserts. Inserts were then purified using the QIAquick PCR Purification kit and sent to the Georgia Genomics Facility for Sanger sequencing on an Applied Biosystems 3730xl DNA Analyzer using BigDye Terminator v3.1 cycle sequencing (Life Technologies).

The recovered *pmoA* nucleotide sequences were aligned (clustalW), revealing 3 unique sequence variants out of 26 total clones analyzed from the ETNP, and 1 unique phylotype out of 2 clones analyzed from the GD. Representatives of each variant were aligned using the software MEGA6 (Tamura et al., 2013) with environmental NC10-like *pmoA* sequences from Genbank, *pmoA* from the sequenced 'Ca. M. oxyfera genome, *pmoA* sequences from known aerobic methanotrophs, and Thaumarchaeota ammonia monooxygenase (*amoA*) sequences (outgroup). Aligned nucleotides were trimmed to the maximum possible length spanning all sequences, translated into amino acids in MEGA (standard genetic code), yielding a final alignment of 88 sites and 53 unique sequences – GenBank Accession numbers of database sequences are provided in Extended Data Fig. 3. Aligned amino acids were used for phylogenetic reconstruction via maximum likelihood (ML) and neighbor-joining (NJ) methods using the Dayoff model bootstrapped at 1000 replicates, with uniform rates and complete deletion. Both ML and NJ methods resulted in nearly identical topologies. Only ML results are shown.

3.3.7 Transcriptome sequencing and analysis

Community cDNA sequencing was used to characterize microbial gene transcription in biomass (Sterivex filter fraction) from a subset of OMZ samples. From the ETNP, these included 2014 samples (n=5) from the lower oxycline (75 m) and OMZ core (300 m) at station 6, and the upper OMZ (100 m, secondary chlorophyll maximum), nitrite maximum (150 m), and OMZ core at station 10. These data were analyzed along with five station 6 datasets generated previously as in Ganesh et al., 2015; 2013 datasets were collected on June 19th, 2013 and spanned the upper oxycline (30 m), lower oxycline (85 m), oxic-nitrite interface (91 m), secondary chlorophyll maximum (100 m), secondary nitrite maximum OMZ (125 m), and OMZ core (300 m) at station 6. From the GD, metatranscriptomes were generated from the Sterivex filter fraction of samples from 90, 100, and 120 m within the anoxic zone.

Community RNA was prepared for sequencing using the ScriptSeq^{TM} v2 RNA-Seq Library preparation kit (Epicentre). cDNA was synthesized from fragmented total RNA (rRNA was not removed) using reverse transcriptase and amplified and barcoded using ScriptSeq™ Index PCR Primers (Epicenter) to generate single-indexed cDNA libraries. cDNA libraries were pooled and sequenced on an Illumina MiSeq using a 500 cycle kit. Sequence counts are listed in Extended Data Table 3.

Analysis of transcripts followed that of Ganesh et al., 2015. Barcoded sequences were de-multiplexed and low quality reads (Phred score < 25) were removed. Paired-end sequences were merged using custom scripts incorporating the FASTX toolkit (http://hannonlab.cshl.edu/fastx_toolkit/index.html) and USEARCH algorithm, with

criteria of minimum 10% overlap and 95% nucleotide identity within the overlapping region. rRNA transcripts were identified with riboPicker (Schmieder et al., 2012) (and taxonomically classified using open reference picking in the software pipeline QIIME v1.8.0 (Caporaso et al., 2010) according to standard protocols. Merged non-rRNA sequences were queried via BLASTX against the NCBI-nr database (November 2013). To assess the representation and expressed gene content of NC10-like bacteria, transcripts with top matches to genes of *Candidatus* Methylomirabilis oxyfera were parsed with custom scripts, with representation expressed as a percentage of the total number of sequences with BLASTX matches (>bit score 50) to NCBI-nr genes (Fig. 3.3A). In addition, an 'M. oxyfera'-like transcript pool was identified using the lowest common ancestor (LCA) criteria in MEtaGenome ANalyzer 5 (MEGAN5; Huson et al., 2011), according to the NCBI taxonomy. We present both top match and LCA results, as the LCA approach may underestimate the relative abundance of taxonomic groups with limited representation in sequence databases. The NC10 phylum is represented in nr by a single genome (*Ca*. M. oxyfera). Using the LCA approach, slowly-evolving (conserved) genes with top matches to 'M. oxyfera' may match genes of other taxa at only marginally lower bit scores and therefore potentially be classified only to "Bacteria". In a separate analysis, recruitment of OMZ transcripts to 'M. oxyfera' was evaluated by BLASTX against the protein-coding portion of the genome. Protein-coding transcripts with top matches to known methanogen-containing archaeal lineages also were determined using MEGAN5 based on annotations of BLASTX-identified genes.

3.3.8 Assembly and phylogenetic analysis of qNor transcripts

For each metatranscriptome (n = 13), non-rRNA reads with top matches (bit score > 50) to 'M. oxyfera' via BLASTX against NCBI nr were assembled using the de novo assembler in CLC Genomics workbench 8 (http://www.clcbio.com), with a minimum contig length cutoff of 500 bp. Eight of 13 assemblies yielded contigs > 500 bp (n = 33 total). Protein-coding genes on these contigs were identified by BLASTX against NCBI nr. The search identified two full-length genes (from samples 2014 ETNP Stn10 150 m and 2013 ETNP Stn6 300 m) with matches to 'M. oxyfera' nitric oxide reductases (NOR). The corresponding amino acid sequences were aligned with NOR sequences from Ettwig et al., 2012 via Multiple Alignment using Fast Fourier Transform (MAFFT). The alignment was trimmed manually and visually inspected for substitutions in quinol binding and catalytic sites. The trimmed alignment, of 15 sequences spanning 520 aa, was used for phylogenetic analysis in MEGA6 by the Maximum Likelihood (ML) criterion. ML heuristic searches used the Le and Gascuel substitution model with a discrete Gamma distribution to model rate differences among sites and initial tree(s) obtained by Neighbor-Joining based on pairwise distances estimated using a JTT model [model selection was done using the best-fit model selection tool in MEGA6]. The tree with the highest log likelihood, along with clade bootstrap values (1000 replicates), is shown in figure C.5.

3.3.9 16S rRNA gene amplicon analysis

We used 16S rRNA gene amplicon sequencing of 2013 ETNP and 2015 GD samples to explore the distribution of methanogens in the OMZ (Figure C.6) (Amplicon

samples from other ETNP sites were not available at the time of sequencing). ETNP data from station 6 were reported in Ganesh et al., 2015; station 10 data have not been reported previously. GD data were generated in this study. Briefly, amplicons were synthesized using Platinum® PCR SuperMix (Life Technologies) with primers F515 and R806, encompassing the V4 region of the 16S rRNA gene (Caporaso et al., 2011). These primers are used primarily for bacterial 16S rRNA genes analysis, but also amplify archaeal sequences. Both forward and reverse primers were barcoded and appended with Illumina-specific adapters. Thermal cycling involved: denaturation at 94°C (3 min), followed by 30 cycles of denaturation at 94°C (45 sec), primer annealing at 55°C (45 sec) and primer extension at 72°C (90 sec), followed by extension at 72°C for 10 min. Amplicons were analyzed by gel electrophoresis to verify size (~400 bp) and purified using RapidTip2 PCR purification tips (Diffinity Genomics). Amplicons from different samples were pooled at equimolar concentrations and sequenced on an Illumina MiSeq using a 500 cycle kit with 5% PhiX as a control.

Demultiplexed amplicon read pairs were quality trimmed with Trim Galore (Babraham Bioinformatics), using a base Phred33 score threshold of Q25 and a minimum length cutoff of 100bp. High quality paired reads were then merged using the software FLASH. These pre-processed merged reads were then analyzed using the software pipeline QIIME v1.8.0[43], according to standard protocols. Briefly, reads were first screened for chimeras using QIIME's identify_chimeric_seqs.py script with Usearch61. Non-chimeric sequences were clustered into Operational Taxonomic Units (OTUs) at 97% sequence similarity using open-reference OTU picking protocol with the script

pick_open_reference_otus.py. Taxonomy was assigned to representative OTUs from each cluster using the Greengenes reference database (Aug 2013 release) in QIIME.

3.3.10 Rate measurements

Process rates were determined using stable isotope tracers (^{15}N, ^{13}C) added to incubations of seawater from stations 6, 8, and 10 in the ETNP and station 1 in the GD. All incubations followed procedures to minimize oxygen contamination, as described by De Brabandere et al., 2014. Water for incubations was taken directly from Niskin bottles or the PPS and transferred to 250 ml glass bottles. Bottles were overflowed (three volume equivalents) and sealed without bubbles with deoxygenated butyl rubber stoppers and stored in the dark at *in situ* temperature. Amendments of $^{15}NO_2^-$ + $^{13}CH_4$ and $^{15}NO_2^-$ + $^{13}CH_4$ + acetylene were conducted at all depths and all stations. Each bottle was spiked with ^{15}N-labelled substrate, purged with a helium - carbon dioxide (800 ppm) mixture for approximately 20 minutes, dispensed into 12-ml exetainers (Labco, UK) using a slight overpressure, and immediately capped with deoxygenated lids. Headspaces of 2 ml helium were introduced into each exetainer and flushed twice. After headspace flushing, $^{13}CH_4$ (as gas or saturated water) and acetylene (as saturated water) additions were injected directly into each exetainer through the septum. Final concentrations were 5 µM $^{15}NO_2^-$, 1 µM $^{13}CH_4$, and 200 µM acetylene. For each treatment, duplicate exetainers were preserved with 100 µl of 50% (w/v) $ZnCl_2$ at the start of the incubation, and again at 18 and 36 hours at stations 6 and 8 and 24, 48, 96 and 240 hours at station 10 and station 1 GD.

Production of $^{14}N^{15}N$ and $^{15}N^{15}N$ was determined using a gas-chromatography isotope ratio mass spectrometer (GC-IRMS), as in Dalsgaard et al., 2012. Rates were calculated based on the slope of the linear regression of $^{14}N^{15}N$ and $^{15}N^{15}N$ with time. T-tests were applied to determine if rates were significantly different from zero ($p < 0.05$).

The production of ^{13}C-DIC from $^{13}CH_4$ additions was determined following acidification by GC-IRMS, using the method outlined in Torres et al., 2005. The detection limit of this method was 0.6 nM d^{-1}, based on two times the standard error.

3.4 Results and Discussion

Methane concentrations were elevated in the anoxic zone in both the ETNP and GD. In the ETNP, the highest concentrations, reaching ~26 nM at station 6, were located in a broad maximum at the center of the OMZ, at seawater densities of 26.7 to 27 kg m^{-3}, and decreased with distance from shore, as well as above and below the OMZ (ca 2-8 nM; Figure 3.1). This pattern is in agreement with previous studies in the ETNP, hypothesizing that the CH_4 maximum at the OMZ core, along an isopycnal of 26.8 kg m^{-3}, represents a CH_4 plume advected offshore from organic rich sediments along the central American coast (Sansone et al., 2001; Pack et al., 2015). The methane profile in the GD also suggested a sediment methane source, with concentrations at trace levels above the oxycline and increasing progressively with depth to ~78 nM at 180 m in the sulfidic bottom water. Concentrations were ~6 nM at the GD nitrite maximum (100 m).

PCR-based assays were used to identify and quantify NC10 bacteria. Assays

followed established protocols using primers based on freshwater NC10 isolates and flanking a 200-bp fragment of the 16S rRNA gene (Ettwig et al., 2009). We tested the specificity of these primers using a subset of samples from the OMZ core in the ETNP (300 m, station 6). Cloning and sequencing of PCR products revealed sequences with 97% nucleotide similarity to *Ca.* M. oxyfera and 99% similarity to uncultured wetland NC10 clones. Cloned products were used to generate standards for quantitative PCR counts of NC10 16S rRNA genes. NC10 gene counts were low throughout the two study areas (< 200 copies ml^{-1}) but higher counts were exclusively associated with anoxic depths while NC10 genes were undetectable or near the detection limit (6 copies ml^{-1}) above and below the ETNP OMZ and above the GD OMZ (Figure 3.1). In the ETNP, counts increased with proximity to shore and peaked at ~0.02-0.05% of total 16S RNA gene counts within the OMZ (average: 0.015%). At all stations, maximum counts occurred at 300-400 m, below the OMZ nitrite maximum and at the top of the OMZ methane-enriched layer (Figure 3.1), suggesting that in addition to anoxia, NC10 distributions are linked to methane rather than organic flux from above, in which case counts would be predicted to peak higher in the OMZ core where organotrophic activity is highest (Babbin et al., 2014). The percentage of NC10 counts in the GD was an order of magnitude smaller compared to the ETNP (average: 0.003% of total), peaking at 90 m (0.006%) at the top of the nitrite maximum and methane zone (Figure 3.1).

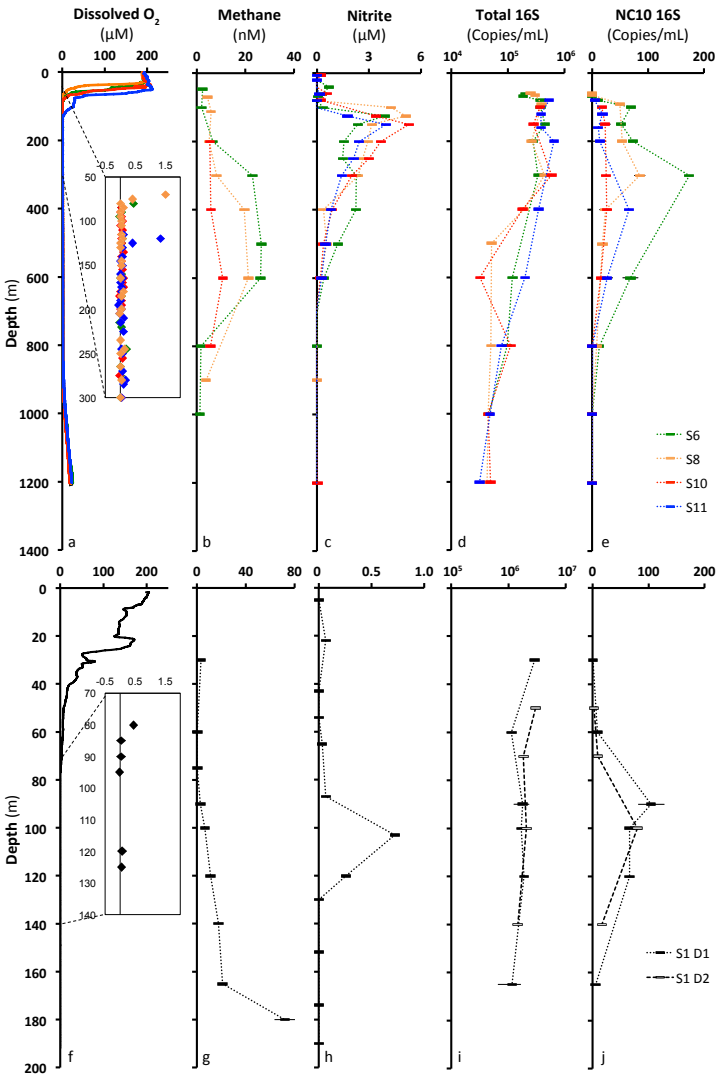

Figure 3.1 Water column chemistry and microbial biomass in the ETNP OMZ in May 2014 (a-e) and GD OMZ in January 2015 (f-j). ETNP stations (colors) span a near shore (S6) to offshore (S11) gradient (Extended Data Fig. 1). **a,f** Dissolved oxygen, based on the SBE43 sensor (a) and Clark type O_2 electrode (f), with an inset showing higher resolution STOX sensor measurements. **b,g,** Methane. **c,h** Nitrite. **d-j,** Total (d,i) and NC10-specific (e,j) 16S rRNA gene counts, based on quantitative PCR analyses of the 0.2-1.6 μm biomass fraction. Connecting lines between data points have been added for clarity and do not indicate values between depths.

The function and diversity of the OMZ NC10 community was further examined by amplification and sequencing a 320-bp fragment of the *pmoA* gene encoding pMMO, which catalyzes the initial CH_4-oxidation step in methanotrophy. Amplification with NC10-specific primers (Luesken et al., 2011) recovered *pmoA* sequences from all OMZ samples within a targeted subset selected from both sites. Phylogenetic analysis of cloned sequences (representing 28 clones: 26 from ETNP, 2 from GD) revealed four closely related phylotypes (3 from ETNP, 1 from GD) related to *pmoA* from NC10 environmental clones and *Ca.* M. oxyfera (Figure 3.2, C.2), with highest similarity (98% amino acid identity) to sequences from anoxic, nitrite-rich sediments of the South China Sea (Chen et al., 2015), suggesting the potential for methane oxidation in OMZ NC10 bacteria and an NC10 lineage specific to ocean waters.

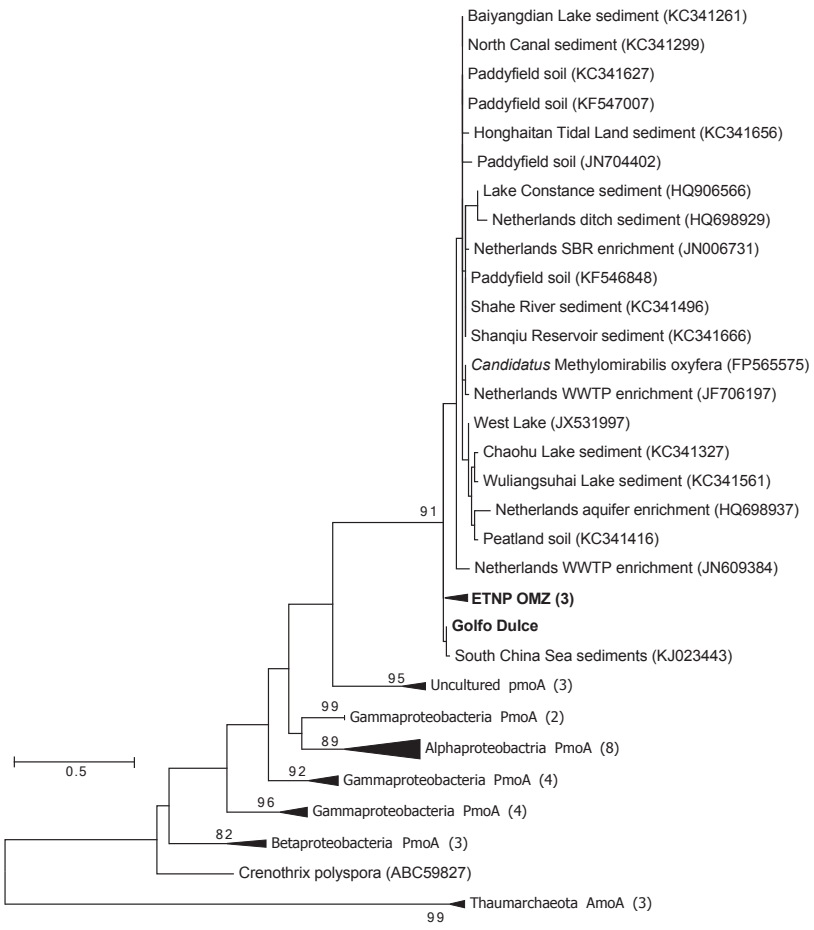

Figure 3.2 Particulate methane monooxygenase subunit A (PmoA) gene phylogeny. PmoA sequences (n=53) recovered from the ETNP and GD are highlighted in bold within the larger clade of NC10-like sequences from other studies, separated from PmoA of aerobic methanotrophic clades and an ammonia monooxygenase (AmoA) outgroup. Reconstruction is based on Maximum Likelihood analysis of 88 amino acids using the Dayhoff substitution model. Bootstrap values greater than 70 are shown, along with NCBI Accession numbers for database sequences. Numbers in parentheses represent the number of unique sequences included in each collapsed node – Taxon identifiers and Accession numbers for all sequences are in Extended Data Fig. 3. The scale bar represents 50 amino-acid changes per 100 amino acids.

Metatranscriptomes confirmed that NC10-like bacteria are metabolically active within OMZs (Figure 3.3). Community RNA from 5 ETNP samples (stations 6 and 10, 2014) and 3 GD samples from upper and core anoxic zone depths was used to create cDNA libraries and shotgun sequenced using Illumina technology. These sequence sets were analyzed along with 5 datasets spanning the oxic zone and OMZ at ETNP station 6 in June 2013; the latter were generated in a prior study using the same methods (Ganesh et al., 2015) and reanalyzed here. The relative abundance of rRNA transcripts classified as NC10 varied widely and increased with decreasing oxygen, peaking at the ETNP core (300 m) and at 90 m in the GD (Figure C.3), consistent with the depths of maximum NC10 16S gene counts (Figure 3.1). The inverse relationship with oxygen was clearest in the 2013 ETNP data, in which *'*M. oxyfera' representation increased from below detection in the oxic zone (30 m) to 0.02% of total rRNA transcripts at the OMZ core (300 m). For all samples, BLASTX against the NCBI non-redundant (nr) protein database identified mRNA transcripts with top matches to the *Ca.* M. oxyfera genome (Figure 3.3A). These trends were supported when BLASTX-identified mRNA transcripts were assigned taxonomy based on a lowest common ancestor (LCA) algorithm (Figure C.4). However, the abundance of 'M. oxyfera'-like transcripts was lower using the LCA approach, likely due to limited representation of NC10 in the nr database, which could prevent accurate assignment of slowly evolving genes. *'*M. oxyfera'-like mRNA transcripts varied widely in relative abundance and, with the exception of the 150 m sample from ETNP station 10, paralleled the distribution of NC10 rRNA transcripts (Fig. 3), increasing with declining oxygen and peaking at ~0.1% of total mRNA transcripts in the ETNP OMZ. Based on top BLAST matches, queries against NCBI-nr identified 210

unique ‘M. oxyfera’ genes across all ETNP samples (range: 2-113 per sample), with an average amino acid identity (AAI) of 66% to matching OMZ transcripts, and 33 genes across GD samples (average AAI: 57%). These AAI values fall within the genome-wide range observed for bacteria categorized in the same genus, although lower values have been observed among strains of the same species (Konstantinidis et al., 2005).

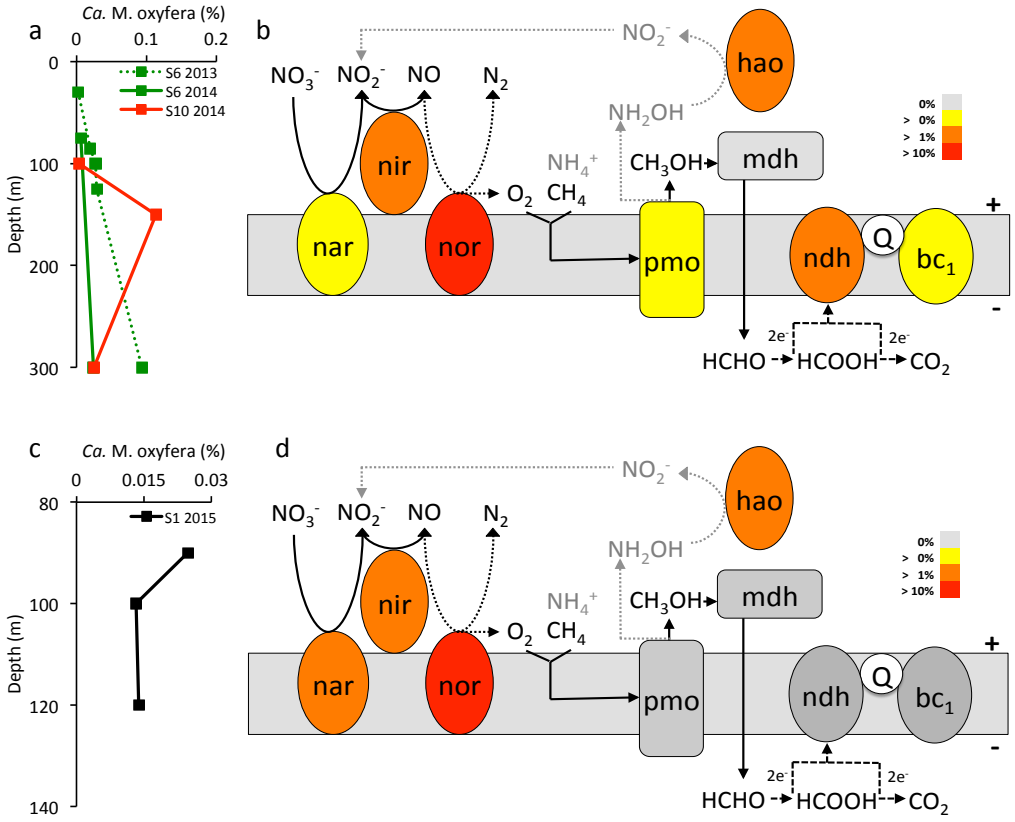

Figure 3.3 Transcription of denitrification-dependent AOM genes in the ETNP (a,b) and GD OMZs (c,d). a,c Abundances of transcripts with top matches (bit score > 50) to *Candidatus* M. oxyfera genes during BLASTX against the NCBI-nr database, as a % of the total number of mRNA transcripts in each sample. **b,d** % abundances of 'M. oxyfera'-like transcripts matching genes of the proposed pathway for denitrification-dependent AOM (diagram modified from (Wu et al., 2011, Wu et al., 2012). Data in **b** and **d** were binned over all samples shown in **a** and **c**, respectively, with abundance colored as a percentage of the total mRNA transcripts matching 'M. oxyfera' genes. nar = nitrate reductase, nir = nitrite reductase, nor = nitric oxide reductase, mdh = methanol dehydrogenase, pmo = particulate methane monooxygenase, bc1 = cytochrome bc1 complex, ndh = NAD(P)H dehydrogenase complex, Q = coenzyme Q, hao = hydroxylamine oxidoreductase. Light gray shows potential non-specific oxidation of ammonium by pmo, followed by detoxification of hydroxylamine to nitrite by hao. Counts reflect matches to all subunits of each enzyme.

Genes with predicted roles in dissimilatory N transformations in NC10 were detected among 'M. oxyfera'-like transcripts assignable by both top match and LCA approaches (Figure 3.3, Figure C.4). These included genes for reduction of nitrate to nitrite (*narGH*), nitrite to NO (*nirS*), and NO to N_2O (*norZ*). Two *norZ* genes, encoding quinol-dependent nitric-oxide reductases (qNor), were the most abundant sequences, together representing 45% of all transcripts with top matches to 'M. oxyfera' and 51% of transcripts assignable by LCA. For two samples (ETNP station 6, 300 m (2013) and station 10, 150 m (2014)), assemblies of qNor transcript fragments yielded full-length gene sequences. These sequences clustered unambiguously in a clade of unique qNor variants (bootstrap = 100; Figure C.5), including loci DAMO_2434 and 2437 of the 'M. oxyfera' genome. N_2O does not appear as an intermediate during nitrite reduction in 'M. oxyfera' enrichments[3] and it has been hypothesized that the qNor encoded by DAMO_2434 and 2437 functions not as a traditional N_2O-producing NO reductase but instead as a NO dismutase (NOD) to convert two NO molecules to N_2 and O_2 (Ettwig et al., 2012). Indeed, DAMO_2434 and 2437 have substitutions at key residues in both the quinol-binding and catalytic sites (Ettwig et al., 2012). The qNor sequences recovered in the ETNP also lack conservation of the canonical quinol-binding motif and contain catalytic site substitutions identical to those of DAMO_2434 and 2437. The identification of these candidate NODs raises the possibility of nitrite-dependent O_2 production in the OMZ.

The 'M. oxyfera' transcript pool from the ETNP also contned sequences suggestive of methane oxidation by n-damo, including the methane-oxidizing pmo enzyme, although these were at low abundance (<1% of total 'M. oxyfera' reads; Fig. 3) and not detectable via LCA. All detected pMMO transcripts matched 'M. oxyfera' pmo as a top BLASTX

hit; pmo transcripts matching aerobic methanotrophs were not detected. In contrast, 'M. oxyfera'-like pmo was not detected in the GD datasets. Rather, transcripts most similar to both soluble and particulate MMO of putative aerobic methylotrophs were recovered in the upper depths of the GD (90, 100 m), despite anoxic conditions at these depths. The pmo enzyme is related structurally to ammonia monooxygenase and may function non-specifically to oxidize ammonia to toxic hydroxylamine, which in other methanotrophs is then detoxified by hydroxylamine oxidoreductase (*hao*) (Stein et al., 2011). Interestingly, transcripts matching 'M. oxyfera' *hao* were highly represented in both ETNP and GD OMZs (Figure 3.3, Figure C.4), raising the possibility of ammonia oxidation by the resident NC10 population. Other 'M. oxyfera' genes of the predicted n-damo pathway were not identified via queries against NCBI-nr, but were detected by BLASTX directly against the 'M. oxyfera' genome. Many of the identified genes shared high amino acid identity (>65%) to OMZ transcripts, including genes for methanol dehydrogenase (*mdh*) catalyzing the second step of methane oxidation and genes of the Calvin-Benson cycle mediating carbon fixation in NC10 bacteria. Although our analyses do not localize OMZ 'M. oxyfera'-like genes to a contiguous genome, they confirm that key genes for n-damo are present and transcribed in OMZs, indicating that resident NC10 bacteria are metabolically active and likely mediating OMZ N transformations. However, overall low levels of NC10-assigned transcripts involved in methane oxidation raise the question of whether the OMZ NC10 population also utilizes energy substrates other than methane. Alternatively, low representation of specific transcripts may be due to misclassification, which is possible if the OMZ NC10 population is sufficiently divergent from the 'M. oxyfera' reference.

To search for a distinct biogeochemical indication of n-damo activity, we conducted anoxic 10-day incubations of OMZ water with ^{13}C-labeled methane and ^{15}N-labeled nitrite to measure rates of anaerobic methane oxidation and N_2 production. At all analyzed depths in the ETNP (100, 150, and 300 m at station 10), methane oxidation measurements were below the detection limit (0.6 nM d^{-1}; Table 3.1). Rates at two of the three analyzed depths in the GD (100, 120 m) also were below detection. Such low rates are consistent with published rates from the ETNP of typically $\leq$ 0.1 nM d^{-1} (range 7 x 10^{-5} – 1.6 nM d^{-1}; aerobic and anaerobic oxidation not discerned described in Pack et al., 2015) and with the low NC10 16S rRNA gene counts observed at both GD and ETNP sites, which would correspond to rates < 0.02 nM d^{-1} assuming specific rates similar to those determined in enrichment cultures (0.09 – 0.2 fmol CH_4 per 16S rRNA gene copy per day; Ettwig et al., 2009).

Table 3.1 Process rates*, as measured during 10-day anoxic incubations.

Treatment:		$^{15}NO_2^- + {}^{13}CH_4$		$^{15}NO_2^- + {}^{13}CH_4$ + Acetylene	
		$^{15}N\text{-}N_2$ production†	^{13}C-DIC production	$^{15}N\text{-}N_2$ production‡	^{13}C-DIC production
ETNP	100 m	1.1±0.5	<0.6	<0.5	<0.6
	150 m	0.4±0.1	<0.6	<0.5	<0.6
	300m	13.8±1.8	<0.6	<0.5	<0.6
GD	90 m	151.9±39.7	2.6±0.7	7.8±2.3	<0.6
	100 m	192.7±19.8	<0.6	3.7±1.0	<0.6
	120 m	431.9±79.8	<0.6	6.9±0.7	<0.6

*All rates are nM d^{-1}, with errors representing the standard error of the slope of regression of produced $^{15}N\text{-}N_2$ or ^{13}C-DIC as a function of time.

† $^{15}N\text{-}N_2$ production was not partitioned into anammox and denitrification, due to the likely dilution of the labeled nitrite pool as a result of dissimilatory nitrate reduction to nitrite over the 10-day incubation period.

‡ The detected N_2 production rates under acetylene in the GD are likely residual denitrification (Jenson et al., 2007).

In contrast, at 90 m in the GD, the depth of maximum NC10 gene abundance, methane oxidation was measured at 2.6 ± 0.7 nM d^{-1} but was inhibited under identical conditions with the addition of acetylene, an inhibitor of pmo. Although oxygen concentration was not continuously recorded during these incubations, prior analyses indicate that oxygen content stays below 80 nM using our incubation protocol (Ganesh et al., 2015). Together, these results raise the possibility of OMZ methane consumption by pmo-catalyzed AOM, and therefore potentially n-damo. However, the activity of pmo-utilizing aerobic methanotrophs in this study remains unconstrained, but is suggested by the recovery of MMO transcripts from putative aerobic methylotrophs at this depth. Similar co-occurrence of NC10 and aerobic methanotrophs has been documented previously in a lake hypolimnion (Kojima et al., 2014). Although rates of aerobic methane oxidation generally decrease sharply under sub-micromolar oxygen concentrations (Ren et al., 1997; Gerritse et al., 1993; van Bodegom et al., 2001), a contribution of aerobic methanotrophy to the oxidation rates observed in the upper GD cannot be ruled out based on previous studies suggesting aerobic methane oxidation (Tavormina et al., 2010) and/or a combined use of oxygen and nitrate (Kits et al., 2015) can occur in sub-oxic environments.

Given a predicted 4:3 ratio of N_2 production to CH_4 oxidation during n-damo (Ettwig et al., 2010), the low methane oxidation rates observed in most OMZ samples indicate a minor contribution of n-damo to N_2 production in the OMZ compared to denitrification and anammox. Contributions from denitrification and anammox peaked at 0.3 – 2 nM d^{-1} and 1 – 5 nM d^{-1}, respectively, at nearby stations 3 and 7 in the ETNP and 8 nM d^{-1} and 115 nM d^{-1} respectively, at station 1 in the GD (Figure C.1), consistent with previous

measurements from these regions (Ganesh et al., 2015; Dalsgaard et al., 2003; Babbin et al., 2014), with the differences between sites reflecting the coastal and offshore locations. The conversion rates of ^{15}N-labeled nitrite to N_2 in our 10-day methane oxidation assays (0.4 to 13.8 nM d^{-1} for the ETNP, 152 to 432 nM d^{-1} for the GD; Table 3.1) were broadly consistent with these ranges, although the long incubation may have caused a stimulation of activity through bottle effects (Thamdrup et al., 2006). If coupled to oxidative processes other than methane oxidation, NO dismutation could make a larger contribution to N_2 production than suggested by our estimates.

These combined molecular and biogeochemical data identify marine OMZs as an unrecognized niche for NC10 bacteria potentially conducting n-damo. Here, the detection of NC10 in both open-ocean and coastal OMZs suggests that these bacteria are widespread in low oxygen pelagic zones. Prior studies have reported sulfate-dependent ANME archaea in anoxic water columns (Jakobs et al., 2013), and this group may be the dominant AOM community in waters replete with sulfate and devoid of nitrite. However, the unique conditions of nitrite accumulation common in anoxic OMZs may enable n-damo to effectively compete for available methane. Additionally, n-damo may have a competitive advantage over ANME under the low methane concentrations of pelagic OMZs, as the affinity of pMMO for methane is generally orders of magnitude higher than that of methyl-coenzyme M reductase, the methane-activating enzyme of methanotrophic archaea (Baani et al., 2008; Nauhaus et al., 2002; Smith et al., 1991; Ettwig et al., 2008).

Coastal, shelf, or slope sediments may be a source of methane to OMZ waters (Sansone et al., 2001; Pack et al., 2015), but methane could potentially also be generated

internally by OMZ methanogens. In support of this hypothesis, deep sequencing of 16S rRNA gene amplicons generated from 2013 ETNP (stations 6 and 10) and GD samples revealed sequences matching methanogenic Euryarchaeota. These groups were undetectable at oxic depths (30 m), but increased along the transition into the OMZ to peak in relative abundance either at (ETNP) or just below (GD) the nitrite maximum (Figure C.6). Similarly, methanogen rRNA transcripts in ETNP and GD metatranscriptomes increased in relative abundance as oxygen declined, accounting for ~0.01-0.08% of all rRNA transcripts at OMZ depths. Diverse mRNA transcripts with top matches to methanogens also were identified in metatranscriptome datasets (Figure C.6), including transcripts encoding steps of the classical pathway catalyzing CO_2 reduction to methane (Reeve et al., 1997), although total counts of methanogenesis enzyme transcripts were low (<0.003% of mRNA sequences). These results raise the possibility of active methanogens in OMZs and hence an internal anaerobic methane cycle coupled to denitrification.

N_2 production by NC10 bacteria would represent an overlooked third route of nitrogen loss in OMZs, along with classical denitrification and anammox. The latter are undoubtedly the dominant OMZ N sinks, given the low methane oxidation rates observed here and the low NC10 bacterial numbers indicated by qPCR. However, n-damo may substantially affect the oceanic OMZ methane inventory. In the ETNP, for example, at a methane concentration of 20 nM and NC10 16S rRNA gene abundance of 100 copies ml^{-1} as found at the inshore stations (Figure 3.1), and assuming specific rates of 0.09 – 0.2 fmol CH_4 per 16S rRNA gene copy per day (Ettwig et al., 2009), we estimate a turnover time for methane of 2.7 – 6.1 years. This is similar to a recently estimated water age of

3.9 ± 0.8 years for the ETNP OMZ core (DeVries et al., 2012), which indicates that NC10 bacteria may be as important as ventilation for controlling these large open-ocean methane pools. With a much shorter estimated water residence of 35 – 57 days (Ferdelman et al., 2006), the GD OMZ is a more dynamic system, which may explain the coexistence of NC10 bacteria with a large population of [putative] aerobic methanotrophs. Although the relative importance of these two populations to methane oxidation is not clear, the establishment of an NC10 population here emphasizes that n-damo may also be active in other low-oxygen pelagic zones enriched in both methane and nitrogen oxides, including oil spills and seasonal hypoxic zones (deadzones). Additionally, the presence of NC10 in the OMZ raises the possibility for interactions with other metabolic pathways, including competition with anammox for nitrite, or potentially for ammonia if NC10 monooxygenases act nonspecifically. Understanding the diversity and dynamics of coupled chemical cycles in low-oxygen waters is critical, as zones of oxygen loss are predicted to increase in both area and frequency during climate change.

Acknowledgements

We thank the crew of the *R/V New Horizon* for help in sample collection, Niels Peter Revsbech and Morten Larsen for oxygen concentration analysis in the GD, and Alvaro Morales for coordinating and supporting work at the GD field site. This work was supported by the National Science Foundation (1151698 to FJS), the Sloan Foundation (RC944 to FJS), the Danish National Research Foundation DNRF53, the Danish Council of Independent Research, and the European Research Council 'Oxygen' grant (267233; supporting LAB and BT).

3.5 References

Baani, M., Liesack, W. (2008). Two isozymes of particulate methane monooxygenase with different methane oxidation kinetics are found in Methylocystis sp strain SCZ. Proceedings of the National Academy of Sciences of the United States of America, 105(29), 10203-10208. doi:10.1073/pnas.0702643105

Babbin, A. R., Keil, R. G., Devol, A. H., Ward, B. B. (2014). Organic Matter Stoichiometry, Flux, and Oxygen Control Nitrogen Loss in the Ocean. Science, 344(6182), 406-408. doi:10.1126/science.1248364

Boetius, A., Ravenschlag, K., Schubert, C. J., Rickert, D., Widdel, F., Gieseke, A., et al. (2000). A marine microbial consortium apparently mediating anaerobic oxidation of methane. Nature, 407(6804), 623-626. doi:10.1038/35036572

Caporaso, J. G., Kuczynski, J., Stombaugh, J., Bittinger, K., Bushman, F. D., Costello, E. K., et al. (2010). QIIME allows analysis of high-throughput community sequencing data. Nature Methods, 7(5), 335-336. doi:10.1038/nmeth.f.303

Caporaso, J. G., Lauber, C. L., Walters, W. A., Berg-Lyons, D., Lozupone, C. A., Turnbaugh, P. J., et al. (2011). Global patterns of 16S rRNA diversity at a depth of millions of sequences per sample. Proceedings of the National Academy of Sciences of the United States of America, 108, 4516-4522. doi:10.1073/pnas.1000080107

Chen, J., Jiang, X. W., Gu, J. D. (2015). Existence of Novel Phylotypes of Nitrite-Dependent Anaerobic Methane-Oxidizing Bacteria in Surface and Subsurface Sediments of the South China Sea. Geomicrobiology Journal, 32(1), 1-9. doi:10.1080/01490451.2014.917742

Codispoti, L. A., Brandes, J. A., Christensen, J. P., Devol, A. H., Naqvi, S. W. A., Paerl, H. W., Yoshinari, T. (2001). The oceanic fixed nitrogen and nitrous oxide budgets: Moving targets as we enter the anthropocene? Scientia Marina, 65, 85-105.

Dalsgaard, T., Canfield, D. E., Petersen, J., Thamdrup, B., Acuna-Gonzalez, J. (2003). N-2 production by the anammox reaction in the anoxic water column of Golfo Dulce, Costa Rica. Nature, 422(6932), 606-608. doi:10.1038/nature01526

Dalsgaard, T., Stewart, F. J., Thamdrup, B., De Brabandere, L., Revsbech, N. P., Ulloa, O., et al. (2014). Oxygen at Nanomolar Levels Reversibly Suppresses Process Rates and Gene Expression in Anammox and Denitrification in the Oxygen Minimum Zone off Northern Chile. Mbio, 5(6), 14. doi:10.1128/mBio.01966-14

Dalsgaard, T., Thamdrup, B., Farias, L., Revsbech, N. P. (2012). Anammox and denitrification in the oxygen minimum zone of the eastern South Pacific. Limnology and Oceanography, 57(5), 1331-1346. doi:10.4319/lo.2012.57.5.1331

De Brabandere, L., Canfield, D. E., Dalsgaard, T., Friederich, G. E., Revsbech, N. P., Ulloa, O., Thamdrup, B. (2014). Vertical partitioning of nitrogen-loss processes across the oxic-anoxic interface of an oceanic oxygen minimum zone. Environmental Microbiology, 16(10), 3041-3054. doi:10.1111/1462-2920.12255

Deutzmann, J. S., Schink, B. (2011). Anaerobic Oxidation of Methane in Sediments of Lake Constance, an Oligotrophic Freshwater Lake. Applied and Environmental Microbiology, 77(13), 4429-4436. doi:10.1128/aem.00340-11

Deutzmann, J. S., Stief, P., Brandes, J., Schink, B. (2014). Anaerobic methane oxidation coupled to denitrification is the dominant methane sink in a deep lake. Proceedings of the National Academy of Sciences of the United States of America, 111(51), 18273-18278. doi:10.1073/pnas.1411617111

DeVries, T., Deutsch, C., Primeau, F., Chang, B., Devol, A. (2012). Global rates of water-column denitrification derived from nitrogen gas measurements. Nature Geoscience, 5(8), 547-550. doi:10.1038/ngeo1515

Ettwig, K. F., Butler, M. K., Le Paslier, D., Pelletier, E., Mangenot, S., Kuypers, M. M. M., et al. Strous, M. (2010). Nitrite-driven anaerobic methane oxidation by oxygenic bacteria. Nature, 464(7288), 543-+. doi:10.1038/nature08883

Ettwig, K. F., Shima, S., van de Pas-Schoonen, K. T., Kahnt, J., Medema, M. H., op den Camp, H. J. M., et al. (2008). Denitrifying bacteria anaerobically oxidize methane in the absence of Archaea. Environmental Microbiology, 10(11), 3164-3173. doi:10.1111/j.1462-2920.2008.01724.x

Ettwig, K. F., Speth, D. R., Reimann, J., Wu, M. L., Jetten, M. S. M., Keltjens, J. T. (2012). Bacterial oxygen production in the dark. Biochimica Et Biophysica Acta-Bioenergetics, 1817, S155-S155. doi:10.1016/j.bbabio.2012.06.406

Ettwig, K. F., van Alen, T., van de Pas-Schoonen, K. T., Jetten, M. S. M., Strous, M. (2009). Enrichment and Molecular Detection of Denitrifying Methanotrophic Bacteria of the NC10 Phylum. Applied and Environmental Microbiology, 75(11), 3656-3662. doi:10.1128/aem.00067-09

Ferdelman, T. G., Thamdrup, B., Canfield, D. E., Glud, R. N., Kuever, J., Lillebaek, R., et al. (2006). Biogeochemical controls on the oxygen, nitrogen and sulfur distributions in the water column of Golfo Dulce: an anoxic basin on the Pacific coast of Costa Rica revisited. Revista De Biologia Tropical, 54, 171-191.

Ganesh, S., Bristow, L. A., Larsen, M., Sarode, N., Thamdrup, B., Stewart, F. J. (2015). Size-fraction partitioning of community gene transcription and nitrogen metabolism in a marine oxygen minimum zone. ISME J, in Press†

Gerritse, J., Gottschal, J. C. (1993). 2-Membered mixed cultures of methanogenic and aerobic-bacteria in o2-limited chemostats. Journal of General Microbiology, 139, 1853-1860.

Gruber, N., Sarmiento, J. L. (1997). Global patterns of marine nitrogen fixation and denitrification. Global Biogeochemical Cycles, 11(2), 235-266. doi:10.1029/97gb00077

Haroon, M. F., Hu, S. H., Shi, Y., Imelfort, M., Keller, J., Hugenholtz, P., et al. (2013). Anaerobic oxidation of methane coupled to nitrate reduction in a novel archaeal lineage. Nature, 500(7464), 567-+. doi:10.1038/nature12375

He, Z. F., Geng, S., Cai, C. Y., Liu, S., Liu, Y., Pan, Y. W., et al. (2015). Anaerobic Oxidation of Methane Coupled to Nitrite Reduction by Halophilic Marine NC10 Bacteria. Applied and Environmental Microbiology, 81(16), 5538-5545. doi:10.1128/aem.00984-15

Huson, D. H., Mitra, S., Ruscheweyh, H. J., Weber, N., Schuster, S. C. (2011). Integrative analysis of environmental sequences using MEGAN4. Genome Research, 21(9), 1552-1560. doi:10.1101/gr.120618.111

Jakobs, G., Rehder, G., Jost, G., Kiesslich, K., Labrenz, M., Schmale, O. (2013). Comparative studies of pelagic microbial methane oxidation within the redox zones of the Gotland Deep and Landsort Deep (central Baltic Sea). Biogeosciences, 10(12), 7863-7875. doi:10.5194/bg-10-7863-2013

Jensen, M. M., Thamdrup, B., Dalsgaard, T. (2007). Effects of specific inhibitors on anammox and denitrification in marine sediments. Applied and Environmental Microbiology, 73(10), 3151-3158. doi:10.1128/aem.01898-06

Kirschke, S., Bousquet, P., Ciais, P., Saunois, M., Canadell, J. G., Dlugokencky, E. J., et al. (2013). Three decades of global methane sources and sinks. Nature Geoscience, 6(10), 813-823. doi:10.1038/ngeo1955

Kits, K. D., Klotz, M. G., Stein, L. Y. (2015). Methane oxidation coupled to nitrate reduction under hypoxia by the Gammaproteobacterium Methylomonas denitrificans, sp nov type strain FJG1. Environmental Microbiology, 17(9), 3219-3232. doi:10.1111/1462-2920.12772

Kojima, H., Tokizawa, R., Kogure, K., Kobayashi, Y., Itoh, M., Shiah, F. K., et al. (2014). Community structure of planktonic methane-oxidizing bacteria in a subtropical reservoir characterized by dominance of phylotype closely related to nitrite reducer. Scientific Reports, 4. doi:10.1038/srep05728

Konstantinidis, K. T., Tiedje, J. M. (2005). Towards a genome-based taxonomy for prokaryotes. Journal of Bacteriology, 187(18), 6258-6264. doi:10.1128/jb.187.18.6258-6264.2005

Luesken, F. A., Zhu, B. L., van Alen, T. A., Butler, M. K., Diaz, M. R., Song, B., et al. (2011). pmoA Primers for Detection of Anaerobic Methanotrophs. Applied and Environmental Microbiology, 77(11), 3877-3880. doi:10.1128/aem.02960-10

Naqvi, S. W. A., Bange, H. W., Farias, L., Monteiro, P. M. S., Scranton, M. I., Zhang, J. (2010). Marine hypoxia/anoxia as a source of CH4 and N2O. Biogeosciences, 7(7), 2159-2190. doi:10.5194/bg-7-2159-2010

Nauhaus, K., Boetius, A., Kruger, M., Widdel, F. (2002). In vitro demonstration of anaerobic oxidation of methane coupled to sulphate reduction in sediment from a marine gas hydrate area. Environmental Microbiology, 4(5), 296-305. doi:10.1046/j.1462-2920.2002.00299.x

Nordi, K. A., Thamdrup, B. (2014). Nitrate-dependent anaerobic methane oxidation in a freshwater sediment. Geochimica Et Cosmochimica Acta, 132, 141-150. doi:10.1016/j.gca.2014.01.032

Pack, M. A., Heintz, M. B., Reeburgh, W. S., Trumbore, S. E., Valentine, D. L., Xu, X. M., Druffel, E. R. M. (2015). Methane oxidation in the eastern tropical North Pacific Ocean water column. Journal of Geophysical Research-Biogeosciences, 120(6), 1078-1092. doi:10.1002/2014jg002900

Raghoebarsing, A. A., Pol, A., van de Pas-Schoonen, K. T., Smolders, A. J. P., Ettwig, K. F., Rijpstra, W. I. C., et al. (2006). A microbial consortium couples anaerobic methane oxidation to denitrification. Nature, 440(7086), 918-921. doi:10.1038/nature04617

Reeburgh, W. S. (2007). Oceanic methane biogeochemistry. Chemical Reviews, 107(2), 486-513. doi:10.1021/cr050362v

Reeve, J. N., Nolling, J., Morgan, R. M., Smith, D. R. (1997). Methanogenesis: Genes, genomes, and who's on first? Journal of Bacteriology, 179(19), 5975-5986.

Ren, T., Amaral, J. A., Knowles, R. (1997). The response of methane consumption by pure cultures of methanotrophic bacteria to oxygen. Canadian Journal of Microbiology, 43(10), 925-928.

Revsbech, N. P. (1989). An oxygen microsensor with a guard cathode. Limnology and Oceanography, 34(2), 474-478.

Revsbech, N. P., Thamdrup, B., Dalsgaard, T., Canfield, D. E. (2011). Construction of stox oxygen sensors and their application for determination of o-2 concentrations in oxygen minimum zones. In M. G. Klotz (Ed.), Methods in Enzymology: Research on Nitrification and Related Processes, Vol 486, Part A (Vol. 486, pp. 325-341). San Diego: Elsevier Academic Press Inc.

Sansone, F. J., Graham, A. W., Berelson, W. M. (2004). Methane along the western Mexican margin. Limnology and Oceanography, 49(6), 2242-2255.

Sansone, F. J., Popp, B. N., Gasc, A., Graham, A. W., Rust, T. M. (2001). Highly elevated methane in the eastern tropical North Pacific and associated isotopically

enriched fluxes to the atmosphere. Geophysical Research Letters, 28(24), 4567-4570. doi:10.1029/2001gl013460

Schmieder, R., Lim, Y. W., Edwards, R. (2012). Identification and removal of ribosomal RNA sequences from metatranscriptomes. Bioinformatics, 28(3), 433-435. doi:10.1093/bioinformatics/btr669

Shen, L. D., Wu, H. S., Gao, Z. Q. (2015). Distribution and environmental significance of nitrite-dependent anaerobic methane-oxidising bacteria in natural ecosystems. Applied Microbiology and Biotechnology, 99(1), 133-142. doi:10.1007/s00253-014-6200-y

Smith, R. L., Howes, B. L., Garabedian, S. P. (1991). In situ measurement of methane oxidation in groundwater by using natural-gradient tracer tests. Applied and Environmental Microbiology, 57(7), 1997-2004.

Stein, L. Y., Klotz, M. G. (2011). Nitrifying and denitrifying pathways of methanotrophic bacteria. Biochemical Society Transactions, 39, 1826-1831. doi:10.1042/bst20110712

Stocker, T., Qin, D., Plattner, G., Tignor, M., Allen, S., Boschung, J., et al. (2013). IPCC, 2013: climate change 2013: the physical science basis.†Contribution of working group I to the fifth assessment report of the intergovernmental panel on climate change. Retrieved from Cambridge, United Kingdom and New York, NY USA:

Stramma, L., Johnson, G. C., Sprintall, J., Mohrholz, V. (2008). Expanding oxygen-minimum zones in the tropical oceans. Science, 320(5876), 655-658. doi:10.1126/science.1153847

Tamura, K., Stecher, G., Peterson, D., Filipski, A., Kumar, S. (2013). MEGA6: Molecular Evolutionary Genetics Analysis Version 6.0. Molecular Biology and Evolution, 30(12), 2725-2729. doi:10.1093/molbev/mst197

Tavormina, P. L., Ussler, W., Joye, S. B., Harrison, B. K., Orphan, V. J. (2010). Distributions of putative aerobic methanotrophs in diverse pelagic marine environments. Isme Journal, 4(5), 700-710. doi:10.1038/ismej.2009.155

Thamdrup, B. (2012). New Pathways and Processes in the Global Nitrogen Cycle. In D. J. Futuyma (Ed.), Annual Review of Ecology, Evolution, and Systematics, Vol 43 (Vol. 43, pp. 407-428). Palo Alto: Annual Reviews.

Thamdrup, B., Dalsgaard, T., Jensen, M. M., Ulloa, O., Farias, L., Escribano, R. (2006). Anaerobic ammonium oxidation in the oxygen-deficient waters off northern Chile. Limnology and Oceanography, 51(5), 2145-2156.

Thamdrup, B., Dalsgaard, T., Revsbech, N. P. (2012). Widespread functional anoxia in the oxygen minimum zone of the Eastern South Pacific. Deep-Sea Research Part I-Oceanographic Research Papers, 65, 36-45. doi:10.1016/j.dsr.2012.03.001

Tiano, L., Garcia-Robledo, E., Dalsgaard, T., Devol, A. H., Ward, B. B., Ulloa, O., et al. (2014). Oxygen distribution and aerobic respiration in the north and south eastern tropical Pacific oxygen minimum zones. Deep-Sea Research Part I-Oceanographic Research Papers, 94, 173-183. doi:10.1016/j.dsr.2014.10.001

Tiano, L., Garcia-Robledo, E., Revsbech, N. P. (2014). A New Highly Sensitive Method to Assess Respiration Rates and Kinetics of Natural Planktonic Communities by Use of the Switchable Trace Oxygen Sensor and Reduced Oxygen Concentrations. Plos One, 9(8). doi:10.1371/journal.pone.0105399

Torres, M. E., Mix, A. C., Rugh, W. D. (2005). Precise delta C-13 analysis of dissolved inorganic carbon in natural waters using automated headspace sampling and continuous-flow mass spectrometry. Limnology and Oceanography-Methods, 3, 349-360.

Van Bodegom, P., Goudriaan, J., Leffelaar, P. (2001). A mechanistic model on methane oxidation in a rice rhizosphere. Biogeochemistry, 55(2), 145-177. doi:10.1023/a:1010640515283

Wu, M. L., Ettwig, K. F., Jetten, M. S. M., Strous, M., Keltjens, J. T., van Niftrik, L. (2011). A new intra-aerobic metabolism in the nitrite-dependent anaerobic methane-oxidizing bacterium Candidatus 'Methylomirabilis oxyfera'. Biochemical Society Transactions, 39, 243-248. doi:10.1042/bst0390243

Wu, M. L., van Teeseling, M. C. F., Willems, M. J. R., van Donselaar, E. G., Klingl, A., Rachel, R., et al. van Niftrik, L. (2012). Ultrastructure of the Denitrifying Methanotroph "Candidatus Methylomirabilis oxyfera," a Novel Polygon-Shaped Bacterium. Journal of Bacteriology, 194(2), 284-291. doi:10.1128/jb.05816-11

CHAPTER 4.

METAGENOMIC BINNING RECOVERS A TRANSCRIPTIONALLY ACTIVE GAMMAPROTEOBACTERIUM LINKING METHANOTROPHY TO PARTIAL DENITRIFICATION IN AN ANOXIC OXYGEN MINIMUM ZONE

Disclaimer: This chapter was published in a shortened version with the same title, along with the supplementary material in Appendix D, in the journal Frontiers in Marine Science on Feburary 7, 2017.

Citation: **Padilla, C. C., Bertagnolli, A.D., Bristow L.A., Sarode, N., Glass, J.B., Thamdrup, B., Stewart, F. J.** (2017). Metagenomic binning recovers a transcriptionally active Gammaproteobacterium linking methanotrophy to partial denitrification in an anoxic oxygen minimum zone. *Frontiers in Marine Science*, *4*, 23-23.

4.1 Abstract

Diverse planktonic microorganisms play a crucial role in mediating methane flux from the ocean to the atmosphere. The distribution and composition of the marine methanotroph community is determined partly by oxygen availability. The low oxygen conditions of oxygen minimum zones (OMZs) may select for methanotrophs that oxidize methane using inorganic nitrogen compounds (e.g., nitrate, nitrite) in place of oxygen. However, environmental evidence for methane-nitrogen linkages in OMZs remains sparse, as does our knowledge of the genomic content and metabolic capacity of organisms catalyzing OMZ methane oxidation. Here, binning of metagenome sequences from a coastal anoxic OMZ recovered the first near complete (95%) draft genome representing the methanotroph clade OPU3. Phylogenetic reconstruction of concatenated single copy marker genes confirmed the OPU3-like bacterium as a divergent member of the type Ia methanotrophs, with an estimated genome size half that of other sequenced taxa in this group. The proportional abundance of this bacterium peaked at 4% of the total microbial community at the top of the anoxic zone in areas of nitrite and nitrate availability but declining methane concentrations. Genes mediating dissimilatory nitrate and nitrite reduction were identified in the OPU3 genome, and transcribed in conjunction with key enzymes catalyzing methane oxidation to formaldehyde and the ribulose monophosphate (RuMP) pathway for formaldehyde assimilation, suggesting partial denitrification linked to methane oxidation. Together, these data provide the first field-based evidence for methanotrophic partial denitrification by the OPU3 cluster under anoxic conditions, supporting a role for OMZs as key sites in pelagic methane turnover.

4.2 Introduction

Methane (CH_4) is a potent greenhouse gas with 25 times the warming potential per-mol compared to CO_2 (IPCC 2013). The oceans contribute up to 4% of annual global methane emissions (Kirschke et al., 2013), with the sea-to-air flux of methane determined largely by the balance of methane production and consumption by marine microbes. Methane production has been observed under both oxic and anoxic conditions, although the mechanisms of production differ, via either archaeal methanogenesis in sediments (Reeburgh, 2007; Valentine, 2011) or aerobic catabolism of methylated phosphorous-containing compounds (Karl et al., 2008; Damm et al., 2010; Carini et al. 2014). Likewise, the metabolic pathways used to consume methane include both aerobic methanotrophy and anaerobic oxidation of methane (AOM). The latter process is mediated by prokaryotes using alternative oxidants such as sulfate (SO_4^{2-}) (Knittel and Boetius, 2009) or through the putative generation of intracellular oxygen from nitrate (NO_3^-) and nitrite (NO_2^-) (Raghoebarsing et al., 2006; Ettwig et al., 2010). While marine methanotrophy has been studied extensively over the past decades (Reeburgh, 2007; Valentine, 2011), the variables controlling the diversity, distribution, and activity of the dominant pelagic methanotrophs are still not well understood, and genomic data for the diverse members of the marine methanotroph community remains sparse.

Oceanic oxygen minimum zones (OMZs) may be important sites for pelagic methane cycling. OMZs form at mid-water depths where heterotrophic respiration rates exceed the introduction of oxygen (Wyrtki, 1962; Helly and Levin, 2004; Wright et al., 2012). In the major OMZs of the Eastern Pacific, oxygen falls below the detection of modern sensors (Thamdrup et al., 2012; Tiano et al., 2014), creating anoxic conditions

dominated by anaerobic microbial metabolisms (Naqvi et al., 2010; Stewart et al., 2012; Ulloa et al., 2012). Notably, OMZs contribute up to half of oceanic nitrogen loss, primarily through the anaerobic processes of denitrification or anaerobic ammonia oxidation (anammox) (Codispoti et al., 2001; Thamdrup, 2012). OMZs are also the largest pool of pelagic methane in the global ocean (Sansone et al., 2001), and represent potentially important sources of methane to the atmosphere (Naqvi et al., 2010). Methane maxima in OMZs may be due either to advection from nearby sediments (Sansone et al., 2001; Pack et al., 2015) or potentially from internal production by methanogenesis (Padilla et al., 2016), although the latter remains to be verified experimentally. Overlapping zones of elevated methane and oxidized nitrogen concentrations in OMZs suggest a pelagic niche for microbes conducting AOM coupled to reductive nitrogen transformations. With OMZs predicted to expand with increasing seawater temperatures (Stramma et al., 2008; Long et al., 2016), characterizing methane-consuming microbial populations in OMZs is critical for understanding greenhouse gas and nutrient budgets during global warming.

Diverse bacteria may be responsible for linking methane oxidation to pathways of nitrogen loss under anoxia. A recent study confirmed that OMZs harbor transcriptionally active bacteria of the candidate division NC10 (Padilla et al., 2016), a group hypothesized to dismutate nitric oxide (NO) into N_2 and O_2 gas, with the latter used as the terminal oxidant in an intra-aerobic methanotrophy pathway (Ettwig et al., 2010). Bacterial groups canonically associated with aerobic methanotrophy may also play a role in nitrogen loss by directly using nitrate or nitrite as terminal oxidants in AOM. Evidence for these groups, predominantly of the gammaproteobacterial order Methylococcales, has

been found in both culture-dependent and -independent studies of diverse low oxygen environments (Kalyuzhnaya et al., 2013; Chistoserdova, 2015; Kits et al., 2015a,b; Danilova et al., 2016), including meromictic lakes (Biderre-Pettit et al., 2011; Blees et al., 2013) and marine water columns (Hayashi et al., 2007; Tavormina et al., 2013). Studies with isolates of two methanotrophic Methylococcales genera (*Methylomonas* and *Methylomicrobium*) show that hypoxic conditions stimulate denitrification to produce N_2O accompanied by increased cellular ATP yields (Kits et al., 2015a,b). Thus, such low oxygen-adapted methanotrophs may act as both a source of nitrous oxide and a sink for methane, depending on oxygen availability.

It remains unclear whether similar physiological mechanisms are used by planktonic methanotrophs in natural OMZ communities. While NC10 bacteria occur in OMZs, our prior work showing low NC10 abundance in a zone of comparatively high methane oxidation rates in a coastal OMZ suggests that other microbial players contribute to OMZ methanotrophy (Padilla et al., 2016). Indeed, PCR-based surveys of the methanotroph marker gene particulate methane monooxygenase (*pmo*) have identified diverse marine clades of the Methylococcales, designated as operational *pmo* units (OPUs), as being widely distributed through pelagic and sediment low oxygen environments (Tavormina et al., 2008, 2010). The OPU3 clade has been detected in a wide range of marine habitats, including the deep sea (Jensen et al., 2008; Lesniewski et al., 2012), methane seeps and oil spills (Wasmund et al., 2009; Tavormina et al., 2010; Kessler et al., 2011; Rivers et al., 2013), and OMZs (Hayaski et al., 2007; Tavormina et al., 2013). These studies suggest a low-to-no oxygen niche for OPU3, with members of this group being particularly prevalent in Eastern Pacific OMZs (Tavormina et al., 2008,

2010, 2013; Kneif, 2015). These OPU clades cluster apart from other denitrifying methanotrophs (Figure 4.1; Tavormina et al., 2008; Tavormina et al., 2010). However, no information regarding the genomic capacities and *in situ* activity of these groups has been reported.

Here, we report a near-complete genome from the OPU3 clade. The genome was recovered by binning of metagenome sequences from the anoxic coastal OMZ in Golfo Dulce (GD), Costa Rica. Like other anoxic OMZs, the GD anoxic, non-sulfidic zone is enriched in nitrite (~0.75 μM at the time of sampling) and supports an active anaerobic microbial community mediating nitrogen loss, notably through both the anammox process and denitrification (Dalsgaard et al., 2003). As reported in Padilla et al. (2016), methane concentrations at the time of sampling for the current study increased with depth into the GD anoxic zone, from <5 nM at the base of the oxycline (~80 m) to >70 nM near the sediment-water interface (~190 m), suggesting methane efflux from sediments (Figure 4.2). In contrast, methane-oxidation rates were highest (2.6±0.7 nM d^{-1}) at the top of the anoxic zone below the oxycline (90 m), but below detection deeper in the water column. This pattern is consistent with the periphery of OMZs as sites of active methane consumption (Ward et al., 1989; Sansone et al., 2001; Naqvi et al., 2010; Pack et al., 2015), potentially with methanotrophs at these transition depths adapted for both aerobic and anaerobic methane oxidation to accommodate fluctuation in oxycline depth or oxygen intrusions. Here, metagenomic data, interpreted alongside 16S rRNA amplicon sequences and phylogenetic analyses, identify an OPU3 bacterium as a dominant member of the anoxic GD community. Mapping of coupled mRNA transcripts to the OPU3 genome provides the first environmental transcriptional evidence of methanotrophic

denitrification outside of the NC10 phylum in an OMZ, further confirming OMZs as key sites of oceanic methane-nitrogen linkages.

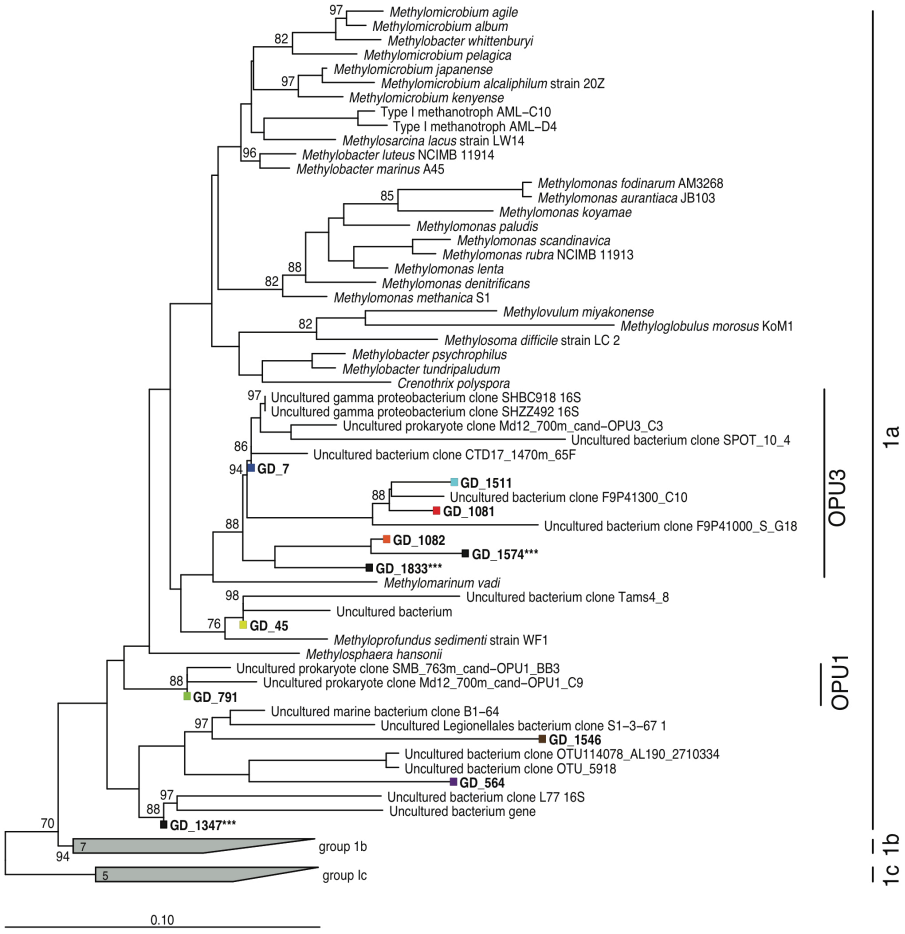

Figure 4.1 Methanotroph 16S rRNA gene phylogeny. Neighbor-joining phylogeny based on partial full-length 16S rRNA genes, with phylogenetic approximation of OTUs (colors) recovered from pooled gDNA and cDNA amplicon fragments assessed by parsimonious placement. Scale bar denotes nucleotide substitutions. Asterisks denote OTUs that were present at low abundance in non-rarefied datasets but lost when the datasets were subsampled to an even sequence depth. Bootstrap values ≥ 70 are displayed.

4.3 Materials and Methods

4.3.1 Sample collection

The collection of samples used in this study was described in Padilla et al. (2016). Briefly, discrete water samples from depths of 30, 60, 90, 100, 120, and 165 m were collected using a hand-deployed Niskin bottle in late January from a site at the northern head of the coastal basin of GD, Costa Rica (Figure D.1). Microbial biomass was collected for molecular analysis by filtration of seawater (~1-3L) through a glass fiber disc pre-filter (GF/A, 47 mm, 1.6 μm pore-size, Whatman) and a primary collection filter (Sterivex™, 0.22 μm pore-size, Millipore) using a peristaltic pump immediately after recovery. Filters were preserved in RNA stabilizing buffer (25 mM Sodium Citrate, 10 mM EDTA, 5.3M Ammonium sulfate, pH 5.2), flash-frozen in liquid nitrogen, and stored at -80°C. Replicate filters for DNA analysis were collected from similar water volumes following RNA collection, preserved with lysis buffer (50mM Tris-HCl, 40 mM EDTA, 0.73 M Sucrose), and stored at -80°C. Dissolved oxygen concentrations were measured with a Clark-type O_2 electrode (Revsbech, 1989) mounted on a hand-deployed CTD (Sea Sun Technology).

4.3.2 Chemical analysis

Nitrite and dissolved methane concentrations at the time of biomass collection were first reported in Padilla et al. (2016) and are presented again here for context (Figure 4.2). Samples for nitrate were filtered (0.45 μm cellulose acetate) and frozen until analysis.

Concentrations of nitrate + nitrite were determined using chemiluminescence after reduction to nitric oxide with acidic vanadium (III) (Braman and Hendrix, 1989).

4.3.3 DNA extraction

DNA was extracted from Sterivex filters (>0.2 μm biomass size fraction) using a phenol:chloroform protocol. Cells were lysed by adding lysozyme (2 mg in 40 μl of lysis buffer per filter) directly to the Sterivex cartridge, sealing the ends, and incubating for 45 min at 37°C. Proteinase K (1 mg in 100 μl lysis buffer, with 100 μl 20% SDS) was added, and cartridges were resealed and incubated for 2 hours at 55°C. The lysate was removed, and the DNA was extracted once with phenol:chloroform:isoamyl alcohol (25:24:1) and once with chloroform:isoamyl alcohol (24:1) and then concentrated by spin dialysis using Ultra-4 (100 kDA, Amicon) centrifugal filters.

4.3.4 RNA extraction

RNA was extracted from Sterivex filters using a modification of the *mir*Vana™ miRNA Isolation kit (Ambion). Filter cartridges were thawed on ice, RNA stabilizing buffer was then expelled and discarded, and cells were lysed by adding Lysis buffer and miRNA Homogenate Additive (Ambion) directly to the cartridges. Following vortexing and incubation on ice, lysates were transferred to RNAase-free tubes and processed via acid-phenol:chloroform extraction according to the kit protocol. The TURBO DNA-

free™ kit (Ambion) was used to remove DNA, and the extract was purified using the RNeasy MinElute Cleanup Kit (Qiagen).

4.3.5 16S rRNA gene and transcript analysis

Fragments of the 16S rRNA molecule were analyzed to assess the taxonomic composition in both the community DNA (gDNA) and RNA (cDNA) pools. gDNA amplicon data was generated previously (Padilla et al. 2016) and re-analyzed here to focus on the methanotrophic community. cDNA amplicon data was generated in this study, as follows. Approximately 50 ng of RNA from each sample was reverse transcribed into cDNA using the Superscript First-Strand synthesis system for RT-PCR (Invitrogen), following protocols of Campbell et al. (2008). Amplicon generation and sequencing was done using an established pipeline in our lab (e.g., Padilla et al., 2015, 2016). Briefly, amplicons were synthesized using Platinum® PCR SuperMix (Life Technologies) with primers F515 and R806, encompassing the V4 region of the 16S rRNA gene (Caporaso *et al.,* 2011). Both forward and reverse primers were barcoded and appended with Illumina-specific adapters according to Kozich *et al.* (2013). Equal amounts of cDNA were used for each PCR reaction to avoid biases due to variable template concentrations (Kennedy et al., 2014). Thermal cycling involved: denaturation at 94°C (3 min), followed by 30 cycles of denaturation at 94°C (45 sec), primer annealing at 55°C (45 sec) and primer extension at 72°C (90 sec), followed by extension at 72°C for 10 min. Amplicons were analyzed by gel electrophoresis to verify size (~400 bp, including barcodes and adaptor sequences) and purified using the Diffinity RapidTip2

PCR purification tips (Diffinity Genomics, NY). Amplicons from different samples were pooled at equimolar concentrations and sequenced on an Illumina MiSeq using a 500-cycle kit.

For both gDNA datasets (from Padilla et al. 2016) and cDNA datasets (this study), barcoded sequences were de-multiplexed, trimmed (length cutoff 100 bp), and filtered to remove low quality reads (average Phred score < 25) using Trim Galore! (http://www.bioinformatics.babraham.ac.uk/projects/trim_galore/). Paired-end reads were then merged using FLASH (Magoč and Salzberg, 2011), with program parameters of a minimum average length of 250 nt for each read, minimum average length of 300 nt for paired read fragments, and a maximum allowable fragment standard deviation of 30 nt. The number of trimmed and merged reads per sample ranged from 3,844 – 95,351 for both gDNA and cDNA amplicon pools. Chimeric sequences were detected by reference-based searches using USEARCH (Edgar 2010) against the SILVA rRNA database 119. Amplicon sequences were then processed using 'UPARSE' as implemented in USEARCH. Briefly, sequences were dereplicated, sorted by size, and clustered into operational taxonomic units (OTUs) at 97% sequence similarity. Sequences from all samples were then mapped back to the OTU file using 'usearch_global', and sample/OTU matrices were produced from the resulting output with the python script 'uc2otutable.py'. Methanotrophic sequences were identified in the amplicon OTUs by BLASTN against SILVA 119, followed by keyword parsing to identify all sequences matching a known methanotroph-containing genus. Top database matches (hits) to these sequences were also identified via BLASTN against the nt database. The SINA aligner with the ARB output designation was used to align sequences representing all identified

putative methanotroph OTUs in our data (n=11; both gDNA and cDNA amplicons pooled), the sequences most closely related to these OTUs via BLASTN, and the methanotrophs isolated in culture in Knife et al. (2015). The resulting ".arb" file was imported into ARB (Ludwig et al. 2004)). A reference phylogenetic tree was compiled using near full-length sequences (1300 bp or greater) with the Feldstein correction, a custom filter based on the associated nucleotide-alignment, and bootstrap support of 1000 re-samplings. Short sequences (1300 or less), including the amplicon sequences, were then inserted into the near full-length reference tree using the parsimony tool in the ARB environment. Proportional abundances of identified methanotroph OTUs (Figure 4.2) were calculated after rarefaction based on the sample with the lowest number of reads (3,844 reads) for both gDNA and cDNA. In rarefying the data some OTUs that were either in low abundance or unique to specific samples were removed; their contribution to the total (all samples) community is expected to be negligible.

4.3.6 Metagenome (DNA) sequencing

A single depth, 90 m at the peak of measured OMZ methane oxidation rates (Padilla et al. 2016) and methanotroph abundance based on amplicon sequence data, was selected for metagenome sequencing. Community DNA was processed using the Nextera XT DNA Sample Prep kit and sequenced using a paired-end Illumina MiSeq 600 kit.

4.3.7 Metatranscriptome (cDNA) sequencing

Metatranscriptomes from three depths within the anoxic zone (90, 100, 120 m) were analyzed to assess methanotroph transcriptional activity. Three datasets representing these depths were generated previously (Padilla et al. 2016) and were reanalyzed in this study. To increase the number of sequences representing the methanotroph-enriched 90 m depth, a fourth dataset was generated using an aliquot of the total RNA used in Padilla et al. (2016). For this aliquot, the Ribo-Zero™ rRNA Removal Kit for bacteria (Epicentre) was used to deplete ribosomal RNA (rRNA) sequences prior to sequencing. rRNA was not depleted from the RNA aliquots used to generate the Padilla et al. (2016) datasets. For all samples, cDNA was prepared for sequencing using the ScriptSeq™ v2 RNA-Seq Library preparation kit (Epicentre) and sequenced on an Illumina MiSeq using a 500 cycle kit.

4.3.8 Metagenomic analysis

Sequences were trimmed using the same methods as described above for the amplicon analysis. Quality trimmed forward and reverse sequences were merged and assembled into contigs using SPAdes 3.7.0 (Nurk et al., 2013) with the '-meta' option. The number of contigs, contig length, GC content, N50, and L50 assembly statistics were calculated with metaQUAST (Mikheenko et al., 2015). Contigs ≥ 500 nt were organized into genome bins based on tetranucleotide frequency and sequence coverage using MaxBin 2.0 (Wu et al., 2016). Bin completeness and contamination levels were estimated based on the representation of lineage-specific marker gene sets using CheckM (Parks et al., 2014). For each bin with ≥ 50% completeness and ≤ 10% contamination,

the program Prodigal (Hyatt et al., 2010) was used to predict open reading frames (ORFs). Predicted ORFs were queried via BLASTP against the NCBI-nr database (April 2016) (criteria for a significant match: amino acid ID ≥ 40% over ≥ 70% of the alignment, and bit score ≥ 50) and assigned to a prokaryotic KEGG Orthology (KO) identifier (Kanehisa and Goto, 2000) using the MetaGenome Analyzer 5 (MEGAN5; Hudson et al., 2011), with taxonomic classification in MEGAN5 via the Lowest Common Ancestor (LCA) algorithm based on the NCBI taxonomy using the default settings. Annotations are reported in Supplementary Tables 4 and 5.

Based on high completeness and low contamination (see below), a single bin (bin 010) taxonomically affiliated with OPU3-like Methylococcales bacteria was selected for comparative analysis. The identity of this bin was further confirmed based on phylogenetic analysis of 107 concatenated single copy marker genes present in this bin and in the genomes (n=36) of known methanotrophic taxa from the Gammaproteobacteria, Alphaproteobacteria, Verrucomicrobia, and the NC10 candidate phylum. Marker genes were identified using Hidden Markov Models (HMMs) via HMMER3 (http://hmmer.janerlia.org/; Finn et al., 2011) with default settings. Identified genes were aligned using clustalW (Sievers et al., 2011), then concatenated using the alignment tool 'Aln.cat.rb' in the enve-omics package (Rodriguez and Konstantinidis, PeerJ, Preprints). The resulting alignment was inspected manually for errors and then used to generate a maximum likelihood phylogeny inferred with the Dayhoff substitution model with 100 bootstrap iterations using MEGA6 (Tamura et al., 2013). For each genome in the phylogeny, the presence/absence of key genes of dissimilatory and assimilatory nitrogen metabolism was evaluated via BLASTX using the KEGG

Automated Annotation Server (KAAS). Each genome was individually assessed with the bi-directional best-hit option on default settings and the results were manually searched for subunits of nitrogen metabolism genes, with the results (presence/absence) mapped onto the concatenated marker gene phylogeny. Gene content in bin 010 relative to the 36 other gammaproteobacterial methanotroph genomes included in this analysis was evaluated via reciprocal BLASTP using the two-way amino-acid identity script in the enve-omics packages (Konstantinidis and Tiedje, 2005) with a bit score threshold of 50, and match criteria of >35% amino acid identity over >65% of each gene.

Phylogenetic analysis was used to further examine the taxonomic affiliation of key genes of the denitrification process recovered in bin 010: *narG* and *nirK*. The amino acid sequence from each gene was aligned against a representative sequence set, identified based on top BLASTP results, using MUSCLE with default settings (Edgar, 2004). The alignments were manually inspected and used to generate maximum likelihood phylogenies using MEGA6.0 with the Dayhoff substitution model and 1000 bootstrap iterations. To further characterize taxonomic affiliations, the taxonomic annotation of all genes occurring on the same contig as key marker genes of denitrification and methanotrophy (*nar, nir, pmo*) was determined via BLASTX against NCBI-nr (Figure D.2).

4.3.9 Metatranscriptome analysis

Reads were filtered by quality and merged as described above. The program *ribopicke*r (Schmieder et al., 2012) was used to remove rRNA sequences from

metatranscriptome datasets. To characterize the transcript pool affiliated with the OPU3 genomic bin described above, transcripts were mapped to bin 010 ORFs using BLASTX with match criteria of >90% amino acid identity over >60% of the transcript length and bit score >50. To compare transcript levels among bin 010 ORFS, the number of transcripts with significant BLASTX matches per ORF was normalized to variation in ORF length, and then expressed as a proportion of total transcripts mapping to bin 010. To also characterize the transcript pool at the community level, merged non-rRNA datasets were queried via DIAMOND (Buchfink et al., 2015) against the NCBI-nr database (April 2016) using the sensitive search setting. DIAMOND-identified protein-coding transcripts were assigned to functional categories as above based on Kegg Ortholog (KO) identifiers and taxonomically classified according to the NCBI taxonomy using the LCA algorithm in MEGAN5. Transcript counts per KO were normalized to the total number of mRNA transcripts assigned to a prokaryotic KO. To show variations in contributions of bin 010 to community mRNA transcription with depth, the number of transcripts with significant BLASTX matches to bin 010 ORFs was expressed as a proportion of total prokaryotic mRNA transcripts assignable to a KO.

All sequence data, including the bin 010 assembly, have been submitted to the Sequence Read Archive at NCBI under the following BioProject ID's: PRJNA328797 and PRJNA277357.

4.4 Results and discussion

4.4.1 Methanotroph community composition and transcription

Deep-coverage sequencing of 16S rRNA gene (gDNA) and transcript (cDNA) amplicons revealed an abundant, diverse, and active methanotroph community in the Golfo Dulce OMZ. All sequences that matched putative aerobic methanotrophs were classified as type Ia Gammaproteobacteria methanotrophs. Across all depths, 11 OTUs from the gDNA dataset were identified as Methylococcales by BLASTN. Eight of these OTUs remained after rarefaction (3,844 reads) of the total gDNA and cDNA amplicon pools. Phylogenetic analysis classified these eight OTUs as most closely related to methanotrophs of the OPU3 and OPU1 clusters and the genus *Methyloprofundus* (Figure 4.1), with six of the eight belonging to the OPU3 clade. A single OPU3 OTU (GD_7) dominated the methanotroph sequence dataset, constituting ~35-75% of the Methylococcales pool in both the gDNA and cDNA datasets at all depths (Figure 4.2). Only one OTU from the OPU1 clade (GD_791) was detected and was confined primarily to the 60 m sample where O_2 concentration was ~25 μM. Together, these eight OTUs, which collectively represented 1.8% of the total gDNA combined over all depths, were undetected or at low abundance (0.4%) above or within the oxycline (30 and 60 m, respectively) but increased to 4-5% of the gDNA pool in the upper anoxic zone (90 and 100 m) where O_2 concentrations fell below detection, <50 nM, and nitrite accumulated (Figure 2). Notably, OTU GD_7, the dominant OPU3 bacterium, constituted 4% of the total microbial community (gDNA pool) at 90 m. These OTUs then decreased to <1% of the community deeper in the anoxic zone at 120 m, and at 165 m where nitrate and nitrite were depleted and methane accumulated. The proportional representation of these 8 OTUs was ~2-fold higher in the cDNA compared to the gDNA datasets at all depths, indicating a transcriptionally active Methylococcales community.

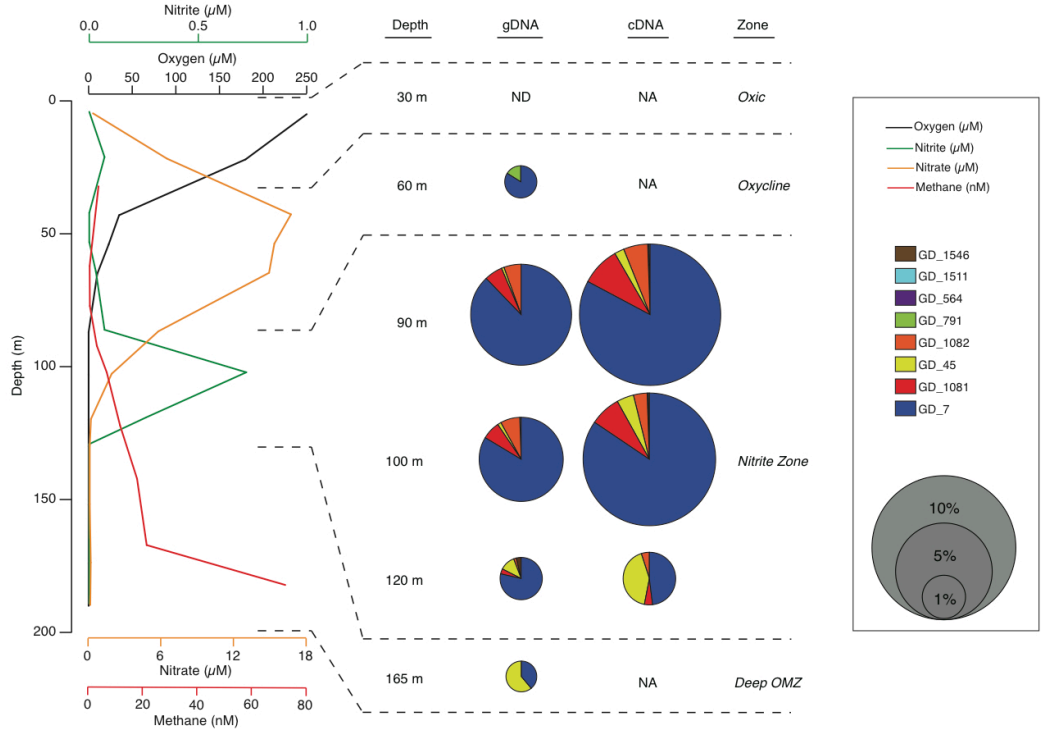

Figure 4.2 Water column chemistry and Methylococcales OTU abundances in the GD water column. Dissolved oxygen (measured by Clark type electrodes; black line), nitrite (green), nitrate (yellow), and methane (red) concentrations through the oxic zone (~0-30 m), oxycline (~30-80 m), anoxic nitrite-enriched zone (~80-140 m), and deeper anoxic zone (~140 m to sediment-water interface at ~190 m). Chemical data are from Padilla et al. (2016). Bubble plots show abundances of Methylococcales OTUs as a percentage of total community 16S rRNA gene (gDNA) and transcript (cDNA) amplicons. ND = Not detected, NA = No available data for that sample.

4.4.2 Recovery of the genome of an OPU3-like methanotrophic denitrifier

Metagenomic analysis confirmed the potential for coupled methanotrophy and denitrification in the Golfo Dulce OMZ. Genomic DNA from within the secondary nitrite maximum at 90 m was deeply sequenced, assembled into contigs, and binned into OTUs resulting in 52 draft genomes (bins) ranging from 12.4% to 100% completeness and 0 to 86% contamination. Of these, bin 010 contained a single near-full length (1405 bp) 16S rRNA gene fragment identical to that of OTU GD_7 identified in the amplicon analysis (above). The contig containing this fragment consisted solely of the 16S rRNA gene and exhibited an average per-base coverage of 6.6, nearly identical to the bin-wide average (all contigs) of 6.7. The bin contamination level was 6% based on duplicated marker genes, a level consistent with that reported in other studies drawing conclusions of genome content based on binning (see Sekiguchi et al., 2015 (6 - 7%); Campanaro et al., 2016 (3 - 5%); Güllert et al., 2016 (5 - 10%)). On average, duplicate marker genes in bin 010 shared 81% amino acid identity, within the genome-wide range observed for bacterial strains categorized in the same species (Kostas and Tiedje, 2005), suggesting that contaminant sequences in this bin are from closely related taxa.

Given the high abundance of OTU GD_7 at >4% in both the gDNA and cDNA amplicon pools (Figure 4.2), suggesting a substantial contribution to OMZ community processes, bin 010 was selected for in-depth characterization. The genome represented by this bin, hereafter designated GD_7, was estimated to be 95.3% complete, with 2,011 coding sequences distributed over 305 contigs and a total of 2,106,486 nt. The estimated GD_7 genome size, at 2.2 Mbp, is consistent with that of pelagic free-living bacteria (Raes et al., 2007; Shi et al., 2011), but substantially smaller than that of most other

gammaproteobacterial methanotrophs (~4-5 Mbp; Figure 4.3). LCA-based taxonomic classification of GD_7 coding sequences indicated an affiliation with the order Methylococcales. Phylogenetic analysis of 107 housekeeping genes (concatenated) from available methanotroph genomes confirmed GD_7 as basal but most closely related to the type-Ia methanotrophs of the Methylococcales, a diverse group of bacteria with some members shown experimentally to couple methane oxidation to denitrification (Figure 4.3; Kits et al., 2015a,b).

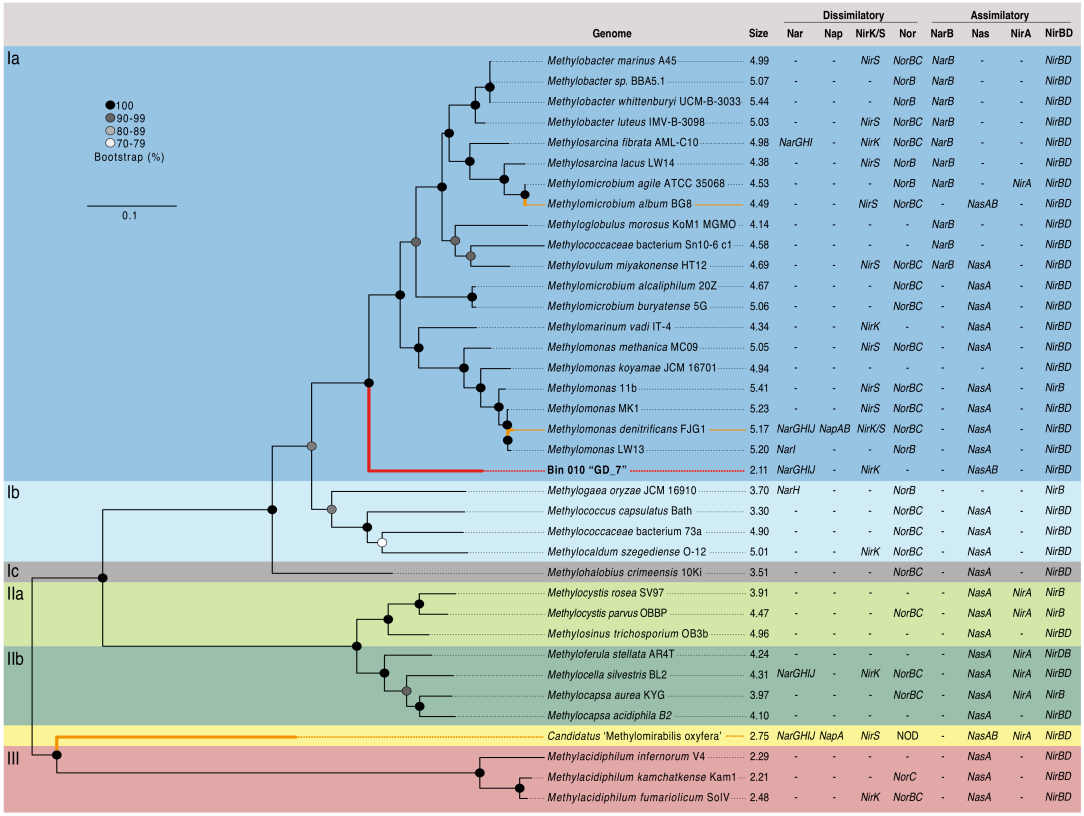

Figure 4.3 Concatenated gene phylogeny of methanotrophic genomes and description of N utilizing genes. Phylogeny based on the concatenated alignment of 107 single copy housekeeping genes from OTU GD_7 (bin 010) and known methanotroph genomes (n=36). Maximum likelihood phylogeny was inferred based on the Dayhoff substitution model, bootstrapped 100 times; bootstrap support values ≥ 70 are displayed. Phylogenetic classification (Ia, Ib, Ic, IIa, IIb, III) is based on a recent review (Kneif, 2015). Genome size in megabases and presence/absence of key genes of dissimilatory and assimilatory nitrogen metabolism are displayed next to taxon names. Experimentally confirmed denitrifying taxa are highlighted with bold orange branches, with the assembled bin 010 denoted by the bold red branch. The scale bar represents amino acid substitutions per site. Abbreviations are as follows: Nar – membrane bound nitrate/nitrite oxidoreductase, Nap – periplasmic nitrate/nitrite oxidoreductase, NirK – copper containing nitrite reductase, NirS – cytochrome cd1 nitrite reductase, Nor – nitric oxide reductase, NOD – nitric oxide dismutase (putative), NarB – ferredoxin nitrate reductase, Nas – assimilatory nitrate reductase, NirA – assimilatory nitrite reductase, NirBD – assimilatory nitrite reductase.

Below we discuss a subset of key functional genes recovered in the GD_7 bin. As the inferred genome is fragmentary and exhibits 6% contamination (above), confirmation that the recovered genes are co-localized on the same chromosome in OPU3 requires further analysis of a pure culture or a closed genome. Similarly, as the recovered GD_7 genome is not 100% complete, we cannot definitively conclude that specific genes are absent from this genome. However, the gene content described below, when contextualized relative to that of other methanotrophs, prior results, and the environmental conditions of Golfo Dulce, is strongly suggestive of key metabolic functions in GD_7.

The genome content of GD_7 indicates the potential for methanotrophic denitrification. GD_7 contains genes required for energy generation by methane oxidation, including those encoding the three subunits of particulate methane monooxygenase (*pmoCAB*) for methane oxidation to methanol, which together co-occur on a contig with diverse other genes having close homologs in other gammproteobacterial methanotrophs (inferred from top BLASTX matches; Supplementary Figure 4.2). Also present are genes for the lanthanide-dependent (*xoxF*) methanol dehydrogenase involved in methanol oxidation to formaldehyde, NAD(P)-dependent methylene-H_4MPT dehydrogenase (*mtd*) involved in formaldehyde oxidation to formate, and formate dehydrogenase (*fdh*) for formate oxidation to CO_2. The presence of XoxF type methanol dehydrogenases, but absence of the calcium-dependent MxaF type, has also been reported for pelagic non-methanotrophic methylotrophs with relatively small genomes (Giovannoni et al. 2008) and is consistent with recent studies suggesting the prevalence

of XoxF compared to MxaF in natural systems (Keltjens et al., 2014; Ramachandran and Walsh, 2015).

GD_7 also contains two operons encoding a dissimilatory nitrate reductase (*nar*), as well as genes for synthesis of the essential *nar* molybdenum cofactor. Of the downstream genes of the denitrification pathway, only the *nirK* gene encoding nitric oxide (NO)-producing nitrite reductase was detected in GD_7. The two *nar* operons, as well as *nir*, were recovered on contigs alongside other functional genes with homology to those of gammaproteobacterial methanotrophs (Figure D.2). Phylogenetic analysis of marker genes *nirK* and *narG*, with the latter encoding the alpha subunit of Nar, also supports a methanotroph affiliation. One of the *narG* copies (ORF 1321) clusters with high support in a clade containing denitrifying gammaproteobacterial methanotrophs, including *Methylomonas denitrificans* (Figure 4.4a). Likewise, GD_7 *nirK* clusters with a sequence from the gammaproteobacterial Methylothermaceae and that of the nitrite-oxidizing bacterium *Nitrospina gracilis,* although the function of NirK in *Nitrospina* remains unclear (Lücker et al., 2013) (Figure 4b). In contrast, the second *nar* operon may have an origin outside of the gammaproteobacteria, as analysis of the corresponding *narG* copy (ORF 1413) reveals a closer affiliation to *narG* from a genus of Chlorobi bacteria (*Ignavibacterium*) containing facultatively anaerobic chemoheterotrophic members (Figure 4.4a).

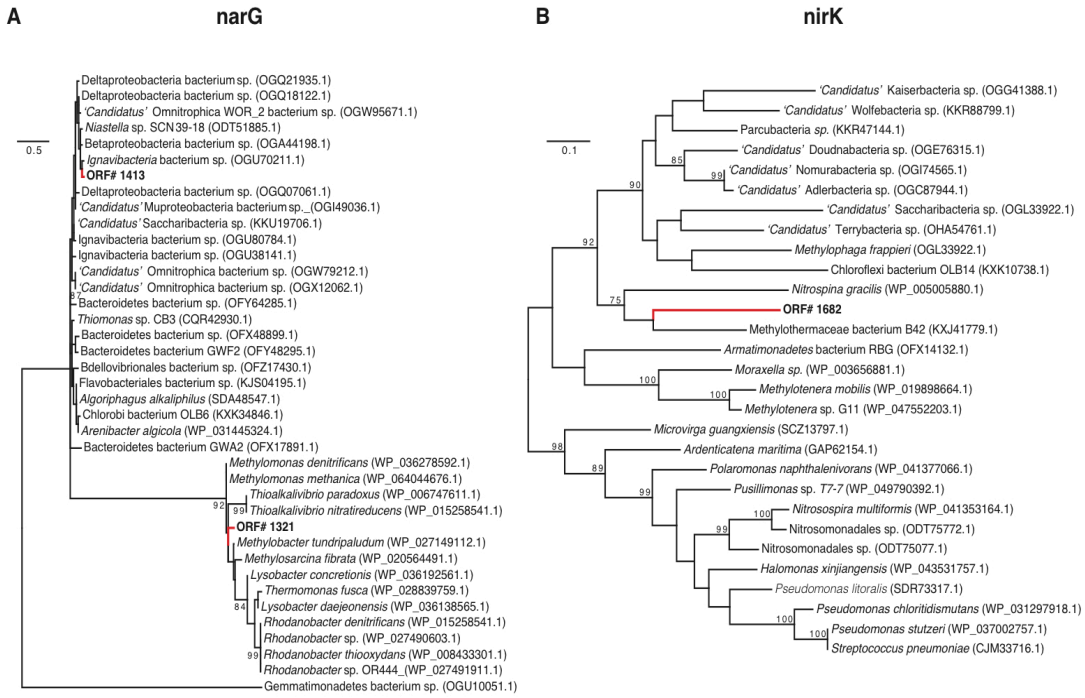

Figure 4.4 Nitrate reductase (*narG*) and nitrite reductase (*nirK*) phylogenies. The trees include closely related sequences identified as top matches to GD_7 *narG* and *nirK* amino sequences through BLASTP queries against NCBI-nr. Unrooted phylogenies were inferred based on maximum likelihood analysis using the Dayhoff substitution model with 1000 bootstrap iterations. Bootstrap values >70 are displayed, along with NCBI accession numbers. Scale bars for *narG* and *nirK* represent 50 and 10 changes per 100 amino acids (respectively).

These results suggest that certain genes for partial denitrification in GD_7 share ancestry with those of gammaproteobacterial methanotrophs, while others, notably ORF 1413, may have been acquired horizontally (Figure 4.4a). Horizontal acquisition of denitrification genes in methanotrophs may be common, as the presence of *nar* and *nir* genes is independent of methanotrophic phylogenetic histories (Figure 4.3). Indeed, the co-occurrence of divergent denitrification genes in the same genome is not unusual. Many bacteria, for example, encode divergent *nar* copies (Philippot, 2002; Tsementzi et al., 2016), potentially as an adaptation to variable oxygen conditions (Iobbi-Nivol et al., 1990). Although multiple *nar* operons have yet to be reported in other methanotrophs, a marine methylotroph was shown to encode two *nar* enzymes, with one copy playing a role in regulating the other depending on oxygen availability (Mauffery et al., 2015). Some denitrifying methanotrophs also encode the perisplasmic dissimilatory nitrate reductase (*Nap*), hypothesized to function primarily under nitrate-limiting conditions (Figure 3; Ferguson and Richardson, 2004); however, *nap* genes were not detected in GD_7. In contrast to *Methylomonas denitrificans* FJG1, *Methylomicrobium album* BG8, and *Candidatus* 'Methylomirablis oxyfera', GD-7 does not appear to harbor an NO-reductase (*nor*), and is therefore likely incapable of producing N_2O as an intermediate or end-product (Figure 4.3; Kits et al., 2015a,b). In *M. denitrificans* FJG1, *M. album* BG8, and potentially GD-7, nitrate is likely utilized for respiratory purposes. This is in contrast to NC10 members, which likely utilize nitric oxide (derived from nitrate and nitrite reduction) for dismutation with concomitant production of intracellular oxygen. Rather, our data identify a partial methanotrophic denitrification pathway in GD_7, with NO as the likely respiratory end product.

GD_7 also contains genes encoding key enzymes of C_1 carbon assimilation from methane, including those of the ribulose monophosphate (RuMP) pathway for incorporation of methanol-derived formaldehyde and regeneration of ribulose-5-phosphate (Figure D.3). Key enzymes of the serine pathway for formaldehyde assimilation were also detected (Table 4.1), with ten of the serine cycle genes recovered on the same contig. Diagnostic enzymes of the ethylmalonyl-CoA (EMC) pathway (ethylmalonyl-CoA mutase, crotonyl- CoA reductase/carboxylase), used by some serine cycle-utilizing methanotrophs for glyoxylate regeneration (Christoserdova, 2011), were not detected in GD_7. Neither were isocitrate lyase and malate synthase, suggesting glyoxylate generation does not occur via the glyoxylate cycle in GD_7. This pattern, the presence of serine cycle genes and absence of an EMC pathway and glyoxylate shunt, has been reported in other type 1 methanotrophs (Poehlein et al., 2013; de la Torre et al., 2015). In GD_7, all enzymes of the Citric Acid (TCA) cycle are present, as are genes of glycolysis and for pyruvate dehydrogenase for acetyl-CoA generation. However, GD_7 appears to lack the genes encoding the Entner-Doudoroff Pathway, which would be atypical of Type I methanotrophs that have been hypothesized to depend primarily on Entner-Doudoroff cleavage reactions over glycolysis (Kalyuzhnaya et al., 2013). However, we cannot rule out that these or other genes were not detected due to incomplete coverage (~95%) of this genome bin. Together, these patterns suggest C_1 incorporation from methane via the RuMP pathway, with acetyl-CoA synthesis via pyruvate for entry into the TCA cycle for biosynthesis.

Table 4.1. Representation of methane oxidation and denitrification genes present (+/-) in GD_7 (bin 010) and abundance in the coupled 90 m metatranscriptome.

Function	Gene description	Bin[a]	%OPU3[b]	ORF #[c]
Methane oxidation				
	Particulate methane monooxygenase subunit A	+	1.18	1481
	Particulate methane monooxygenase subunit B	+	0.47	1480
	Particulate methane monooxygenase subunit C	+	4.57	1482
	Soluble methane monooxygenase subunit A	-	-	-
	Soluble methane monooxygenase subunit B	-	-	-
	Soluble methane monooxygenase subunit C	-	-	-
Methanol conversion				
	Methanol dehydrogenase (*xoxF*)	+	0.56	1041
Formaldehyde oxidation				
	Beta-ribofuranosylaminobenzene phosphate synthase	+	-	938, 1429
	H4MPT-dependent formaldehyde activating enzyme	+	0.65	943
	Methylene-H4MPT dehydrogenase (MtdB)	+	0.02	1057 - 1058
	Methenyl-H4MPT cyclohydrolase	+	0.03	940, 1431
	Formyltransferase/Hydrolase Complex	+	0.02	799 – 801, 910 - 913
Formic acid production				
	Formate dehydrogenase	+	0.07	954 - 956
RuMP cycle				
	3-hexulose-6-phosphate synthetase	+	2.85	749
	6-phospho-3-hexuloisomerase	+	1.55	748
	Glucose-6-phosphate isomerase	+	0.05	1736
	Glucose-6-phosphate dehydrogenase	+	0.07	316
	6-phosphogluconate dehygdrogenase	+	0.23	480
	Phosphofructokinase	+	< 0.01	882
	Fructose bisphosphate aldolase	+	0.60	744, 1303
	Transaldolase	+	1.97	745
	Transketolase	+	-	747
Serine cycle				
	Methylene-H4/Methylene-H4MPT dehydrogenase (MtdA)	+	-	277
	Methenyl-H4F cyclohydrolase	+	-	378
	Formyl-H4F ligase	+	-	274
	Serine-glyoxylate aminotransferase	+	0.02	280
	Hydroxypyruvate reductase	+	-	279
	Glycerate kinase	+	0.06	276
	Enolase	+	0.11	122
	Phosphoenolpyruvate carboxylase	-	-	-
	Malate dehydrogenase	+	0.03	278
	Malate thiokinase (Malate-CoA ligase)	+	0.01	282 - 283
	Malyl-CoA/Methylmalyl-CoA lyase	+	-	281
	Serine hydroxymethyltransferase	+	0.06	275
Citric Acid Cycle (TCA)				
	Citrate synthase	+	0.16	1049, 1554
	Aconitate hydratase	+	0.24	1050
	Isocitrate dehydrogenase	+	0.02	1051
	2-oxoglutarate dehydrogenase	+	0.02	751 - 752
	Succinyl-CoA synthetase	+	0.02	590 - 591
	Succinate dehydrogenase	+	0.05	1053 - 1056
	Fumarate hydratase	+	0.03	1105
	Malate dehydrogenase	+	0.03	278
Denitrification				
	Respitpory nitrate reductase alpha chain	+	0.37	1321, 1410
	Respitpory nitrate reductase beta chain	+	0.02	1322, 1411
	Respitpory nitrate reductase gamma chain	+	0.17	1324, 1413
	Respitpory nitrate reductase delta chain	+	0.04	1323, 1412
	Periplasmic nitrate reductase subunit A	-	-	-
	Periplasmic nitrate reductase subunit B	-	-	-
	Periplasmic nitrate reductase subunit C	-	-	-

[a] Gene detected in GD_7 (bin 010) from 90 m

[b] Percent of OPU3 transcripts mapped to GD_7 (bin 010) calculated as ((Number of hits mapping ORF / ORF length) / Total mapped reads to GD_7)

[c] ORF # corresponds to numbers in Supplementary Table

Reciprocal BLASTP against all methanotrophic bacteria in Figure 3 identified 102 protein-coding genes in GD_7 that lack close homologs in other methanotroph genomes (based on the imposed BLAST criteria: bit score > 50, with >35% amino acid identity across >65% of the gene). Of this divergent gene set, 47 encode hypothetical proteins. The remaining annotated genes are associated with diverse functions, including flagellum synthesis or regulation, phage tail synthesis, and diverse functions of amino acid or peptide metabolism, as well as an arginase potentially involved in urea generation. Genes in this divergent set may be candidates for follow-up studies to better understand niche-specific adaptations in GD_7.

4.4.3 OPU3 transcription in the OMZ

To characterize the Methylococcales-like transcript pool, we examined transcripts from 90, 100, and 120 m that mapped with high identity to GD_7. To increase coverage across the bin, we analyzed an additional 90 m dataset from which rRNA was removed prior to sequencing. This step increased data yield but altered the abundance of mapped transcripts (expressed as a % of total prokaryotic mRNA; Figure 4.5), suggesting that rRNA subtraction may also have removed certain mRNA transcripts. This procedure does not affect our conclusions, however, as our goal was to characterize the range of genes actively transcribed by GD_7; variation in transcription among genes is presented in only a general sense (e.g., Figure 4.5). Nonetheless, the rRNA-subtracted dataset is not considered when evaluating changes across depths (below).

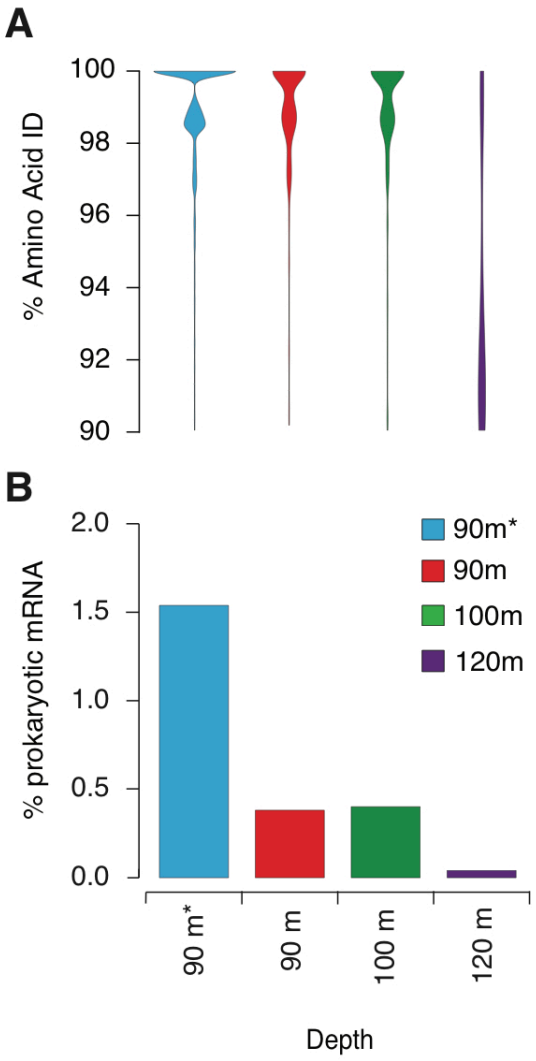

Figure 4.5 Transcripts mapping to GD_7. (A) Violin plots indicating the proportion of mRNA reads at each amino acid %ID in each sample. (B) Percentage of mRNA recruited to the bin from each sample as a proportion of prokaryotic mRNA assigned by MEGAN5. Asterisk (*) 90 m sample denotes rRNA removal prior to sequencing using Ribo-Zero™ rRNA Removal Kit for bacteria (Epicentre). Transcript mapping to GD_7 is based on BLASTX with the following criteria: bit score ≥ 50, amino acid ID ≥ 90%, and alignment length ≥ 60% of the gene.

Metatranscriptome analysis confirmed that Methylococcales bacteria were transcriptionally active in the Golfo Dulce OMZ. Across all datasets, a total of 24,989 reads representing 764 genes were recruited via BLASTX to GD_7 contigs with high identity (>90% AAI; bit scores > 50) across 60% of the transcript fragment. The proportional representation of these mapped transcripts peaked at 90 and 100 m at ~0.5% of total mRNA reads (non-rRNA-subtracted dataset) before decreasing to <0.1% deeper in the anoxic zone (120 m sample; Figure 4.5b). Indeed, at 90 and 100 m, the vast majority (~90%) of recruited transcripts share greater than 98% AAI with genes of GD_7 (Figure 4.5a; Figure D.4). In contrast, at 120 m, the majority of mapped reads share less than 94% AAI. These patterns suggest discrete OPU3-like populations based on depth, with GD_7 confined primarily to the upper OMZ where both nitrite- and nitrate are enriched compared to greater depths in the anoxic zone (Figure 4.2).

Transcripts involved in methanotrophy and denitrification were among the most abundant of those recruiting to GD_7, based on the mRNA-enriched 90 m dataset (Figures D.4 and D.5). Mapped transcripts included all genes of the aerobic methane oxidation pathway (Table 4.1), with *pmoA* and *pmoC* being particularly abundant, as well as genes of the RuMP pathway. Denitrification transcripts included *narG* and *nirK*, both of which were detected at 90 and 100 m, but absent from the 120 m dataset. Interestingly, only transcripts mapping to *narG* ORF 1413 were detected, suggesting differential regulation of Nar expression and therefore the potential for functional variation between the two enzyme variants (ORF 1321, 1413). Terminal oxidase genes, though present in GD_7, were not detected in the mapped transcript pool, suggesting that any oxygen being utilized is for methane oxidation rather than respiration. Genes for fatty acid metabolism

were also among the most abundant transcripts recruiting to GD_7, as were those mediating flagellar biosynthesis and regulation. The high transcription of flagellar genes is consistent with prior reports of the importance of motility in type 1 methanotrophs from low oxygen environments (Danilova et al., 2016), suggesting a need to traverse redox gradients to access zones of optimal substrate (e.g., methane) or oxygen conditions, potentially including those at the micron scale on suspended or sinking particles. Enzymes involved in amino acid metabolism were also abundant in the GD_7 transcript pool (Figure D.5), with proline dehydrogenase being among the most highly transcribed GD_7-specific protein at 90 m. This enzyme is involved in proline catabolism, producing reductant in the form of reduced co-enzyme Q10 (i.e., ubiquinol). Although use of proline for reductant has been reported for diverse bacteria under both oxic and anoxic conditions (Deutsch and Soffer, 1975; Barker, 1981), the potential contribution of amino acid catabolism to reductant pools in methanotrophs, including OPU3 members, remains uncharacterized. Genes encoding enzymes of the methylcitrate pathway (MCA) involved in propionate catabolism were also highly transcribed (Figure D.5). These included methylcitrate synthase, methylcitrate dehydrogenase and aconitate hydratase, although the MCA gene encoding methylisocitrate lyase was not detected. MCA genes and transcripts have been reported in aquatic betaproteobacterial methylotrophs, raising the hypothesis that propionate, which can be produced via demethylation of compounds such as dimethylsulfoniopropionate, may be an important carbon substrate in these bacteria (Kalyuzhnaya et al., 2008, 2010). The potential for propionate catabolism in OPU3 should be further evaluated.

Taxonomic classification of the bulk metatranscriptome based on lowest common ancestry (LCA) corroborated the transcriptional activity of a Methylococcales community in the OMZ. The majority (~80%) of LCA-identified Methylococcales transcripts could not be assigned to a genus (Supplementary Figure 6). Of those transcripts that could be classified, most are affiliated with *Methylomonas*, *Methylobacter*, or *Methylomicrobium*. The proportional abundance of total Methylococcales transcripts across depths was nearly identical to that of the transcript pool mapping to GD_7 (Figure 4.4, Figure D.6), indicating that the vast majority of Methylococcales transcripts were affiliated with this OPU3 taxon and that its contribution to community transcription peaked at 90 and 100 m just below the oxycline. As in the GD_7 transcript pool, biochemical functions highly represented in the bulk Methylococcales transcripts were predominantly associated with methane oxidation and C_1 assimilation, with transcripts encoding *pmoCAB* among the most abundant (data not shown).

4.5 Conclusion

These results provide the first environmental meta-omic evidence for coupled methanotrophy and partial denitrification in the OPU3 bacterial clade. The recovery of a near complete genome for GD_7, interpreted alongside community composition data and linked metatranscriptome analysis identifying transcripts of methane-oxidation, C_1 assimilation via the RuMP pathway, and partial denitrification, implicate this abundant OTU as a potentially significant player in methane-driven nitrogen transformations in the Golfo Dulce. The localized distribution at 90 m of transcripts with high identity to GD_7

(Figure 4.4b), along with the recovery of diverse other OPU3 OTUs, suggests the potential for temporal or spatial variation in the contribution of different OPU3 ecotypes to community metabolism, likely driven by local concentrations of methane, oxidized nitrogen, or dissolved oxygen.

Our results suggest that GD_7 is adapted to conditions at the upper OMZ periphery where oxygen is absent but nitrate, nitrite, and methane are all available. Prior studies have suggested a low-to-no oxygen niche for the OPU3 group as a whole, notably as pelagic methane concentrations typically increase with decreasing oxygen content (Sansone et al., 2001; Pack et al., 2015). Indeed, the abundance of OPU3-like OTUs has been shown to increase with decreasing oxygen further off the Costa Rican coast (Tavormina et al., 2013). However, the activity of methanotrophic denitrifiers in the OMZ water column may also be driven strongly by nitrite conditions; for example, in *Methylomicrobium album*, transcription of methanotrophy genes and nitrous oxide production via denitrification was dependent on both nitrite availability and low oxygen conditions, whereas denitrification gene transcription was stimulated only by nitrite availability (Kits et al., 2015a). In the GD, the distribution of OPU3 amplicons and transcriptional activity, notably those of GD_7, mirror that of the nitrite profile (Figure 2). The high abundance of OPU3 genes and transcripts in the upper OMZ corresponds with the previously reported maximum in methane oxidation rates at 90 m, whereas rates lower in the OMZ were undetectable at the time of collection (Padilla et al., 2016). Despite the anoxia at 90 m, it remains possible that the rates reported in Padilla et al (2016) represent a combination of both aerobic and denitrification-dependent methane oxidation, potentially due to inter-individual variation in an OPU population or variation

among OPU ecotypes. Genomes and gene expression studies targeting diverse OPU phylotypes from the GD and other low oxygen marine habitats would be valuable for resolving these possibilities. Characterizing the metabolic diversity of pelagic methane utilizing bacteria is critical for predicting linkages between greenhouse gas, carbon, and nutrient fluxes. This is particularly important for microbial communities along the steep redox gradients of OMZs, as these habitats are predicted to expand in response to climate change.

Acknowledgements

We thank Alvaro Morales for coordinating work at the GD field site and Pete Girguis for analysis of methane concentrations.

4.6 References

Barker, H.A. (1981). Amino acid degradation by anaerobic bacteria. *Ann. Rev. Biochem*. 50, 23-40. doi: 10.1146/annurev.bi.50.070181.000323.

Biderre-Petit, C., Jezequel, D., Dugat-Bony, E., Lopes, F., Kuever, J., Borrel, G., et al. (2011). Identification of microbial communities involved in the methane cycle of a freshwater meromictic lake. *FEMS Microbiol. Ecol.* 77, 533-545. doi: 10.1111/j.1574-6941.2011.01134.x.

Blees, J., Niemann, H., Wenk, C.B., Zopfi, J., Schubert, C.J., Kirf, M.K., et al. (2014). Micro-aerobic bacterial methane oxidation in the chemocline and anoxic water column of deep south-Alpine Lake Lugano (Switzerland). *Limnol. Oceanogr.* 59, 311-324. doi: 10.4319/lo.2014.59.2.0311.

Boetius, A., Ravenschlag, K., Schubert, C.J., Rickert, D., Widdel, F., Gieseke, A., et al. (2000). A marine microbial consortium apparently mediating anaerobic oxidation of methane. *Nature* 407, 623-626. doi: 10.1038/35036572.

Braman, R.S., Hendrix SA. (1989). Nanogram nitrite and nitrate determination in environmental and biological materials by vanadium (III) reduction with chemiluminescence detection. *Anal. Chem.* 61, 2715-2718.

Buchfink, B., Xie, C., and Huson, D.H. (2015). Fast and sensitive protein alignment using DIAMOND. *Nat. Methods* 12, 59-60. doi: 10.1038/nmeth.3176.

Campanaro S., Treu L., Kougias P.G., De Francisci D., Valle G., Angelidaki I. (2016). Metagenomic analysis of functional characterization of the biogas microbiome using high throughput shotgun sequencing and a novel binning strategy. *Biotech. for Biofuel*. 9, 1. doi: 10.1186/s13068-016-0441-1.

Campbell, B.J., Yu, L., Straza, T.R.A., Kirchman, D.L. (2009). Temporal changes in bacterial rRNA and rRNA genies in Delaware (USA) coastal waters. *Aquat. Microb. Ecol.* 57, 123-135. doi: 10.3354/ame01335.

Caporaso, J.G., Lauber, C.L., Walters, W.A., Berg-Lyons, D., Lozupone, C.A., Turnbaugh, P.J., et al. (2011). Global patterns of 16S rRNA diversity at a depth of millions of sequences per sample. *P. Natl. Acad. Sci. USA.* 108, 4516-4522. doi: 10.1073/pnas.1000080107.

Carini, P., White, A.E., Campbell, E.O., Giovannoni, S.J. (2014). Methane production by phosphate-starved SAR11 chemoheterotrophic marine bacteria. *Nat. Comm.* 5, 4346. doi: 10.1038/ncomms5346.

Chistoserdova, L. (2015). Methylotrophs in natural habitats: current insights through metagenomics. *Appl. Microbiol. Biot.* 99, 5763-5779. doi: 10.1007/s00253-015-6713-z.

Codispoti, L.A., Brandes, J.A., Christensen, J.P., Devol, A.H., Naqvi, S.W.A., Paerl, H.W., et al. (2001). The oceanic fixed nitrogen and nitrous oxide budgets: moving targets as we enter the anthropocene? *Sci. Mar.* 65, 85-105. doi: 10.3989/scimar.2001.65s285

Dalsgaard, T., Canfield, D.E., Petersen, J., Thamdrup, B., Acuna-Gonzalez, J. (2003). N_2 production by the anammox reaction in the anoxic water column of Golfo Dulce, Costa Rica. *Nature* 422, 606-608. doi: 10.1038/nature01526.

Damm, E., Helmke, E., Thoms, S., Schauer, U., Nothig, E., Bakker, K., et al. (2010). Methane production in aerobic oligotrophic surface water in the central Arctic Ocean. *Biogeosciences* 7, 1099-1108. doi: 10.5194/bg-7-1099-2010

Danilova, O.V., Suzina, N.E., Van De Kamp, J., Svenning, M.M., Bodrossy, L., Dedysh, S.N. (2016). A new cell morphotype among methane oxidizers: a spiral-shaped obligately microaerophilic methanotroph from northern low oxygen environments. *ISME J.* advanced online publication. doi: 10.1038/ismej.2016.48.

de la Torre, A., Metivier, A., Chu, F., Laurens, L.M.L., Beck, D.A.C., Pienkos, P.T., et al. (2015). Genome-scale metabolic reconstructions and theoretical investigation of methane conversion in *Methylomicrobium buryatense* strain 5G(B1). *Microb. Cell. Fact.* 14, 188. doi: 10.1186/s12934-015-0377-3.

Deutch, C.E., Soffer, R.L. (1975). Regulation of proline catabolism by Leucyl,Phenylalanyl-tRNA-Protein Transferase. *Proc. Natl. Acad. Sci*. 72, 405-408.

Edgar, R.C. (2004). MUSCLE: multiple sequence alignment with high accuracy and high throughput. *Nucl. Acids Res.* 32, 1792-1797. doi: 10.1093/nar/gkh340.

Edgar, R.C. (2010). Search and clustering orders of magnitude faster than BLAST. *Bioinformatics* 26, 2460-2461. doi: 10.1093/bioinformatics/btq461.

Ettwig, K.F., Butler, M.K., Le Paslier, D. Pelletier, E., Mangenot, S., Kuypers, M.M.M., et al. (2010). Nitrite-driven anaerobic methane oxidation by oxygenic bacteria. *Nature* 464, 543-548. doi: 10.1038/nature08883.

Ferguson, S.J., Richardson, D.J. (2004). "The enzymes and bioenergetics of bacterial nitrate, nitrite, nitric oxide and nitrous oxide respiration," in Respiration in Archaea and Bacteria. Springer, 169-206.

Finn, R.D., Clements, J., Eddy, S.R. (2011). HMMER web server: interactive sequence similarity searching. *Nucleic Acids Res.* 39, W29-W37. doi: 10.1093/nar/gkr367.

Haroon, M.F., Hu, S.H., Shi, Y., Imelfort, M., Keller, J., Hugenholtz, P., et al. (2013). Anaerobic oxidation of methane coupled to nitrate reduction in a novel archaeal lineage. *Nature* 500, 567-570. doi: 10.1038/nature12375.

Giovannoni, S.J., Hayakawa, D.H., Tripp, H.J., Stingl, U., Givan, S.A., et al. (2008). The small genome of an abundant coastal ocean methylotroph. *Environ. Microbiol*. 10:1771-82. doi: 10.1111/j.1462-2920.2008.01598.x.

Güllert S., Fischer M.A., Turaev D., Noebauer B., Ilmberger N., Wemheuer B., et al. (2016). Deep metagenome and transcriptome analyses of microbial communities affiliated with an industrial biogas fermenter, a cow rumen, and elephant feces reveal major differences in carbohydrate hydrolysis strategies. *Biotech. For Biofuel* 9:121. doi: 10.1186/13068-016-0534-x

Hayashi, T., Obata, H., Gamo, T., Sano, Y., Naganuma, T. (2007). Distribution and phylogenetic characteristics of the genes encoding enzymes relevant to methane oxidation in oxygen minimum zones of the eastern Pacific Ocean. *Res. J. Environ. Sci.* 1, 275-284. doi: 10.392/rjes.2007.275.284

Helly, J.J., Levin, L.A. (2004). Global distribution of naturally occurring marine hypoxia on continental margins. *Deep-Sea Res. Pt. I.* 51, 1159-1168. doi: 10.1016/j.dsr.2004.03.009.

Hudson, D.H., Mitra, S., Ruscheweyh, H.J., Weber, N., Schuster, S.C. (2011). Integrative analysis of environmental sequences using MEGAN4. *Genome. Res.* 21, 1552-1560. doi: 10.1101/gr.120618.111.

Hyatt, D., Chen, G.L., LoCascio, P.F., Land, M.L., Larimer, F.W., Hauser, L.J. (2010). Prodigal: prokaryotic gene recognition and translation initiation site identification. *BMC Bioinformatics* 11, 119. doi: 10.1186/1471-2105-11-119.

Iobbi-Nivol, C. Santini, C.L., Blasco, F., Giordano, G. (1990). Purification and further characterization of the second nitrate reductase of *Escherichia coli* K12. *Eur. J. Biochem.* 188, 679-687. doi: 10.1111/j.1432-10.33.1990.tb15450.x

Jensen, S., Neufeld, J.D., Birkeland, N.K., Hovland, M., Murrell, J.C. (2008). Insight into the microbial community structure of a Norwegian deep-water coral reef environment. *Deep-Sea Res. Pt. I.* 55, 1554-1563. doi: 10.1016/j.dsr.2008.06.008.

Kalvelage, T., Lavik, G., Jensen, M.M., Revsbech, N.P., Loscher, C., Schunck, H., et al. (2015). Aerobic microbial respiration In oceanic oxygen minimum zones. *PLOS One* 10, e0133526. doi: 10.1371/journal.pone.0133526.

Kalyuzhnaya, M.G., Lapidus, A., Ivanova, N., Copeland, A.C., McHardy, A.C., et al. (2008). High-resolution metagenomics targets specific functional types in complex microbial communities. *Nat. Biotechnol.* 26, 1029-34. doi: 10.1038/nbt.1488.

Kalyuzhnaya, M.G., Beck, D.A., Suciu, D., Pozhitkov, A., Lidstrom, M.E., Chistoserdova, L. (2010). Functioning in situ: gene expression in Methylotenera mobilis in its native environment as assessed through transcriptomics. *ISME J.* 4, 388-398. doi: 10.1038/ismej.2009.117.

Kalyuzhnaya, M.G., Yang, S., Rozova, O.N., Smalley, N.E., Clubb, J., Lamb, A., et al. (2013). Highly efficient methane biocatalysis revealed in a methanotrophic bacterium. *Nat. Comm.* 4, 2785. doi: 10.1038/ncomms3785.

Kanehisa, M., Goto, S. (2000). KEGG: Kyoto Encyclopedia of Genes and Genomes. *Nucleic. Acids. Res.* 28, 27-30. doi: 10.1093/nar/28.1.27.

Karl, D.M., Beversdorf, L., Bjorkman, K.M., Church, M.J., Martinez, A., DeLong, E.F. (2008). Aerobic production of methane in the sea. *Nat. Geosci.* 1, 473-478. doi: 10.1038/ngeo234.

Keltjens J.T., Pol, A., Reimann, J., Op den Camp, H.J.M. (2014). PQQ-dependent methanol dehydrogenases: rare-earth elements make a difference. *Appl. Microb. Biotech*. 98, 6163-6183. doi: 10.1007/s00253-014-5766-8.

Kennedy, K., Hall, M.W., Lynch, M.D.J., Moreno-Hagelsieb, G., and Neufeld, J.D. (2014). Evaluating bias of Illumina-based bacterial 16S rRNA gene profiles. *Appl. Environ. Microb.* 80, 5717-5722. doi: 10.1128/aem.01451-14.

Kessler, J.D., Valentine, D.L., Redmond, M.C., Du, M.R., Chan, E.W., Mendes, S.D., et al. (2011). A persistent oxygen anomaly reveals the fate of spilled methane in the deep Gulf of Mexico. *Science* 331, 312-315. doi: 10.1126/science.1199697.

Kirschke, S., Bousquet, P., Ciais, P., Saunois, M., Canadell, J.G., Dlugokencky, E.J., et al. (2013). Three decades of global methane sources and sinks. *Nat. Geosci.* 6, 813-823. doi: 10.1038/ngeo1955.

Kits, K.D., Campbell, D.J., Rosana, A.R., Stein, L.Y. (2015a). Diverse electron sources support denitrification under hypoxia in the obligate methanotroph *Methylomicrobium album* strain BG8. *Front. Microb*. 6, 1072. doi: 10.3389/fmicb.2015.01072.

Kits, K.D., Klotz, M.G., Stein, L.Y. (2015b). Methane oxidation coupled to nitrate reduction under hypoxia by the Gammaproteobacterium *Methylomonas denitrificans*, sp nov type strain FJG1. *Environ. Microb.* 17, 3219-3232. doi: 10.1111/1462-2920.12772.

Knief, C. (2015). Diversity and habitat preferences of cultivated and uncultivated aerobic methanotrophic bacteria evaluated based on *pmoA* as molecular marker. *Front. Microb*. 6, 1346. doi: 10.3389/fmicb.2015.01346.

Knittel, K. Boetius, A. (2009). Anaerobic oxidation of methane: Progress with an unknown process. *Ann. Rev. Microb*. 63: 311-344. doi: 10.1146/annurev.micro.61.080706.093130

Konstantinidis, K.T., Tiedje, J.M. (2005). Towards a genome-based taxonomy for prokaryotes. *J. Bacteriol.* 187, 6258-6264. doi: 10.1128/jb.187.18.6258-6264.2005.

Kozich, J.J., Westcott, S.L., Baxter, N.T., Highlander, S.K., Schloss, P.D. (2013). Development of a dual-index sequencing strategy and curation pipeline for analyzing amplicon sequence data on the MiSeq Illumina sequencing platform. *Appl. Environ. Microb.* 79, 5112-5120. doi: 10.1128/aem.01043-13.

Lesniewski, R.A., Jain, S., Anantharaman, K., Schloss, P.D., Dick, G.J. (2012). The metatranscriptome of a deep-sea hydrothermal plume is dominated by water column methanotrophs and lithotrophs. *ISME J*. 6, 2257-2268. doi: 10.1038/ismej.2012.63.

Long, M.C., Deutsch, C., Ito, T. (2016). Finding forced trends in oceanic oxygen. *Global Biogeochem. Cy*. 30, 381-397. doi: 10.1002/2015gb005310.

Ludwig, W., Strunk, O., Westram, R., Richter, L., Meier, H., Yadhukumar, et al., (2004). ARB: a software environment for sequence data. *Nucleic Acids Res.* 32, 1363-1371. doi: 10.1093/nar/gkh293.

Lüker, S., Nowka, B., Rattei, T., Spieck, E., Daims H. (2013). The genome of *Nitrospina gracilis* illuminates the metabolism and evolution of the major marine nitrite oxidizer. *Front. Microb*. 4, 27. doi: 10.3389/fmicb.2013.00027.

Magoč, T., Salzberg, S.L. (2011). FLASH: fast length adjustment of short reads to improve genome assemblies. *Bioinformatics* 27, 2957-2963. doi: 10.1093/bioinformatics/btr507.

Mauffrey, F., Martineau, C., Villemur, R. (2015). Importance of the two dissimilatory (Nar) nitrate reductases in the growth and nitrate reduction of the methylotrophic marine bacterium *Methylophaga nitratireducenticrescens* JAM1. *Front. Microb*. 6, 1475. doi: 10.3389/fmicb.2015.01475.

Mikheenko, A., Saveliev, V., Gurevich, A. (2016). MetaQUAST: evaluation of metagenome assemblies. *Bioinformatics* 32, 1088-1090. doi: 10.1093/bioinformatics/btv697.

Naqvi, S.W.A., Bange, H.W., Farias, L., Monteiro, P.M.S., Scranton, M.I., and Zhang, J. (2010). Marine hypoxia/anoxia as a source of CH_4 and N_2O. *Biogeosciences* 7, 2159-2190. doi: 10.5194/bg-7-2159-2010.

Nurk, S., Bankevich, A., Antipov, D., Gurevich, A.A., Korobeynikov, A., Lapidus, A., et al. (2013). Assembling single-cell genomes and mini-metagenomes from

chimeric MDA products. *J. Comput. Biol*. 20(10), 714-737. doi: 10.1089/cmb.2013.0084.

Op den Camp, H.J.M., Islam, T., Stott, M.B., Harhangi, H.R., Hynes, A., Schouten, S., et al. (2009). Environmental, genomic and taxonomic perspectives on methanotrophic Verrucomicrobia. *Environ. Microb. Rep.* 1, 293-306. doi: 10.1111/j.1758-2229.2009.00022.x.

Pack, M.A., Heintz, M.B., Reeburgh, W.S., Trumbore, S.E., Valentine, D.L., Xu, X.M., et al. (2015). Methane oxidation in the eastern tropical North Pacific Ocean water column. *J. Geophys. Res. Biogeo.* 120, 1078-1092. doi: 10.1002/2014jg002900.

Padilla, C.C., Bristow, L.A., Sarode, N., Garcia-Robledo, E., ER, R., Benson, C.R., et al. (2016). NC10 bacteria in marine oxygen minimum zones. *ISME J*. 10, 2067-2071. doi: 10.1038/ismej.2015.262.

Padilla, C.C., Ganesh, S., Gantt, S., Huhman, A., Parris, D.J., Sarode, N., et al. (2015). Standard filtration practices may significantly distort planktonic microbial diversity estimates. *Front. Microb.* 6, 547. doi: 10.3389/fmicb.00547.

Parks, D.H., Imelfort, M., Skennerton, C.T., Hugenholtz, P., Tyson, G.W. (2015). CheckM: assessing the quality of microbial genomes recovered from isolates, single cells, and metagenomes. *Genome Res.* 25(7), 1043-1055. doi: 10.1101/gr.186072.114.

Philippot, L. (2002). Denitrifying genes in Bacterial and Archaeal genomes. Biochim. Biophys. Acta 1577, 355-376. doi: 10.1016/s0167-4781(02)00420-7.

Poehlein, A., Deutzmann, J.S., Daniel, R., Simeonova, D.D. (2013). Draft genome sequence of the methanotrophic gammaproteobacterium *Methyloglobulus morosus* DSM 22980 strain KoM1. *Genome Ann.* 1, e01078-01013. doi: 10.1128/genomeA.01078-13

Raes, J., Korbel, J.O., Lercher, M.J., von Mering, C., Bork, P. (2007). Prediction of effective genome size in metagenomic samples. *Genome Biol.* 8, R10. doi: 10.1186/gb-2007-8-1-r10.

Raghoebarsing, A.A., Pol, A., van de Pas-Schoonen, K.T., Smolders, A.J.P., Ettwig, K.F., Rijpstra, W.I.C., et al. (2006). A microbial consortium couples anaerobic methane oxidation to denitrification. *Nature* 440, 918-921. doi: 10.1038/nature04617.

Ramachandran, A., Walsh, D.A. (2015). Investigation of XoxF methanol dehydrogenases reveals new methylotrophic bacteria in pelagic marine and freshwater ecosystems. *FEMS Microbiol. Ecol*. 97, 10. doi: 10.1093/femsec/fiv105.

Reeburgh, W.S. (2007). Oceanic methane biogeochemistry. *Chem. Rev.* 107, 486-513. doi: 10.1021/cr050362v.

Revsbech, N.P. (1989). An oxygen microsensor with a guard cathode. *Limnol. Oceanogr.* 34, 474-478. doi: 10.4319/lo.1989.34.2.0474

Rivers, A.R., Sharma, S., Tringe, S.G., Martin, J., Joye, S.B., Moran, M.A. (2013). Transcriptional response of bathypelagic marine bacterioplankton to the Deepwater Horizon oil spill. *ISME J.* 7, 2315-2329. doi: 10.1038/ismej.2013.129.

Rodriguez-R, L.M., Konstantinidis, K.T. (2016). The enveomics collection: a toolbox for specialized analyses of microbial genomes and metagenomes. *PeerJ Preprints*. No. e1900v1

Sansone, F.J., Popp, B.N., Gasc, A., Graham, A.W., Rust, T.M. (2001). Highly elevated methane in the eastern tropical North Pacific and associated isotopically enriched fluxes to the atmosphere. *Geophys. Res. Lett.* 28, 4567-4570. doi: 10.1029/2001gl013460.

Schmieder, R., Lim, Y.W., Edwards, R. (2012). Identification and removal of ribosomal RNA sequences from metatranscriptomes. *Bioinformatics* 28, 433-435. doi: 10.1093/bioinformatics/btr669.

Sekiguchi Y., Osashi A., Parks D.H., Yamauchi T., Tyson G.W., Hugenholtz P. (2015). First genomics insights into members of a candidate bacterial phylum responsible for wastewater bulking. *PeerJ*.. 3, e740. doi: 10.7717/peerj.740

Shi, Y.M., Tyson, G.W., Eppley, J.M., DeLong, E.F. (2011). Integrated metatranscriptomic and metagenomic analyses of stratified microbial assemblages in the open ocean. *ISME J.* 5, 999-1013. doi: 10.1038/ismej.2010.189.

Sievers, F., Wilm, A., Dineen, D., Gibson, T.J., Karplus, K., Li, W.Z., et al. (2011). Fast, scalable generation of high-quality protein multiple sequence alignments using Clustal Omega. *Mol. Syst. Biol.* 7, 539. doi: 10.1038/msb.2011.75.

Stewart, F.J., Ulloa, O., DeLong, E.F. (2012). Microbial metatranscriptomics in a permanent marine oxygen minimum zone. *Environ. Microbiol.* 14, 23-40. doi: 10.1111/j.1462-2920.2010.02400.x.

Stocker, T., Qin, D., Plattner, G., Tignor, M., Allen, S., Boschung, J., et al. (2013). "IPCC, 2013: climate change 2013: the physical science basis. Contribution of working group I to the fifth assessment report of the intergovernmental panel on climate change". Cambridge, United Kingdom and New York, NY USA: Cambridge University Press.

Stramma, L., Johnson, G.C., Sprintall, J., Mohrholz, V. (2008). Expanding oxygen-minimum zones in the tropical oceans. *Science* 320, 655-658. doi: 10.1126/science.1153847.

Tamura, K., Stecher, G., Peterson, D., Filipski, A., Kumar, S. (2013). MEGA6: Molecular Evolutionary Genetics Analysis Version 6.0. *Mol. Biol. Evol.* 30, 2725-2729. doi: 10.1093/molbev/mst197.

Tavormina, P.L., Orphan, V.J., Kalyuzhnaya, M.G., Jetten, M.S.M., Klotz, M.G. (2011). A novel family of functional operons encoding methane/ammonia monooxygenase-related proteins in gammaproteobacterial methanotrophs. *Environ. Microbiol. Rep.* 3, 91-100. doi: 10.1111/j.1758-2229.2010.00192.x.

Tavormina, P.L., Ussler, W., Joye, S.B., Harrison, B.K., Orphan, V.J. (2010). Distributions of putative aerobic methanotrophs in diverse pelagic marine environments. *ISME J*. 4, 700-710. doi: 10.1038/ismej.2009.155.

Tavormina, P.L., Ussler, W., Orphan, V.J. (2008). Planktonic and sediment-associated aerobic methanotrophs in two seep systems along the North American margin. *Appl. Environ. Microbiol.* 74, 3985-3995. doi: 10.1128/aem.00069-08.

Tavormina, P.L., Ussler, W., Steele, J.A., Connon, S.A., Klotz, M.G., Orphan, V.J. (2013). Abundance and distribution of diverse membrane-bound monooxygenase (Cu-MMO) genes within the Costa Rica oxygen minimum zone. *Environ. Microbiol. Rep.* 5, 414-423. doi: 10.1111/1758-2229.12025

Thamdrup, B. (2012). New pathways and processes in the global nitrogen cycle. *Ann. Rev. Ecol. Evol. S.* 43, 407-428. doi: 10.1146/annurev-ecolsys-102710-145048

Thamdrup, B., Dalsgaard, T., Revsbech, N.P. (2012). Widespread functional anoxia in the oxygen minimum zone of the Eastern South Pacific. *Deep-Sea Res. Pt. I.* 65, 36-45. doi: 10.1016/j.dsr.2012.03.001.

Theodosiou, E., Frick, O., Bühler, B., and Schmid, A. (2015). Metabolic network capacity of *Escherichia coli* for Krebs cycle-dependent proline hydroxylation. *Microb. Cell Fact*. 14:108. doi: 10.1186/s12934-015-0298-1.

Tiano, L. Garcia-Robledo, E. Dalsgaard, T. Devol, A.H., Ward, B.B,. Ulloa, O. (2014). Oxygen distribution and aerobic respiration in the north and south eastern tropical Pacific oxygen minimum zones. *Deep-Sea Res. Pt. I.* 94, 173-183. doi: 10.1016/j/dsr.2014.10.001

Tsementzi, D., Wu, J., Deutsch, S., Nath, S., Rodriguez-R, L.M., Burns, A.S., et al. (2016). SAR11 bacteria linked to ocean anoxia and nitrogen loss. *Nature* 536, 179-183. doi: 10.1038/nature19068

Ulloa, O., Canfield, D.E., DeLong, E.F., Letelier, R.M., Stewart, F.J. (2012). Microbial oceanography of anoxic oxygen minimum zones. *P. Natl. Acad. Sci. USA*. 109, 15996-16003. doi: 10.1073/pnas.1205009109.

Valentine, D.L. (2011). Emerging topics in marine methane biogeochemistry. *Annu. Rev. Mar. Sci.* 3, 147-171. doi: 10.1146/annurev-marine-120709-142734.

Ward, B.B., Kilpatrick, K.A., Wopat, A.E., Minnich, E.C., Lidstrom, M.E. (1989). Methane oxidation in Saanich Inlet during summer stratification. *Cont. Shelf. Res.* 9, 65-75. doi: 10.1016/0278-4343(89)90083-6.

Ward, N., Larsen, O., Sakwa, J., Bruseth, L., Khouri, H., Durkin, A.S., et al. (2004). Genomic insights into methanotrophy: The complete genome sequence of *Methylococcus capsulatus* (Bath). *PLOS Biol*. 2, 1616-1628. doi: 10.1371/journal.pbio.0020303.

Wasmund, K., Kurtboke, D.I., Burns, K.A., Bourne, D.G. (2009). Microbial diversity in sediments associated with a shallow methane seep in the tropical Timor Sea of Australia reveals a novel aerobic methanotroph diversity. *FEMS Microbiol. Ecol.* 68, 142-151. doi: 10.1111/j.1574-6941.2009.00667.x.

Wiezorek A.S., Drake H.L., Kolb, S. Organic acids and ethanol inhibit the oxidation of methane by mire methanotrophs. (2011). *FEMS Microbiol. Ecol*. 77, 28-39. doi: 10.1111/j.1574-6941.2011.01080.x.

Wright, J.J., Konwar, K.M., Hallam, S.J. (2012). Microbial ecology of expanding oxygen minimum zones. *Nat. Rev. Microbiol*. 10, 381-394. doi: 10.1038/nrmicro2778.

Wu, Y.W., Simmons, B.A., Singer, S.W. (2016). MaxBin 2.0: an automated binning algorithm to recover genomes from multiple metagenomic datasets. *Bioinformatics* 32, 605-607. doi: 10.1093/bioinformatics/btv638.

Wyrtki, K. (1962). The oxygen minima in relation to ocean circulation. *Deep-Sea Res.* 9, 11-23. doi: 10.1016/0011-7471(62)90243-7.

CHAPTER 5.

CONCLUSION AND SUGGESTIONS

This dissertation combines metagenomics, transcriptomics, and biochemical rate measurements to confirm OMZs as a niche space for methanotrophy coupled to N loss. A secondary goal of this work is to establish best practices when sampling environments for microbial diversity. In Ch. II it was shown that the volume of seawater filtered impacts diversity estimates of 16S rRNA microbial diversity when using a common method to size-fractionate pelagic microbial populations. In both Ch. III and IV 16S rRNA sequences were initially used to characterize microbial diversity in the ETNP and the GD. While this method failed to recover NC10 sequences in Ch.III, metatranscriptomics and chemical rate data pointed to OMZs as being a suitable niche for the NC10 N-DAMO process. In the Golfo Dulce (Ch. IV), 16S amplicon analysis recovered a high abundance of methanotroph-like sequences, but metagenomic binning recovered *nar* and *nir* enzymes in the OPU3 genome, thus linking this uncultivated group of gammaproteobacteria methanotrophs to denitrification. These findings suggests that implementing 16S amplicon diversity surveys is a crucial first step for characterizing microbial communities, but meta–omic and rate analyses are needed to better contextualize biogeochemical reactions.

5.1 OMZs as a niche for CH_4 oxidation coupled to N loss

The results from this thesis confirm OMZs as a niche for microbial metabolisms linking CH_4 consumption with N loss (Ch. III and IV). These findings identify another route of N loss within OMZs in addition to classical denitrification and anammox. The extent to which denitrification-dependent methanotrophy contributes to N loss and C cycling remains unknown. However, as OMZs expand with global warming, the microbes linking methanotrophy to N loss at these sites may become an important CH_4 sink.

The two mechanisms for OMZ methanotrophy described in this thesis are distinct from each other, although both pathways contribute to N loss. The NC10 N-DAMO reaction (Ch. III), which involves the intracellular generation of O_2, provides a powerful oxidative electron sink in a region that is functionally devoid of O_2. This process extended from the NO_2^- maxima to the OMZ core. NC10 *nar* transcripts, which produce NO_2^- from NO_3^-, were detected in the OMZ core and could provide a crucial NO_2^- source that is removed from the NO_2^- maximum. This allows NC10 to persist in the OMZ core were CH_4 concentrations are highest. Moreover the dismutation reaction could offer a vector of non-photosynthetic O_2 in the OMZ core. Despite the intracellular nature of the O_2 production, microbial cells lyse frequently, thus releasing O_2 into the anoxic core for rapid reduction by other microbes. Some the most abundant microorganisms in the OMZ core transcribe terminal oxidases, including SAR11. These enzymes allow microbes to rapidly make use of any freely available O_2, yielding a powerful thermodynamic advantage in this anoxic habitat (Appendix D).

The second metabolism was detected in a uncultivated gammaproteobacterium from the OPU3 clade. This microbe transcribes genes for methanotrophy and partial

denitrification (Ch. IV). This reaction supports respiration under low O_2 conditions and allows for any available O_2 to be used directly for CH_4 oxidation. While this strategy has been described previously in culture systems, this work provides the first meta-omic evidence for methanotrophy supported by partial denitrification in natural environments. This work also achieved the first description of a potential mechanism for pelagic aerobic methanotrophs to survive in OMZs by assembling the first draft-genome of a pelagic methanotroph that was only detected by marker gene surveys.

This thesis provides compelling evidence that OMZs are suitable niches for denitrification-dependent CH_4 oxidation. However, there are more questions in this topic. For example, other pelagic OPU clades have also been detected at OMZ periphery, these OPUs lack genomic characterization, and have only been described through 16S or *pmo* PCR surveys. Moreover, there are still many questions about the mechanisms that govern the population dynamics and chemical parameters that govern the realized niche space of pelagic methanotrophs.

5.2 Suggestions and further questions

To expand upon the work presented here, there are some key questions that should be further addressed. One of the most pertinent questions is how O_2 concentrations impact the distribution and metabolic activity of pelagic methanotrophs. Given the results from this thesis, O_2 is key oxidant for pelagic methanotrophs either by intracellular generation or by direct utilization from the environment. As OMZs are projected to expand, the role of dissolved O_2 could be a crucial factor in determining

which biochemical processes or microbial populations become selected for as the prominent pathway for CH_4 loss. Recent work in the ETNP shows that increased O_2 concentrations impeded CH_4 oxidation in water taken from the OMZ core (Thamdrup, private communication). As NC10 were the only methanotrophs detected in the OMZ core, this suggests that extracellular oxygen can significantly impact the NC10 N-DAMO processes. This O_2-based inhibition has been described in the transcriptional patterns of the NC10 representative *M. oxyfera*. Roughly half of the genome was down regulated upon exposure to microaerobic conditions (Luesken et al., 2012). It is unclear why NC10 is negatively impacted by microaerobic conditions. However, it has been shown that similar O_2 exposure suppresses the N loss capacity in OMZ microbial communities. NC10 suppression from O_2 exposure could be caused by similar mechanisms. Luesken et al., (2012) reported that most of the N reduction genes were down regulated indicating a strong reliance of the NC10 electron transport chain on denitrification and any external O_2 could disrupt the denitrification pathway.

In the case of OPU3, and other aerobic methanotrophs found in low O_2 environments, it is unclear what the O_2 source is for CH_4 oxidation. In OMZs microaerobic pockets of O_2 can be detected even into the anoxic core. Throughout the OMZ many microbial taxa transcribe terminal oxidases to rapidly take advantage of these O_2 "whiffs" (Appendix D). OPU3 bacteria genomes contain these terminal oxidases, however they were not transcribed in Ch. IV. This is taken as evidence that any available O_2 is used by actively transcribed *pmo*. The distribution of OPU3 in the water column peaks at the upper boundary of the NO_2^- maximum and lower boundary of the chlorophyll maximum. It has been recently demonstrated that high concentrations of

chlorophyll in OMZs generate enough O_2 to support O_2-dependent oxidative metabolisms despite O_2 being undetectable (Appendix D). Confirming this source of O_2 could be achieved with isotopic measurements tracking photosynthetic-generated O_2 through the methanotrophic reactions. Adding ^{18}O labeled CO_2 and to seawater incubations at different light levels the photosynthetic reaction would produce $^{18}O_2$ from the CO_2. In addition ^{13}C labeled CH_4 would also be added to the seawater and the methanotroph reaction would use the $^{18}O_2$ and $^{13}CH_4$ as substrates. The CO_2 resulting from CH_4 oxidation would contain both the labeled substrates as $^{13}C^{18}O_2$. This would be difficult to do as CH_4 oxidation rates in OMZs are very low, and there are many biological reactions that generate CO_2. The sensitivity for this process would need to comparable to using tritiated CH_4 to track CH_4 oxidation.

This dissertation highlights the genomic and metabolic diversity of OMZ methanotrophs. These findings directly support other research that demonstrates the wide range of metabolic strategies for energy generation and C utilization that methanotrophs display in O_2-limiting conditions. One such strategy is to use CH_4-derived C for fermentation (Gilman et al., 2017; Kalyuzhnaya et al., 2013). Aerobic methanotroph strains from the *Methylomicrobium* genus have been shown to excrete fermentation products such as succinate, acetate, lactate, and H_2 under O_2 starvation. As O_2 becomes limiting NADH can accumulate from formaldehyde oxidation to CO_2 by the methanotrophy pathway, with this NADH build up causing an intracellular redox imbalance. Excretion of fermentation products can inhibit oxidative production of NADH by shunting formaldehyde into the RuMP cycle, thus alleviating potential redox imbalance by suppressing NADH generation by formaldehyde and formic acid oxidation

(Gilman et al., 2017). In these cases CH_4 is only used as a C source to generate methanol, which is subsequently used for pyruvate synthesis (Gilman et al., 2017; Kalyuzhnaya et al., 2013). Pyruvate can then be feed into various fermentation pathways.

It is thus far unknown if this type of redox balancing by fermentation could play a role in OMZ methanotrophs. In the anoxic conditions of the ETNP and the GD, transcripts mediating succinate and acetate generation were detected and taxonomically associated with denitrifying methanotrophs. Transcripts encoding genes for succinate generation were detected among OPU3 methanotroph-associated sequences from the GD, while genes for acetate production were detected in NC10-associated transcript pools from both the ETNP and the GD. Key genes for succinate production that were detected in the OPU3 transcript pool included those encoding malate dehydrogenase (Mdh), fumarase (FumA), and succinate dehydrogenases (Sdh). NC10-like transcripts for acetyl CoA synthetase (Acs) and acetate kinase (Ack) were recovered from both sites. The transcription patterns of OPU3, in particular, support methanotroph fermentation. OPU3 appears to generate energy from denitrification, not from CH_4 oxidation, and the succinate production pathway is actively transcribed. However, detection of these transcripts is indirect evidence. The potential for this hybrid metabolism, of denitrification-dependent respiration coupled to fermentation, to contribute to OMZ methane consumption requires further validation.

Along with the further work on describing the biogeochemical constraints on pelagic OMZ methanotrophs, there is a severe lack of genomic data regarding these microorganisms. This has hindered the ability to detect methanotrophs in natural

environments and to assess their metabolic potential. The lack of genomic data on OMZ methanotrophs is, in part, do to their low abundance. Genomic data and better detection of OMZ methanotrophs could become more attainable if certain steps are taken. One such step would be to obtain enrichments or cultures of OMZ methanotrophs. In general, there are very few OMZs microbes with cultured representatives. As such, annotation of microbial sequence data relies on the databases built on organisms that do not always reflect the communities being sampled. Culturing or even enriching microbial taxa from OMZs is no trivial task due to a multitude of reasons: i) the complexity of maintaining anoxic conditions when collecting OMZ water, ii) isolating microbes from natural systems may remove a key substrates, iii) toxins could accumulate in the incubation, iv) culture media may lack substrates as the chemical make up of seawater has yet to be fully characterized, v) viruses may disrupt growth. These are just a few examples of why obtaining oceanic microbial isolates is so difficult. We attempted to enrich for denitrifying methanotrophs in the ETNP and the GD. The results of these enrichments were inclusive, however the enrichment media demonstrated decreasing concentrations of NO_3^- and NO_2^- over the incubation time. Additionally OTUs affiliated with the *Methylophaga* genus appeared to increase with time (Appendix E). Culturing OMZ microbes would allow for profound insight to how microbial populations function in these low O_2 systems.

A second and powerful method would be to design and implement degenerate index primers of both the *pmoA* and *narG* genes for high-throughput sequencing. Such primers exist for the 16S rRNA gene and the ammonia monooxygenase gene, *amoA*. These existing primers have facilitated an unprecedented amount of information about

microbial population dynamics, microbome surveys, and diversity associated with global biogeochemical processes. A similar set of primers could reveal much of the methanotroph population dynamics far beyond OMZ environments. These types of primers would allow for powerful statistical analyses and the ability to find correlations to environmental parameters. Assessing enzymatic diversity patterns at this level will allow research to move beyond descriptive studies and towards predictive modeling. As the planet undergoes changes from warming, it is important to predict what metabolisms and taxa will be selected for and therefore exert strong influence future biogeochemical cycles.

5.3 Final remarks

OMZs are crucial sites for oceanic biogeochemical transformations and impact global chemical budgets. Microbes linking methanotrophy to N loss may have a disproportionate biogeochemical role compared to their abundance. There are very few taxa that encode the ability to consume CH_4 in OMZs, and OMZ methanotrophs appear to constitute a small fraction of OMZ microbes. OMZs represent the largest pool of pelagic CH_4, yet very little of this CH_4 escapes to the atmosphere, it is unclear how so such a small number of cells is responsible for this. As OMZs expand, the role of this process will expand as well. Therefore, characterizing microbial communities implicated in methanotrophy in OMZs is an important step in constraining and predicting OMZs role in global N and C cycles.

APPENDIX A.

CRYPTIC OXYGEN CYCLING IN ANOXIC MARINE ZONES

Disclaimer: This chapter was published with the same title, along with the, in the journal Proceedings of the National Academy of Sciences, USA on July 17, 2017.

Citation: **Garcia-Robledo, E., Padilla, C. C., Bertagnolli, A.D., Aldunate, M., Stewart, F. J., Ulloa, O., Paulmier, A., Gregori, G., Revsbech, N.P.** (2017). Cryptic oxygen cycling in anoxic marine zones. *PNAS USA*, *144*.

A.1 Abstract

Oxygen availability drives changes in microbial diversity and biogeochemical cycling between the aerobic surface layer and the anaerobic core in nitrite-rich anoxic marine zones (AMZs), which constitute huge oxygen-depleted regions in the tropical oceans. The current paradigm is that primary production and nitrification within the oxic surface layer fuel anaerobic processes in the anoxic core of AMZs, where 30–50% of global marine nitrogen loss takes place. Here we demonstrate that oxygenic photosynthesis in the secondary chlorophyll maximum (SCM) releases significant amounts of O_2 to the otherwise anoxic environment. The SCM, commonly found within AMZs, was dominated by the picocyanobacteria Prochlorococcus spp. Free O_2 levels in this layer were, however, undetectable by conventional techniques, reflecting a tight coupling between O_2 production and consumption by aerobic processes under apparent anoxic conditions. Transcriptomic analysis of the microbial community in the seemingly anoxic SCM revealed the enhanced expression of genes for aerobic processes, such as nitrite oxidation. The rates of gross O_2 production and carbon fixation in the SCM were found to be similar to those reported for nitrite oxidation, as well as for anaerobic dissimilatory nitrate reduction and sulfate reduction, suggesting a significant effect of local oxygenic photosynthesis on Pacific AMZ biogeochemical cycling.

A.2 Introduction

In coastal zones of the eastern tropical Pacific Ocean, the upward transportation of nutrient-rich waters results in relatively high primary productivity at surface depths.

Sinking of organic matter produced by surface production coupled with sluggish circulation leads to the formation of oxygen-deficient water masses at intermediate depths below the mixed layer. Due to strong stratification, these oxygen minimum zones (OMZs) extend far offshore over vast swaths of the eastern Pacific. In these regions, oxygen availability plays a major role in structuring organism distributions and biogeochemical processes in the pelagic ocean (Paulmier et al., 2009).

Recently developed sensor techniques (Revsbech et al., 2011) show that in much of the OMZ water column, from about 30–100 m to about 800 m, O_2 concentrations fall below sensor-specific detection limits of down to 3 nmol L^{-1} ($3 \cdot 10^{-9}$moles per liter) (Thamdrup et al., 2012; Tiano et al., 2014). OMZs in the eastern tropical North and South Pacific (ETNP and ETSP, respectively) and in the Arabian Sea are subject to such intense O_2 depletion and therefore have been redefined as anoxic marine zones (AMZs) (Ulloa et al., 2012). In other oceanic OMZs, including in the Bay of Bengal and northeast Pacific, oxygen concentrations may decrease to a few micromolar, but total O_2 depletion occurs only occasionally (Bristow et al., 2017). AMZs are often distinguished from more oxygen-replete OMZs by the accumulation of nitrite, which is typically most pronounced when O_2 falls below the nanomolar detection limit (Ulloa et al., 2012; Bristow et al., 2017; Canfield et al., 2010; Ganesh et al., 2015). Nitrite is a key substrate in microbial N_2 and N_2O production by either denitrification or anaerobic ammonium oxidation (anammox), which together in AMZs mediate 30–50% (Codispoti et al., 2001) of the marine recycling of inorganic nitrogen compounds (nitrate, nitrite, and ammonium) to atmospheric N_2.

Nitrite is also produced and consumed in the aerobic nitrification pathway involving the two-step process of aerobic ammonia and nitrite oxidation (Dalsgaard et al., 2012; Babbin et al., 2014). Despite the absence of measureable O_2 in the core of eastern Pacific AMZs, biomolecular evidence (DNA, RNA, and proteins) indicates the presence of aerobic microbial processes. The expression of genes encoding for nitrification and other O_2-dependent microbial metabolisms, potentially including heterotrophic respiration, have been found well below the oxycline (Stewart et al., 2012; Kalvelage et al., 2015), raising the question of how aerobic processes could persist under apparent anoxia.

In the three oceanic AMZs of the Arabian Sea, ETNP, and ETSP, dense populations of phototrophs have been observed at the base of the photic zone but below the oxycline that separates oxic from anoxic waters (Lavin et al., 2010; Goericke et al., 2000; Cepeda-Morales et al., 2009). This deep secondary chlorophyll maximum (SCM) is mainly composed of novel, yet uncultivated, lineages of the cyanobacterium *Prochlorococcus* (Lavin et al., 2010), with chlorophyll concentrations that can equal that of the primary chlorophyll peak near the surface (Cepeda-Morales et al., 2009). The presence of this large population of putative oxygenic phototrophs has suggested a mechanism by which aerobic metabolism can be maintained in a zone where in situ measurements indicate anoxic conditions (Ulloa et al., 2012). Although an active photosynthetic community produces and releases oxygen to the environment, coupled O_2 consumption by an aerobic microbial community may keep seawater O_2 concentration at very low and possibly subnanomolar levels, thereby resulting in a cryptic O_2cycle. The

existence of such a cryptic oxygen cycle has been suggested by biomolecular evidence (Stewart et al., 2012) but has not yet been demonstrated.

In this study we used a combination of high-resolution oxygen profiling, metabolic rate measurements, and community mRNA sequencing to explore the potential for oxygen cycling in the SCMs of the ETNP off Mexico and the ETSP off Peru. Our results show that the photosynthetic community of the SCM produces significant amounts of O_2, sufficient to maintain an aerobic community in an otherwise anoxic environment. Rates of O_2production and carbon fixation in the SCM in both ETNP and ETSP AMZs are comparable to previously measured rates of aerobic processes like nitrite and ammonium oxidation (Ganesh et al., 2015; Bristow et al., 2016), as well as anaerobic AMZ processes like denitrification, anammox, and sulfate reduction (Canfield et al., 2010; Ganesh et al., 2015). Although the measured metabolic rates exhibit large spatial and temporal variability, our data collectively suggest a significant effect of local photosynthesis on the biogeochemical cycling in Pacific Ocean AMZs.

A.3 Materials and Methods

A.3.1 Sampling sites and in situ measurements

The two main oxygen minimum zones of the ETSP and ETNP were investigated during two cruises during 2014: the Activities of Research Dedicated to the Minimum of Oxygen in the Eastern Pacific cruise on the R/V *L'Atalante* to the ETSP off Peru during late January and February 2014 and the Oxygen Minimum Zone Microbial Biogeochemistry Expedition 2 (OMZoMBiE2) cruise on the R/V *New Horizon* to the

ETNP region off Mexico during May–June 2014. Profiles of physical and chemical variables were obtained with a Seabird SBE-911 CTD system, equipped with a SBE 43 oxygen sensor and a Seapoint Chlorophyll Fluorimeter (R/V *New Horizon*) or a Chelsea Aqua 3 fluorimeter (R/V *L'Atalante*). CTD sensors were calibrated according to the manufacturer. The fluorometers used for the determination of chlorophyll were calibrated using pure chlorophyll solutions in 90% acetone (from 0.1 to 100 μg/L). In the ETNP, a pump profiling system (PPS) was also used for water collection. High-resolution O_2profiling was performed during the CTD and PPS casts during the ETNP cruise. A high-resolution STOX sensor (Revsbech et al., 2011; Revsbech et al., 2009) was used to measure O_2 concentration at nanomolar levels as described previously (Revsbech et al., 2011; Tiano et al., 2014).

A.3.2 Flow cytometry analysis

Samples for cell counts were taken at several depths from the rosette (ETNP and ETSP) and the PPS (ETNP), fixed with glutaraldehyde and stored at −80 °C until analysis. Cell abundance was determined by flow cytometry using a FACSCalibur flow cytometer (Beckton Dickinson). *Prochlorococcus*, *Synechococcus*, and other autofluorescent cells (identified as picoeukaryotes) were counted in untreated samples, whereas autofluorescent plus nonautofluorescent cells (bacteria + archaea, referred as total microbial community) were analyzed by staining the cells with SYBR Green (Molecular Probes) as described previously (Lebaron et al., 1998; Grégori et al., 2001).

A.3.3 Oxygen production and carbon fixation measurements

Water samples from the SCM were collected using Niskin bottles or a PPS. To minimize the O_2 leaking from the polymers of the Niskin bottles, the water was transferred to a 20-L glass bottle previously purged with N_2 gas as soon as the rosette was on deck. If the samples were collected using the PPS, the 20-L glass bottle purged with N_2 gas was filled directly from the outlet of the PPS. A certain O_2 contamination (1–5 $\mu mol \cdot L^{-1}$) during the sampling procedure could not be avoided, and the seawater was therefore immediately degassed in the 20-L bottle by bubbling with N_2 + 0.05% CO_2. A STOX sensor was inserted inside the bottle to determine when anoxia was approached (<100 nmol $O_2 \cdot L^{-1}$). After adjusting the O_2 concentration to 100–400 $nmol \cdot L^{-1}$, samples were siphoned to custom made incubation vessels (n = 12–16) (Tiano et al., 2014; Garcia-Robledo et al., 2016), containing either STOX sensors (ETSP) or a combination of STOX and optode sensors with a measuring range of 0–1,000 $nmol \cdot L^{-1}$ (Garcia-Robledo et al., 2016; Lehner et al., 2015) (ETNP). Each vessel was placed inside a light incubation tube immersed in a constant temperature water bath, enabling maintenance of in situ temperature (14–15 °C) and quantification of very low O_2 transformation rates. The light incubation tubes consisted of a black PVC tube with white LEDs (LF06S-W3F-850; OSRAM) installed along the whole periphery of the tube and with a custom-built waterproof magnetic stirrer fitted at the bottom. The LEDs were covered with a blue filter (131 Marine Blue filter; LEE Filters) to simulate the in situ light spectrum. Oxygen concentrations (Fig. 2) throughout the incubation period (8–12 h) were measured in treatments spanning a range of bluish light intensities slightly above maximum in situ levels (10, 20, and 40 μmol photons m^{-2} s^{-1}) and in darkness (n = 3–4, per treatment).

Rates of oxygen consumption or production (here named NCP) were obtained by linear regression of the oxygen evolution during the incubations. GCP rates were calculated by subtracting the mean respiration value (NCP rate measured in darkness) from the NCP rates measured at different irradiances.

Rates of carbon incorporation were measured simultaneously during the incubations for oxygen measurements using stable (ETNP) or radioactive (ETSP) isotopes. Incubations amended with $Na^{14}C\text{-}HCO_3$ (450 μCi/L final concentration) were done in parallel incubation bottles of only 110 mL following the procedure described by Telling et al. 2010. Incubations amended with $Na^{13}C\text{-}HCO_3$ (0.27 mM ^{13}C final concentration) were done in the same incubation bottles used for O_2measurements. Incorporation of ^{14}C was measured by counting on a Perking Elmer Tri-Carb 2900 TR scintillation counter, whereas the ^{13}C incorporation was analyzed in an Elemental Analyzer (Thermo Elemental Analyzer Flash EA 1112 HT) coupled to an Isotope Ratio Mass Spectrometer (Delta V; Thermo Scientific). The ^{13}C enrichment in the produced organic carbon was calculated as the difference between the amounts of ^{13}C in the sample minus the natural ^{13}C abundance measured on blank filters. Decays per minute values (^{14}C incubations) and ^{13}C incorporation were converted to ^{12}C uptake values or GCP (nmol C L^{-1} h^{-1}) rates using the formula described in Telling et al. 2010.

A.3.3 Rates modeling and upscaling of processes

The photosynthesis–irradiance model described by Jassby and Platt, 1976 was fitted to the measured GCP (nmol L^{-1} h^{-1}) rates for both O_2 production and C assimilation as calculated by equation 1.

$$GCP=GCPmax\times\tanh(\alpha\times E/GCPmax),GCP=GCPmax\times\tanh(\alpha\times E/GCPmax) \quad (1)$$

where GCP_{max} (nmol L^{-1} h^{-1}) is the maximum gross community production rate, reached at saturating irradiances, tan(h) is the hyperbolic tangent, α [(nmol L^{-1} h^{-1}) (µmol photons m^{-2} s^{-1})$^{-1}$] is an index of the photosynthetic efficiency, and E (µmol photons m^{-2} s^{-1}) is the spherical irradiance.

The obtained parameters were normalized by the chlorophyll concentration and used to estimate the in situ O_2production and C fixation using the light and chlorophyll profiles measured in the SCM by the fluorescence and photosynthetic active radiation (PAR) sensors connected to the CTD (ETSP cruise) or the PPS (ETNP cruise). During the ETSP cruise off Peru, casts were consistently repeated every 3–4 h, and thus, the light profiles from the CTD were used in our calculations. During the ETNP cruise, light profiles measured with the PPS during daytime were normalized to the incident irradiance at the surface. The light attenuation profiles were assumed to be constant at each station, and the incident irradiance was used to calculate the change in light profile during the day. The values of incident irradiance were taken from the closest National Radiation station located in San Diego (National Solar Radiation Database, National Oceanic and Atmospheric Administration, United States).

A.3.3 Metatranscriptome analysis

Community cDNA sequencing was used to characterize microbial gene transcription in biomass (retained on 0.22-μm filters) from a subset of AMZ samples at the ETNP region off Mexico. These included samples collected during the OMZoMBiE2 cruise (2014) and a subset of samples previously reported by Padilla et al. 2016. Seawater from discrete depths spanning the oxic zone, SCM, lower oxycline, upper AMZ, and AMZ core was collected using Niskin bottles or the PPS. The sampling, preservation, RNA extraction, and sequencing were done following the procedure described by Padilla et al. 2016. Barcoded sequences were demultiplexed, and low-quality reads (Phred score < 25) were removed. Paired-end sequences were merged using custom scripts incorporating the FASTX toolkit (hannonlab.cshl.edu/fastx_toolkit/index.html) and USEARCH algorithm, with criteria of minimum 10% overlap and 95% nucleotide identity within the overlapping region. Ribosomal RNA (rRNA) transcripts were identified with riboPicker (Schmieder et al., 2012) and removed from the analysis. Merged nonrRNA sequences were queried via DIAMOND using sensitive search parameters (Buchfink et al., 2015) against the National Center for Biotechnology Information (NCBI)-nr database (November 2013). DIAMOND-identified protein-coding transcripts were assigned a functional annotation based Kyoto Encyclopedia of Genes and Genomes (KEGG) orthology (KO) identifiers (Kanehisa et al., 2000) using Metagenome Analyzer 5 (MEGAN5) (Huson et al., 2011), with taxonomic classification assigned using the lowest common ancestor (LCA) algorithm in MEGAN5 based on the NCBI taxonomy. Counts per KO were normalized to the total number of protein coding transcripts classified within bacteria and archaea (i.e., prokaryotes). Transcripts encoding LATO and HATO, *nxr*, and *amo* (all subunits) were identified by the assigned KO

identifiers. NOB abundances were determined by taxonomic LCA assignment according to NCBI taxonomy of DIAMOND-identified mRNA transcripts normalized to the total number of prokaryotic mRNA sequences. Taxonomic affiliation of both LATO and HATO were also assigned according to NCBI taxonomy via the LCA algorithm in MEGAN5.

A.4 Results and discussion

Sampling in both the ETNP and ETSP revealed a typical AMZ O_2 distribution in the upper 200 m of the water column. Oxygen concentrations in the 0–35 m surface layer in the ETNP were stable at 200 μmol kg^{-1}, before declining along a clearly defined oxycline from 35–45 to 60–80 m, and then falling below the detection limit of the switchable trace amount oxygen (STOX) sensors (few nanometers) at 80–100 m (Figure A.1). In the ETSP AMZ off Peru, O_2 concentrations and the depth of the oxycline were more variable and clearly influenced by proximity to the shore, with anoxic depths beginning at ~30 m at the coastal station but at ~70 m for the more oceanic station (Figure A.1*H*). In both the ETNP and ETSP, the chlorophyll concentration below the primary maximum decreased in parallel with O_2 concentration, reaching a minimum before complete O_2depletion and then increasing again to form an SCM in which 90% of the phototrophs were *Prochlorococcus* (Figure A.1). Although the upper region of the SCM was consistently located near the oxic–anoxic interface, maximum in vivo fluorescence and *Prochlorococcus* abundance were usually localized within the anoxic zone a few meters below. Low O_2 concentrations (<500 nmol L^{-1}) were occasionally

found inside the SCM, suggesting intrusion of overlying oxygenated waters or in situ O_2 production and accumulation.

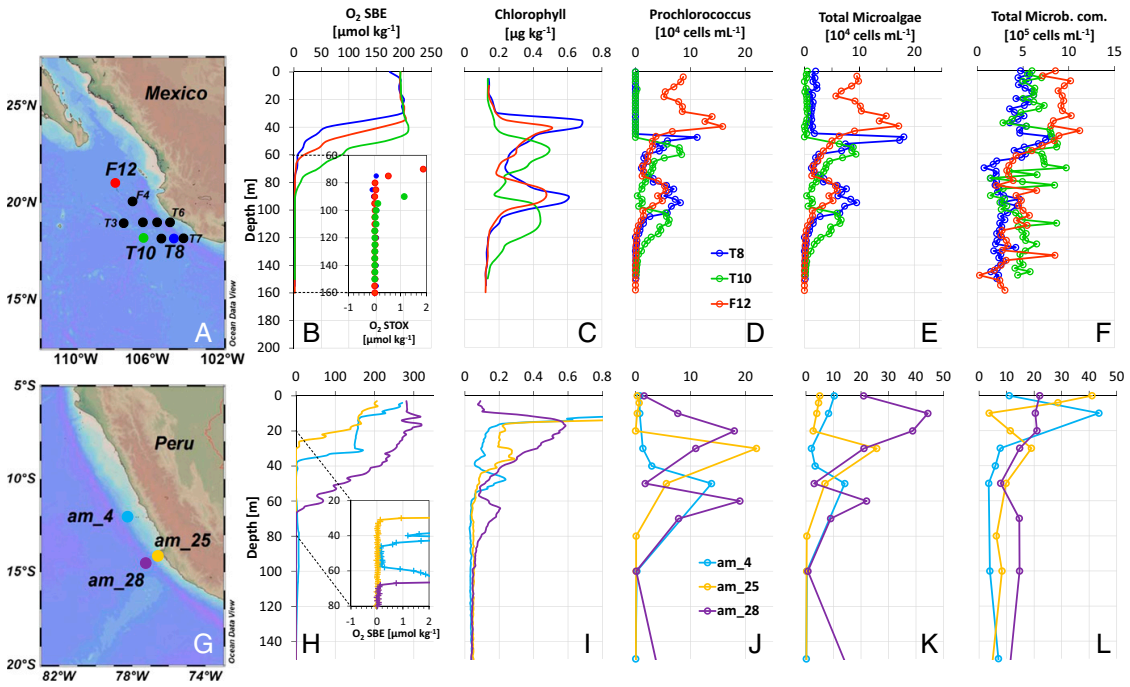

Figure A.1 Maps with sampled stations and main characteristics of the upper part of the (A–F) ETNP AMZ and (G–L) ETSP AMZ. Stations off Mexico (A) and Peru (G) where the SCM was found and sampled. (B and H) Dissolved oxygen profiles, based on SBE43 and STOX sensors (zooming in at low STOX O_2 values in B or corrected SBE O2 in H). (C and I) Profiles of chlorophyll concentration inferred from in vivo fluorescence. (D and J) Prochlorococcus abundance. (E and K) Total microalgae (Prochlorococcus, Synechococcus, and picoeukaryotes) and (F and L) total microbial community (Total Microb. com.) abundance measured by flow cytometry.

A.4.1 Oxygenic photosynthesis and carbon fixation in the SCM

Shipboard experiments using water from the SCM incubated under trace O_2 conditions revealed that O_2 concentration with time differed substantially between dark- and light-incubated samples (Figure A.2 *A* and *D*). Net community production (NCP), corresponding to the slope of the O_2 concentration curves and hence the balance between O_2 production and consumption, gradually increased to more positive values with increasing irradiance. NCP was also variable between stations, reflecting the spatial and temporal variability of the metabolic activity in terms of photosynthesis and respiration rates (Figure A.2 *B* and *E*). At several stations, net consumption of O_2 occurred at all applied irradiances, although a clear decrease in consumption rate was always measured with increasing light intensities. At other stations, a net increase in O_2 was measured when the samples were exposed to an irradiance of only 10 μmol photons m^{-2} s^{-1}. The observed maximum irradiance in situ was, however, only in the range of 2–5 μmol photons m^{-2} s^{-1} at most stations; at such low light levels, net O_2 consumption was always observed.

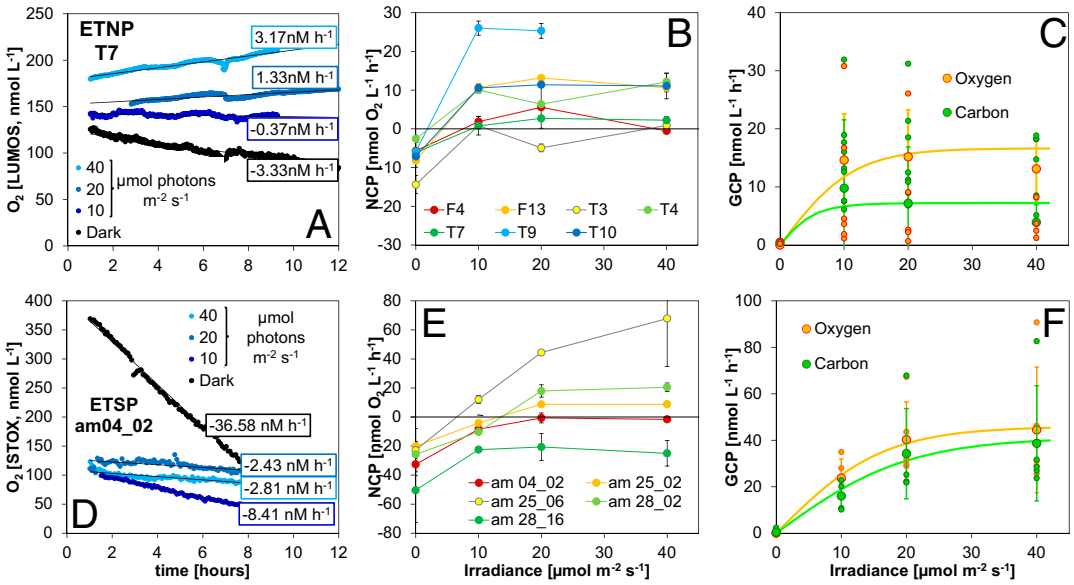

Figure A.2 Oxygen production and carbon fixation during incubations of samples from the SCM off Mexico (A - C) and Peru (D - F). A and D, Evolution of O_2 concentration during incubation of SCM samples exposed to a range of scalar irradiances (0 – 40 µmol photons $m^{-2}s^{-1}$). B and E, Net community production (NCP) rates versus scalar irradiance. C and F, gross community production (GCP): O_2 – GCP was measured by the incorporation of ^{13}C (at ETNP) or ^{14}C (ETSP). Data were fitted to a photosynthesis-irradiance model to calculate maximum rates (GCP_{max}) and the initial slope of the curve (α), an index of the photosynthetic efficiency at low light (values in the main text). Error bars represent the SE.

Tracking O_2 consumption during our experiments allowed for estimates of aerobic respiration rates. O_2 consumption curves were linear down to about 50 nmol L^{-1} during dark incubations (Figure A.2 *A* and *D*). Aerobic respiration by prokaryotes is generally driven by two classes of terminal oxidases: low-affinity terminal oxidases (LATO) with a half saturation constant (*Km*) of about 200 nmol O_2 L^{-1} and high-affinity terminal oxidases (HATO) with *Km* values of 3–8 nmol O_2 L^{-1} (Morris et al., 2013). Marine bacteria possessing HATO can decrease apparent *Km* values of aerobic respiration down to less than 10 nmol O_2 L^{-1} (19), and a linear O_2 decrease may thus be expected down to about 50 nmol O_2 L^{-1}. Therefore, O_2 consumption rates (referred to as respiration for simplicity) obtained at concentrations >50 nmol L^{-1} represent potential respiration rates (*R**) because they were measured above the threshold of O_2 limitation. The estimated *R** rates were significantly higher in the ETSP compared with the ETNP (Figure A.2), consistent with a higher microbial and particle abundance measured in the ETSP (Figure A.1).

Experiments under the unique, almost anoxic conditions, of AMZs have not been performed in previous measurements of photosynthetic activity in the SCM (Johnson et al., 1999). We conducted our experiments at O_2 levels below those sporadically detected by in situ measurements (up to 500 nmol L^{-1}) but far above the *Km* values for HATO. In this range, we can assume that gross community production of O_2 (GCP-O_2) can be calculated as the sum of NCP and *R**. We also validated these production calculations by simultaneously measuring the incorporation of inorganic carbon (using ^{13}C or ^{14}C) into biomass [gross community carbon production (GCP-C)], as has been done previously to quantify *Prochlorococcus* carbon fixation (Johnson et al., 1999; Moore et al., 1999). Both

GCP-O_2 and GCP-C followed a classical photosynthesis–irradiance curve (Figure A.2 *C* and *F*), with maximum (GCP_{max}) values above saturating light intensities (*Ek*) of 10.5 ± 2.0 and 21.4 ± 9.3 µmol photons m^{-2} s^{-1} (0.5 and 1% of the incident light) for the ETNP and ETSP, respectively. The low *Ek* values reflect adaptation to the dim light environment, being similar to values found for the SCM community in the Arabian Sea (Johnson et al., 1999) or in *Prochlorococcus* cultures (Moore et al., 1999). Above *Ek*, mean GCP_{max}-O_2 values in the ETNP and ETSP were 16.6 ± 9.1 and 52.5 ± 30.4 nmol O_2 L^{-1} h^{-1}, respectively, and were generally consistent with maximum GCP-C rates (GCP_{max}-C: 8.1 ± 11.2 and 44.4 ± 30.3 nmol C L^{-1} h^{-1} in the ETNP and ETSP, respectively) (mean values of all stations ± SD in Figure 4.2 *C* and *F*). The parameters describing the photosynthesis characteristics of the SCM community (maximum gross production rates, photosynthetic efficiency, and *Ek*) were similar to the values previously found for the SCM community of the Arabian Sea and the characterization of several *Prochlorococcus* isolates from the Pacific Ocean (Johnson et al., 1999; Moore et al., 1999). The values found for the ETNP were similar to those found for the SCM of the Arabian Sea (Johnson et al., 1999), whereas the ETSP SCM values were more similar to those from the laboratory cultures.

Although it is not yet possible to directly quantify in situ O_2 transformations in the AMZ, in situ GCP rates can be estimated based on water column chlorophyll concentrations and light conditions. The light intensity at the SCM was variable and almost always substantially below 10 µmol photons m^{-2} s^{-1}. Under such conditions, O_2 production rates are lower than potential respiration rates (*R**), and the O_2 produced is immediately consumed by the microbial community, resulting in a cryptic O_2 cycle in the

seemingly anoxic environment of the SCM (Figure A.1). However, at some stations the irradiance in the SCM was similar or close to the *Ek*. The occasional detection of low O_2 concentrations in the SCM (Tiano et al., 204; Ganesh et al., 2015) may thus be explained by photosynthetic activity in the SCM increasing O_2 concentrations to measurable levels. Such daily changes are difficult to measure by discrete sampling, but recurrent measurements in the same water mass might reveal hourly and daily changes in the SCM.

A.4.2 Oxygenic production coupling with aerobic microbial processes

Even if undetectable, O_2production in the SCM may support important (micro)aerobic metabolisms. To explore this prediction, we looked for signatures of such aerobic metabolism in available metatranscriptomes along the AMZ depth gradient in the ETNP during two cruises in 2014 and 2013, focusing on station T6 where the SCM was well developed and for which the metatranscriptome dataset was most comprehensive. Transcripts encoding terminal oxidases, including both LATO and HATO, were detected at all depths (Figure A.3), including deep within the AMZ, where the transcript pool was dominated by sequences affiliated with diverse Gammaproteobacteria and Alphaproteobacteria. The presence of oxidase transcripts within anoxic marine waters has been reported previously (Kalvelage et al., 2015) and may reflect constitutive expression by groups at high abundance in the AMZ core, potentially to capitalize quickly on O_2 if it becomes available (Tsementzi et al., 2016). The relative abundance of both LATO and HATO transcripts exhibits a local peak within the SCM compared with depths

immediately above (base of oxycline) and below the SCM (Figure A.3). Similar trends were observed at stations T4 and T10, although limited sampling affected our ability to fully resolve oxidase distributions immediately above the SCM at these sites. Together, these data provide evidence of a local peak in O_2 scavenging within the SCM.

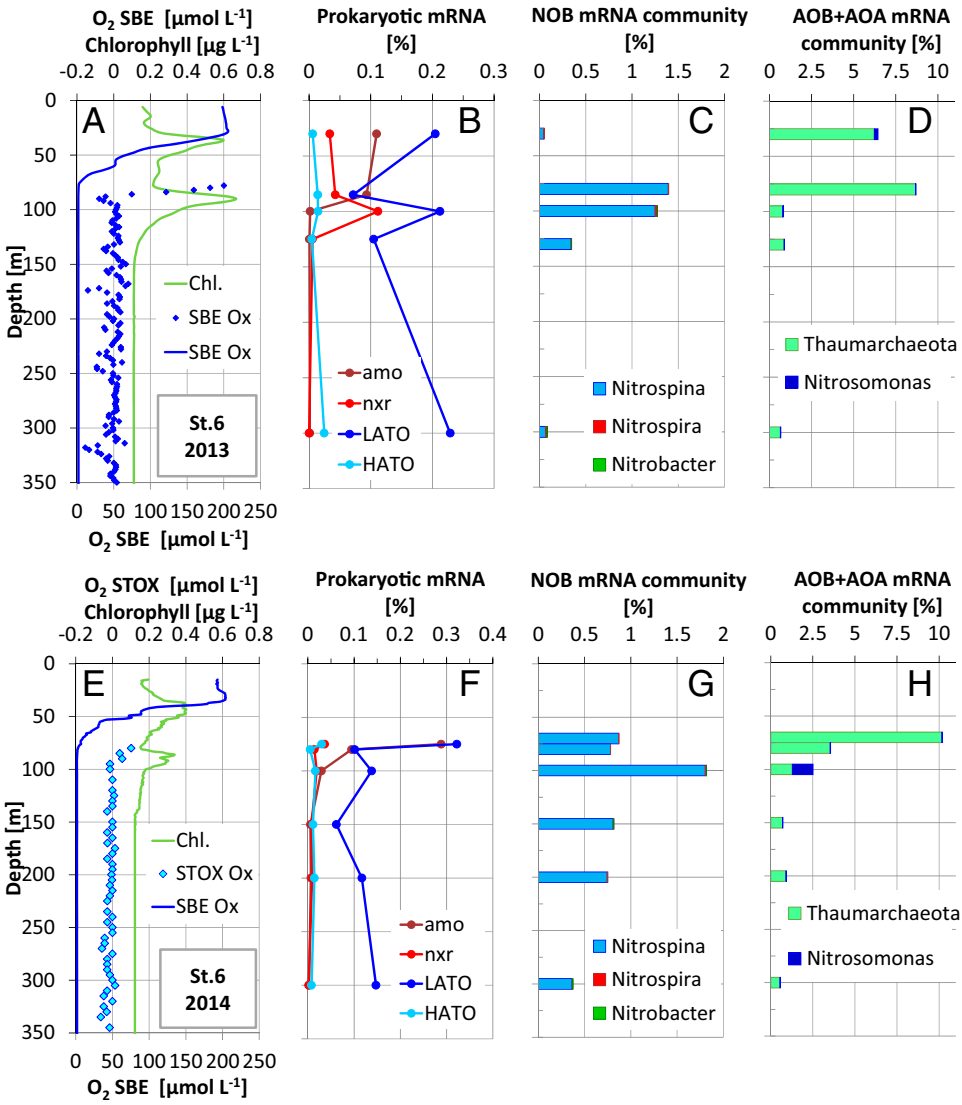

Figure A.3 Water column dissolved oxygen (O2), chorophyll concentrations (Chl), and microbial transcript abundances at station T6 in the ETNP in 2013 (A-D) and 2014 (E-H). A and E, O_2 based on SBE and STOX sensor measurement and chlorophyll inferred from in vivo fluorescence. B and F, abundances of transcripts encoding LATO and HATO, *amo*, and *nxr*, as a percentage of total prokaryotic mRNA. C and G, taxonomic classification of total mRNA affiliated with NOB and (D and H) AOB and AOA, as a percentage of total prokaryotic mRNA.

Oxygen produced in the SCM may also be consumed through key steps of the OMZ nitrogen cycle. Comparatively high rates of autotrophic nitrification (ammonia and nitrite oxidation) are known to occur close to the oxic–anoxic boundary of AMZs (Dalsgaard et al., 2014). Here transcripts affiliated with ammonia oxidizing bacteria (AOB) and ammonia oxidizing archaea (AOA), notably those encoding the ammonia monooxgynease (*amo*) enzyme catalyzing aerobic ammonia oxidation, peaked in the upper part of the oxycline and declined in abundance into the core of the ETNP AMZ (Figure A.3). In contrast, transcripts of nitrite oxidizing bacteria (NOB), primarily those of the marine NOB genus *Nitrospina*, spiked within the SCM, coinciding in most cases with a local enrichment in transcripts encoding nitrite oxidoreductase (*nxr*) (Figure A.3). A prior study showed that potential nitrite oxidation rates at station T6 in the ETNP peaked in the anoxic SCM at 10.8 nmol N L^{-1} h^{-1}, a rate approximately double that of the maximal O_2 respiration rate measured in this study. Taking the stoichiometry of nitrite oxidation into account, we can infer that most of the measured O_2 consumption (R^*) could be due to nitrite oxidation. The nitrite oxidation rates reported at the same stations were measured at low O_2 concentrations (<80 nmol L^{-1}), and we assume that the conditions were similar to our incubations, suggesting that the previous nitrite oxidation and our present R^* rates are directly comparable. The balance between heterotrophic and nitrite oxidizer O_2 consumption may, however, vary as a function of the actual O_2 concentration in the 0 to 100 nmol L^{-1} range that we measured in the ETNP SCM. The co-occurrence of elevated *Nitrospina* transcription and nitrite oxidation rates in the SCM suggests that NOB is fueled by local O_2 production.

Table A.1 Depth-integrated oxygen production and carbon fixation rates.

	GCP, $mmol \cdot m^{-2} \cdot d^{-1}$	
Station	O_2	C
ETNP–Mexico		
T4	0.43	0.15
F4	1.70	0.19
T7	0.48	0.13
T9	0.97	0.93
T10	0.59	0.55
	0.83 ± 0.53	0.39 ± 0.35
ETSP–Peru		
am_04	0.03	0.02
am_25	0.03	0.03
am_28	0.91	0.87
	0.32 ± 0.51	0.31 ± 0.49

A.4.1 Implications for oxygen minimum zones

The results of this study indicate that the SCM is a significant source of O_2 for both nitrite and organic matter oxidation, as well as a source of fixed carbon. Total productivity in terms of O_2 released and C fixed in the SCM was calculated by integrating the GCP profiles over a diel cycle, using measured (ETSP) or estimated (ETNP) scalar irradiance profiles (Table A.1). Higher chlorophyll and estimated irradiance values at the SCM in the ETNP off Mexico resulted in higher mean production rates (0.83/0.39 mmol O_2/C m^{-2} d^{-1}) compared with the ETSP off Peru (0.32/0.31 mmol O_2/C m^{-2} d^{-1}). Although in situ light attenuation profiles were used for the ETNP, cloud coverage and other local factors reducing the incident light could not be included in the calculations, and therefore, the production values should be taken as maximum values. Productivity was also highly variable among sites (0.43–1.70/0.15–0.95, and 0.03–0.91/0.02–0.87 mmol O_2/C m^{-2} d^{-1} for ETNP and ETSP, respectively), reflecting the heterogeneous spatial distribution of the SCM (Figure A.1).

Although primary production in surface waters largely exceeds these values (Kalvelage et al., 2015), the vast majority of surface production is remineralized before reaching the AMZ core. Indeed, the range of particulate organic carbon supply to the AMZ is 0.83–7.81 mmol C m^{-2} d^{-1} (Babbin et al., 2014; Devol et al., 2001) in the ETNP or 1.52–14.70 mmol C m^{-2} d^{-1} in the ETSP (Escribano et al., 2004). This wide range highlights the variability in export rates in these regions. Nonetheless, comparing these estimations with our data, the carbon production in the SCM could provide 5–47% and 2–20% of the organic matter supplied to the anoxic waters of the ETNP and ETSP,

respectively, where part of it is then mineralized by dissimilatory nitrate reduction to nitrite and denitrification (Ganesh et al., 2015; Babbin et al., 2014; Kalvelage et al., 2015; Ward, 2013). Nitrate respiration to nitrite appears as the dominant mineralization step in the ETNP (Ganesh et al., 2015), and mineralization rates of about 1 mmol C m^{-2} d^{-1} can be calculated from published data (Canfield et al., 2010; Kalvelage et al., 2013). These rates are close to the C fixation rate in the SCM, highlighting the relevance of the SCM in OMZ metabolism.

Global warming is expected to result in shoaling of the OMZ oxycline and overall expansion of OMZ volumes (Gilly et al., 2013). Mesoscale physical processes such as local upwelling and anticyclonic eddies that shoal the oxic–anoxic boundary have been shown to enhance the development of SCMs (Goericke et al., 2000; Cepeda-Morales et al., 2009). Oxycline shoaling increases the light intensities in the anoxic cores of the AMZs, thereby potentially stimulating the photosynthetic community. The effects of these changes on microbial communities and microbial biogeochemical cycling in AMZs are difficult to predict, although significant changes in carbon, nitrogen, and sulfur cycling are expected (Gilly et al., 2013). Our data show a significant carbon supply to the anoxic core of the Pacific AMZs by SCM photosynthetic activity, and it is likely that the situation is similar in the Arabian Sea. Although we did not measure nitrogen transformation processes, the nitrifying community was also enriched at the SCM, potentially reflecting elevated metabolic rates. A shoaling of the AMZ coupled with increases in irradiance and SCM photosynthetic activity would increase the carbon and daytime oxygen supply to the upper part of the AMZ. Shoaling of the AMZ due to global warming could thus lead to more extensive areas with high rates of SCM biological

activity, with the diel oxic/anoxic cycles of these SCMs influencing marine productivity and coupled global nitrogen cycling.

A.4 References

Babbin, A. R., Keil, R. G., Devol, A. H., Ward, B. B. (2014). Organic Matter Stoichiometry, Flux, and Oxygen Control Nitrogen Loss in the Ocean. Science, 344(6182), 406-408. doi:10.1126/science.1248364

Bristow, L. A., Callbeck, C. M., Larsen, M., Altabet, M. A., Dekaezemacker, J., Forth, M., et al. (2017). N-2 production rates limited by nitrite availability in the Bay of Bengal oxygen minimum zone. Nature Geoscience, 10(1), 24-29. doi:10.1038/ngeo2847

Bristow, L. A., Dalsgaard, T., Tiano, L., Mills, D. B., Bertagnolli, A. D., Wright, J. J., et al. (2016). Ammonium and nitrite oxidation at nanomolar oxygen concentrations in oxygen minimum zone waters. Proceedings of the National Academy of Sciences of the United States of America, 113(38), 10601-10606. doi:10.1073/pnas.1600359113

Buchfink, B., Xie, C., Huson, D. H. (2015). Fast and sensitive protein alignment using DIAMOND. Nature Methods, 12(1), 59-60.

Canfield, D. E., Stewart, F. J., Thamdrup, B., De Brabandere, L., Dalsgaard, T., Delong, E. F., et al. (2010). A Cryptic Sulfur Cycle in Oxygen-Minimum-Zone Waters off the Chilean Coast. Science, 330(6009), 1375-1378. doi:10.1126/science.1196889

Cepeda-Morales, J., Beier, E., Gaxiola-Castro, G., Lavin, M. F., Godinez, V. M. (2009). Effect of the oxygen minimum zone on the second chlorophyll maximum in the Eastern Tropical Pacific off Mexico. Ciencias Marinas, 35(4), 389-403.

Codispoti, L. A., Brandes, J. A., Christensen, J. P., Devol, A. H., Naqvi, S. W. A., Paerl, H. W., Yoshinari, T. (2001). The oceanic fixed nitrogen and nitrous oxide budgets: Moving targets as we enter the anthropocene? Scientia Marina, 65, 85-105.

Dalsgaard, T., Thamdrup, B., Farias, L., Revsbech, N. P. (2012). Anammox and denitrification in the oxygen minimum zone of the eastern South Pacific. Limnology and Oceanography, 57(5), 1331-1346. doi:10.4319/lo.2012.57.5.1331

Devol, A. H., Hartnett, H. E. (2001). Role of the oxygen-deficient zone in transfer of organic carbon to the deep ocean. Limnology and Oceanography, 46(7), 1684-1690.

Escribano, R., Daneri, G., Farias, L., Gallardo, V. A., Gonzalez, H. E., Gutierrez, D., et al. (2004). Biological and chemical consequences of the 1997-1998 El Nino in the Chilean coastal upwelling system: a synthesis. Deep-Sea Research Part Ii-Topical Studies in Oceanography, 51(20-21), 2389-2411. doi:10.1016/j.dsr2.2004.08.011

Ganesh, S., Bristow, L. A., Larsen, M., Sarode, N., Thamdrup, B., Stewart, F. J. (2015). Size-fraction partitioning of community gene transcription and nitrogen metabolism in a marine oxygen minimum zone. ISME J, in Press†

Garcia-Robledo, E., Borisov, S., Klimant, I., Revsbech, N. P. (2016). Determination of respiration rates in water with sub-micromolar oxygen concentrations. Frontiers in Marine Science, 3, 244.

Gilly, W. F., Beman, J. M., Litvin, S. Y., Robison, B. H. (2013). Oceanographic and Biological Effects of Shoaling of the Oxygen Minimum Zone. Annual Review of Marine Science, Vol 5, 5, 393-420. doi:10.1146/annurev-marine-120710-100849

Goericke, R., Olson, R. J., Shalapyonok, A. (2000). A novel niche for Prochlorococcus sp in low-light suboxic environments in the Arabian Sea and the Eastern Tropical North Pacific. Deep-Sea Research Part I-Oceanographic Research Papers, 47(7), 1183-1205. doi:10.1016/s0967-0637(99)00108-9

Gong, X. Z., Garcia-Robledo, E., Schramm, A., Revsbech, N. P. (2016). Respiratory Kinetics of Marine Bacteria Exposed to Decreasing Oxygen Concentrations. Applied and Environmental Microbiology, 82(5), 1412-1422. doi:10.1128/aem.03669-15

Gregori, G., Citterio, S., Ghiani, A., Labra, M., Sgorbati, S., Brown, S., Denis, M. (2001). Resolution of viable and membrane-compromised bacteria in freshwater and marine waters based on analytical flow cytometry and nucleic acid double staining. Applied and Environmental Microbiology, 67(10), 4662-4670. doi:10.1128/aem.67.10.4662-4670.2001

Huson, D. H., Mitra, S., Ruscheweyh, H. J., Weber, N., Schuster, S. C. (2011). Integrative analysis of environmental sequences using MEGAN4. Genome Research, 21(9), 1552-1560. doi:10.1101/gr.120618.111

Jassby, A. D., Platt, T. (1976). Mathematical formulation of the relationship between photosynthesis and light for phytoplankton. Limnology and oceanography, 21(4), 540-547.

Johnson, Z., Landry, M. L., Bidigare, R. R., Brown, S. L., Campbell, L., Gunderson, J., et al. (1999). Energetics and growth kinetics of a deep Prochlorococcus spp. population in the Arabian Sea. Deep-Sea Research Part Ii-Topical Studies in Oceanography, 46(8-9), 1719-1743. doi:10.1016/s0967-0645(99)00041-7

Kalvelage, T., Lavik, G., Jensen, M. M., Revsbech, N. P., Loscher, C., Schunck, H., et al. (2015). Aerobic Microbial Respiration In Oceanic Oxygen Minimum Zones. Plos One, 10(7). doi:10.1371/journal.pone.0133526

Kalvelage, T., Lavik, G., Lam, P., Contreras, S., Arteaga, L., Loscher, C. R., et al. (2013). Nitrogen cycling driven by organic matter export in the South Pacific oxygen minimum zone. Nature Geoscience, 6(3), 228-234. doi:10.1038/ngeo1739

Kanehisa, M., Goto, S. (2000). KEGG: Kyoto Encyclopedia of Genes and Genomes. Nucleic Acids Research, 28(1), 27-30. doi:10.1093/nar/28.1.27

Lavin, P., Gonzalez, B., Santibanez, J. F., Scanlan, D. J., Ulloa, O. (2010). Novel lineages of Prochlorococcus thrive within the oxygen minimum zone of the eastern tropical South Pacific. Environmental Microbiology Reports, 2(6), 728-738. doi:10.1111/j.1758-2229.2010.00167.x

Lebaron, P., Parthuisot, N., Catala, P. (1998). Comparison of blue nucleic acid dyes for flow cytometric enumeration of bacteria in aquatic systems. Applied and Environmental Microbiology, 64(5), 1725-1730.

Lehner, P., Larndorfer, C., Garcia-Robledo, E., Larsen, M., Borisov, S. M., Revsbech, N. P., et al. (2015). LUMOS - A Sensitive and Reliable Optode System for Measuring Dissolved Oxygen in the Nanomolar Range. Plos One, 10(6). doi:10.1371/journal.pone.0128125

Moore, L. R., Chisholm, S. W. (1999). Photophysiology of the marine cyanobacterium Prochlorococcus: Ecotypic differences among cultured isolates. Limnology and Oceanography, 44(3), 628-638.

Morris, R. L., Schmidt, T. M. (2013). Shallow breathing: bacterial life at low O-2. Nature Reviews Microbiology, 11(3), 205-212. doi:10.1038/nrmicro2970

Padilla, C. C., Bristow, L. A., Sarode, N., Garcia-Robledo, E., ER, R., Benson, C. R., et al. (2016). NC10 bacteria in marine oxygen minimum zones. In (Vol. In Press). ISME J.

Paulmier, A., Ruiz-Pino, D. (2009). Oxygen minimum zones (OMZs) in the modern ocean. Progress in Oceanography, 80(3-4), 113-128. doi:10.1016/j.pocean.2008.08.001

Revsbech, N. P., Larsen, L. H., Gundersen, J., Dalsgaard, T., Ulloa, O., Thamdrup, B. (2009). Determination of ultra-low oxygen concentrations in oxygen minimum zones by the STOX sensor. Limnology and Oceanography-Methods, 7, 371-381.

Revsbech, N. P., Thamdrup, B., Dalsgaard, T., Canfield, D. E. (2011). Construction of STOX sensors and their application for determination of O2 concentrations in oxygen minimum zones. In M. G. Klotz (Ed.), Methods in Enzymology: Research on Nitrification and Related Processes, Vol 486, Part A (Vol. 486, pp. 325-341). San Diego: Elsevier Academic Press Inc.

Schmieder, R., Lim, Y. W., Edwards, R. (2012). Identification and removal of ribosomal RNA sequences from metatranscriptomes. Bioinformatics, 28(3), 433-435. doi:10.1093/bioinformatics/btr669

Stewart, F. J., Ulloa, O., DeLong, E. F. (2012). Microbial metatranscriptomics in a permanent marine oxygen minimum zone. Environmental Microbiology, 14(1), 23-40. doi:10.1111/j.1462-2920.2010.02400.x

Telling, J., Anesio, A. M., Hawkings, J., Tranter, M., Wadham, J. L., Hodson, A. J., et al. (2010). Measuring rates of gross photosynthesis and net community production in cryoconite holes: a comparison of field methods. Annals of Glaciology, 51(56), 153-162. doi:10.3189/172756411795932056

Thamdrup, B., Dalsgaard, T., Revsbech, N. P. (2012). Widespread functional anoxia in the oxygen minimum zone of the Eastern South Pacific. Deep-Sea Research Part I-Oceanographic Research Papers, 65, 36-45. doi:10.1016/j.dsr.2012.03.001

Tiano, L., Garcia-Robledo, E., Dalsgaard, T., Devol, A. H., Ward, B. B., Ulloa, O., et al. (2014). Oxygen distribution and aerobic respiration in the north and south eastern tropical Pacific oxygen minimum zones. Deep-Sea Research Part I-Oceanographic Research Papers, 94, 173-183. doi:10.1016/j.dsr.2014.10.001

Tiano, L., Garcia-Robledo, E., Revsbech, N. P. (2014). A New Highly Sensitive Method to Assess Respiration Rates and Kinetics of Natural Planktonic Communities by Use of the Switchable Trace Oxygen Sensor and Reduced Oxygen Concentrations. Plos One, 9(8). doi:10.1371/journal.pone.0105399

Tsementzi, D., Wu, J., Deutsch, S., Nath, S., Rodriguez-R, L. M., Burns, A. S., et al. (2016). SAR11 bacteria linked to ocean anoxia and nitrogen loss. Nature, 536(7615), 179-183. doi:10.1038/nature19068

Ulloa, O., Canfield, D. E., DeLong, E. F., Letelier, R. M., Stewart, F. J. (2012). Microbial oceanography of anoxic oxygen minimum zones. Proceedings of the National Academy of Sciences of the United States of America, 109(40), 15996-16003. doi:10.1073/pnas.1205009109

Ward, B. B. (2013). How Nitrogen Is Lost. Science, 341(6144), 352-353. doi:10.1126/science.1240314

APPENDIX B.

SUPPLEMENTARY DATA FOR CHAPTER 2 STANDARD FILTRATION PRACTIVES MAY SIGNIFICANTLY DISTORT PLANKTONIC MICROBIAL DIVERSITY ESTIMATES

B.1 Supplementary Tables

Table B.1 Bacterial 16S rRNA gene copies per mL in sample water from experiments 1 and 2. Values are averages across all volume replicates, with standard deviation in parentheses. The ratio of Sterivex to prefilter counts is shown in the last column

exp	Sterivex (0.2-1.6 µm)	prefilter (>1.6 µm)	combined	ratio (Sterivex/prefilter)
1-150m	3.7×10^5 (1.1×10^5)	3.3×10^4 (1.4×10^4)	4.0×10^5 (1.2×10^5)	11.1
2-400m	6.4×10^4 (2.2×10^4)	6.3×10^3 (1.4×10^3)	7.0×10^4 (2.4×10^4)	10.3

Table B.2 Percentages variation (R^2) in weighted UniFrac distances explained by filtered water volume differences, based on adonis tests in QIIME. All P-values are significant following Bonferroni correction for multiple tests.

dataset	R^2, *P-value*
Exp1, prefilter	0.87, *0.01*
Exp1, Sterivex	0.50, *0.001*
Exp2, prefilter	0.74, *0.001*
Exp2, Sterivex	0.81, *0.001*

Table B.3 Abundances of microbial orders in experiment 1, expressed as a percent of toal 16S rRNA gene amplicons.

* average % of replicates
**positive values: fold increase in abundance from the lowest to the highest filtered volumes;
**negative values: fold increase from the highest to the lowest filtered volumes, multiplied by -1
Shading = significant difference in abundance between lowest vs highest volumes (P<0.05; FDR; ba

Sterivex filter fraction (0.2-1.6 μm)

	Filtered water volume*				
Taxon	0.1L	1L	5L	Average (all)	Fold Change**
SAR406, Arctic96B-7	16.2	18.8	25.1	20.0	1.6
Gammaproteobacteria, Oceanospirillales	12.9	11.2	12.5	12.2	-1.0
Alphaproteobacteria, Rickettsiales	11.2	11.5	10.6	11.1	-1.1
Deltaproteobacteria, Sva0853	9.0	10.6	9.1	9.6	1.0
Planctomycetes, Brocadiales	9.0	10.0	8.5	9.2	-1.1
Gammaproteobacteria, Chromatiales	5.3	5.4	4.3	5.0	-1.2
Actinobacteria, Acidimicrobiales	3.0	3.9	3.2	3.4	1.0
SAR406, AB16, ZA3648c	2.1	3.0	3.3	2.8	1.6
Thaumarchaeota, Cenarchaeales	2.7	3.4	2.2	2.8	-1.2
Deltaproteobacteria, Desulfobacterales	2.3	3.2	2.4	2.6	1.0
Gammaproteobacteria, Vibrionales	6.7	0.3	0.1	2.4	-96.5
Euryarchaeota, Thermoplasmata, E2	1.5	2.0	3.2	2.2	2.2
Unassigned	2.1	2.0	1.8	2.0	-1.2
Gammaproteobacteria, Thiotrichales	1.5	1.9	2.5	1.9	1.7
Chloroflexi, SAR202	1.6	2.1	2.0	1.9	1.3
Alphaproteobacteria, Rhodospirillales	1.4	1.8	1.5	1.6	1.0
Gammaproteobacteria, Thiohalorhabdales	1.1	1.4	1.6	1.4	1.4
Alphaproteobacteria, unassigned	0.8	1.2	0.8	0.9	-1.0
Gammaproteobacteria, Alteromonadales	1.5	0.6	0.4	0.8	-3.6
Chloroflexi, Dehalococcoidales	0.6	0.7	0.5	0.6	-1.1
Bacteroidetes, Flavobacteriales	0.4	0.4	0.6	0.5	1.5

Table S3 continued

Prefilter fraction (>1.6 μm)

Taxon	Filtered water volume* 0.1L	1L	5L	Average (all)	Fold Change
Gammaproteobacteria, Vibrionales	54.1	4.6	2.6	17.2	-20.5
Gammaproteobacteria, Thiohalorhabdales	4.4	18.8	17.0	14.1	3.8
Euryarchaeota, Thermoplasmata, E2	1.0	7.9	9.6	6.8	9.8
SAR406, Arctic96B-7	3.1	7.3	6.9	6.0	2.2
Bacteroidetes, Flavobacteriales	1.5	6.7	7.0	5.4	4.7
Gammaproteobacteria, Oceanospirillales	4.7	5.2	5.1	5.0	1.1
Unassigned	1.3	6.7	6.1	4.9	4.6
Gammaproteobacteria, Alteromonadales	7.4	2.8	2.6	4.0	-2.8
Deltaproteobacteria, Myxococcales	0.5	3.6	4.2	3.1	8.4
Planctomycetes, Phycisphaerales	0.2	3.0	3.9	2.7	15.9
SAR406, ZA3648c	0.7	3.1	3.0	2.4	4.1
Gammaproteobacteria, Thiotrichales	0.3	1.8	2.9	1.9	8.7
Gammaproteobacteria, Pseudomonadales	5.2	0.8	0.2	1.7	-21.6
Alphaproteobacteria, Rickettsiales	0.9	2.1	1.9	1.7	2.0
Deltaproteobacteria, unassigned	0.1	1.6	2.0	1.4	27.4
Alphaproteobacteria, Rhodobacterales	3.9	0.2	0.3	1.2	-12.9
Gammaproteobacteria, Chromatiales	0.6	1.3	1.3	1.1	2.0
Planctomycetes, Brocadiales	0.7	1.2	1.2	1.1	1.6
Alphaproteobacteria, Rhodospirillales	0.6	1.1	1.3	1.1	2.2
Planctomycetes, OM190, agg27	0.1	1.0	1.4	0.9	15.5
Actinobacteria, Acidimicrobiales	0.7	1.1	0.8	0.9	1.2
Chloroflexi, SAR202	0.3	0.9	1.0	0.8	3.6
Planctomycetes, OM190,	0.2	1.1	0.9	0.8	4.9
Verrucomicrobia, Verrucomicrobiales	0.1	0.6	1.1	0.7	7.9
Deltaproteobacteria, Desulfobacterales	0.4	1.0	0.7	0.7	2.0
Alphaproteobacteria, Sphingomonadales	2.1	0.2	0.1	0.7	-30.4
Thaumarchaeota, Cenarchaeales	0.3	0.7	0.7	0.6	2.6
Epsilonproteobacteria, Campylobacterales	0.2	0.7	0.7	0.6	3.1
Verrucomicrobia, Arctic97B-4	0.2	0.5	0.7	0.5	3.6
Deltaproteobacteria, Sva0853	0.4	0.4	0.7	0.5	1.8
Deltaproteobacteria, PB19	0.1	0.8	0.5	0.5	6.9
Gammaproteobacteria, Legionellales	0.2	0.6	0.5	0.5	2.8

Table B.4 Abundances of microbial orders in experiment 2, expressed as a percent of toal 16S rRNA gene amplicons.

* average % of replicates
**positive values: fold increase in abundance from the lowest to the highest filtered volumes;
**negative values: fold increase from the highest to the lowest filtered volumes, multiplied by -1
Shading = significant difference in abundance between lowest vs highest volumes (P<0.05; FDR; baySeq)

Sterivex filter fraction (0.2-1.6 μm)

	Filtered water volume*							
Taxon	0.05L	0.1L	0.5L	1L	2L	5L	Average (all)	Fold Change**
SAR406, Arctic96B-7	12.3	14.4	21.2	19.7	24.2	26.0	19.7	2.1
Planctomycetes, Brocadiales	16.0	11.3	21.7	19.7	20.0	15.6	17.4	-1.0
Unassigned	4.4	4.6	6.9	6.5	7.4	8.8	6.4	2.0
Alphaproteobacteria, Rickettsiales	4.5	3.9	7.6	7.0	7.5	6.7	6.2	1.5
Gammaproteobacteria, Vibrionales	22.0	7.8	2.4	0.6	0.2	0.4	5.6	-51.0
Gammaproteobacteria, Chromatiales	1.3	7.0	2.3	12.3	1.4	2.3	4.4	1.8
Deltaproteobacteria, Sva0853	3.6	3.1	5.4	4.9	5.1	4.3	4.4	1.2
Chloroflexi, SAR202	2.0	1.9	3.2	3.0	4.4	4.2	3.1	2.1
Actinobacteria, Acidimicrobiales	2.4	2.4	3.2	2.8	3.2	3.0	2.8	1.2
Gammaproteobacteria, Oceanospirillales	2.6	2.4	2.7	2.4	2.6	2.7	2.6	1.0
Alphaproteobacteria, Rhodospirillales	2.1	1.9	2.8	2.6	3.0	2.6	2.5	1.3
Gammaproteobacteria, Alteromonadales	4.9	4.6	1.2	0.5	0.4	0.3	2.0	-15.6
SAR406, ZA3648c	1.0	1.1	2.1	2.0	2.3	2.4	1.8	2.3
Chloroflexi, Dehalococcoidales	1.0	1.0	1.5	1.4	2.1	1.8	1.5	1.7
Euryarchaeota, Thermoplasmata, E2	0.6	1.1	1.1	1.1	1.9	2.8	1.4	4.4
Crenarchaeota, MBGA	1.2	1.0	1.7	1.4	1.7	1.5	1.4	1.3
Gammaproteobacteria, Thiohalorhabdales	0.9	1.2	1.2	1.0	1.4	2.4	1.4	2.8
Alphaproteobacteria, Kiloniellales	3.3	4.0	0.2	0.1	0.0	0.0	1.3	-93.6
Gammaproteobacteria, Thiotrichales	0.7	0.8	1.3	1.1	1.3	1.5	1.1	2.0
Thaumarchaeota, Cenarchaeales	1.0	0.5	1.3	1.3	1.3	1.2	1.1	1.2
Deltaproteobacteria, Desulfobacterales	0.9	1.1	1.4	1.1	1.1	1.0	1.1	1.2
Alphaproteobacteria, Rhodobacterales	4.1	1.4	0.3	0.1	0.1	0.0	1.0	-85.7
Bacteroidetes, Flavobacteriales	0.2	2.8	0.4	0.4	0.3	0.9	0.8	3.7
Planctomycetes, Planctomycetales	0.0	4.5	0.0	0.1	0.0	0.0	0.8	-11.4
Deltaproteobacteria, Entotheonellales	0.6	0.6	1.0	0.7	0.9	0.8	0.8	1.2
Acidobacteria, iii1-15	0.6	0.4	0.7	0.6	0.8	0.7	0.6	1.2
Betaproteobacteria, Methylophilales	0.0	3.8	0.0	0.0	0.0	0.0	0.6	-1.2
Chloroflexi, H39	0.2	0.3	0.5	0.6	0.6	0.7	0.5	3.5

Table S4 continued

Prefilter fraction (>1.6 μm)

Taxon	Filtered water volume*						Average (all)	Fold Change
	0.05L	0.1L	0.5L	1L	2L	5L		
Gammaproteobacteria, Vibrionales	62.2	49.6	38.5	4.7	2.6	1.9	26.6	-33.4
Gammaproteobacteria, Chromatiales	2.2	1.4	2.8	27.9	58.1	38.7	21.8	17.6
Gammaproteobacteria, Alteromonadales	8.1	8.8	7.5	2.3	1.6	1.8	5.0	-4.5
SAR406, Arctic96B-7	0.9	4.2	7.0	7.0	4.2	6.6	5.0	7.7
Gammaproteobacteria, Oceanospirillales	7.5	7.9	4.4	3.4	2.0	1.7	4.5	-4.4
Euryarchaeota, Thermoplasmata, E2	0.4	2.0	4.5	6.2	4.2	7.1	4.1	19.5
Unassigned	0.6	2.6	5.3	5.9	3.3	4.4	3.7	7.1
Gammaproteobacteria, Thiohalorhabdales	0.6	1.4	3.3	7.5	2.6	4.6	3.3	7.6
Firmicutes, Bacillales	5.1	4.3	1.0	0.3	0.0	0.5	1.9	-10.2
Epsilonproteobacteria, Campylobacterales	0.1	0.2	0.9	2.7	4.2	1.9	1.7	20.0
Alphaproteobacteria, Rickettsiales	0.4	1.1	2.5	2.3	1.4	2.0	1.6	4.7
Bacteroidetes, Flavobacteriales	0.3	1.0	1.5	3.0	1.5	1.4	1.5	4.2
Planctomycetes, Brocadiales	0.6	1.6	2.4	1.6	1.2	1.3	1.4	2.3
Gammaproteobacteria, Thiotrichales	0.0	0.5	1.3	2.4	1.4	2.5	1.3	65.0
Alphaproteobacteria, Rhodobacterales	3.2	2.4	0.7	0.1	0.2	0.1	1.1	-49.0
Alphaproteobacteria, Rhodospirillales	0.3	0.8	1.5	1.9	0.6	1.2	1.0	4.5
SAR406, ZA3648c	0.2	0.6	1.3	2.4	0.6	0.9	1.0	5.2
Chloroflexi, SAR202,	0.2	0.7	1.6	1.3	0.5	0.9	0.9	4.1
Deltaproteobacteria, Myxococcales	0.2	0.4	0.5	1.4	0.5	1.4	0.8	8.5
Planctomycetes, Phycisphaerales	0.2	0.5	0.4	1.9	0.2	1.1	0.7	6.3
Actinobacteria, Acidimicrobiales	0.2	0.3	1.2	0.8	0.7	0.8	0.7	4.8
Alphaproteobacteria, Kiloniellales	1.6	1.3	0.3	0.0	0.0	0.1	0.6	-23.2
Alphaproteobacteria, Sphingomonadales	1.0	0.7	0.0	0.0	0.0	1.2	0.5	1.2
Bacteroidetes, Bacteroidales	0.1	0.1	0.4	0.4	0.8	0.9	0.5	10.9

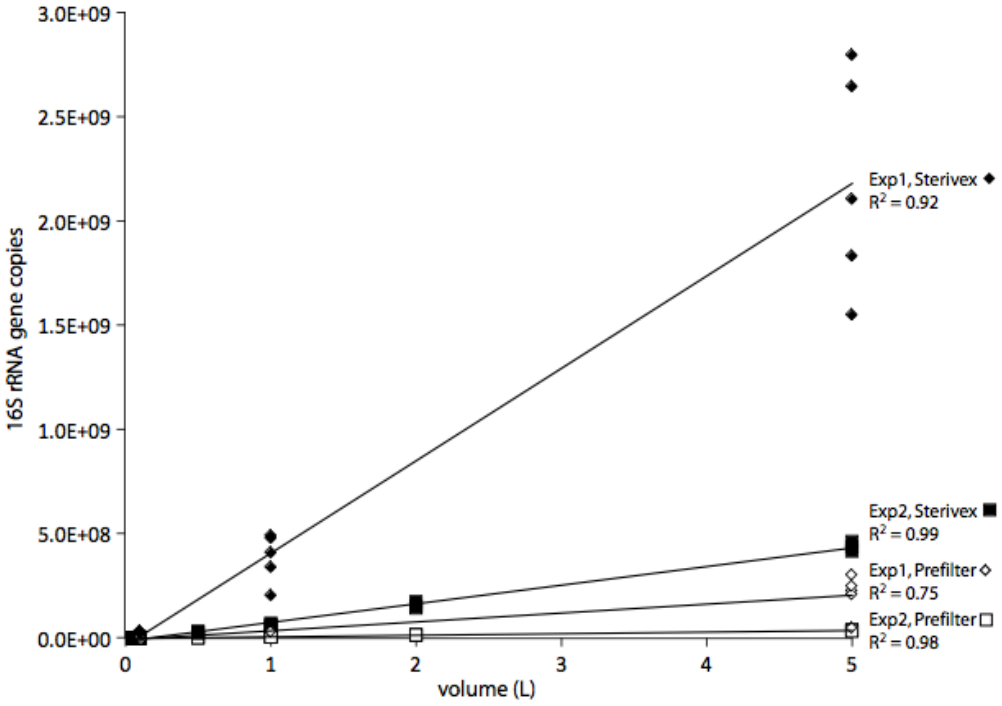

Figure B.1 Total bacterial 16S rRNA gene counts as function of filtered water volume.

APPENDIX C.

SUPPLEMENTARY DATA FOR CHAPTER 3
NC10 BACTERIA IN MARINE OXYGEN MINIMUM ZONES

C.1 Supplementary figures

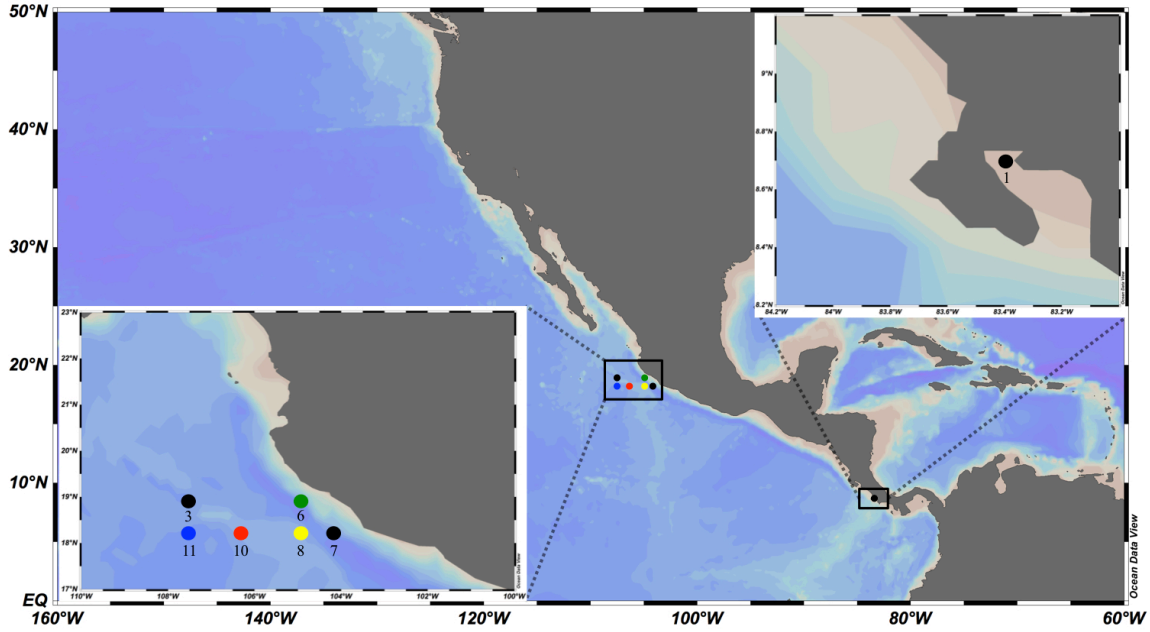

Figure C.1 Sampling sites in the ETNP and GD OMZs off Mexico and Costa Rica, respectively. ETNP samples for analysis of methane concentrations and biochemical and molecular analysis of n-damo bacteria were collected at stations 6, 8, 10, and 11 in May 2014. Additional samples used for molecular analysis were collected at stations 6 and 10 in July 2013. Stations 3 and 7 are also shown (black circles), as these indicate sites of measured anammox and denitrification rates in 2014 (as described in the main text). All samples from the GD were collected at station 1 at the far northern head of Golfo Dulce.

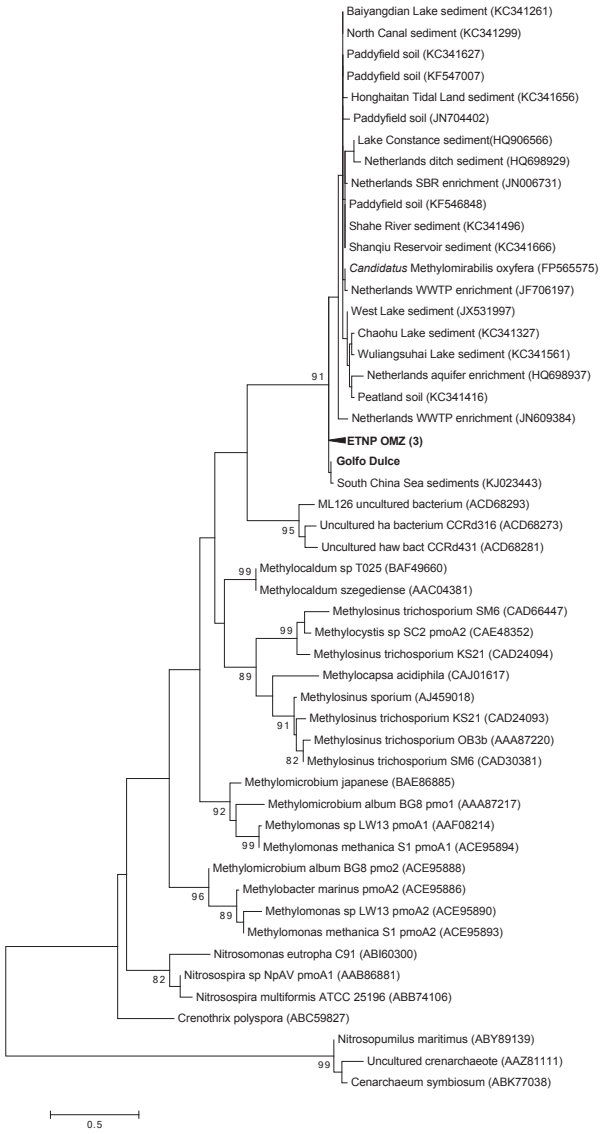

Figure C.2 PmoA gene phylogeny. Uncollapsed version of the particulate methane monooxygenase subunit A (PmoA) gene phylogeny shown in Figure 2 (main text). PmoA sequences (n=53) recovered from the ETNP are highlighted in bold within the larger clade of NC10-like sequences from other studies, separated from PmoA of aerobic methanotrophic clades and an ammonia monooxygenase (AmoA) outgroup. Reconstruction is based on Maximum Likelihood analysis of 88 amino acids using the Dayhoff substitution model. Bootstrap values greater than 70 are shown, along with NCBI accession numbers for database sequences. The scale bar represents 50 amino-acid changes per 100 amino acids.

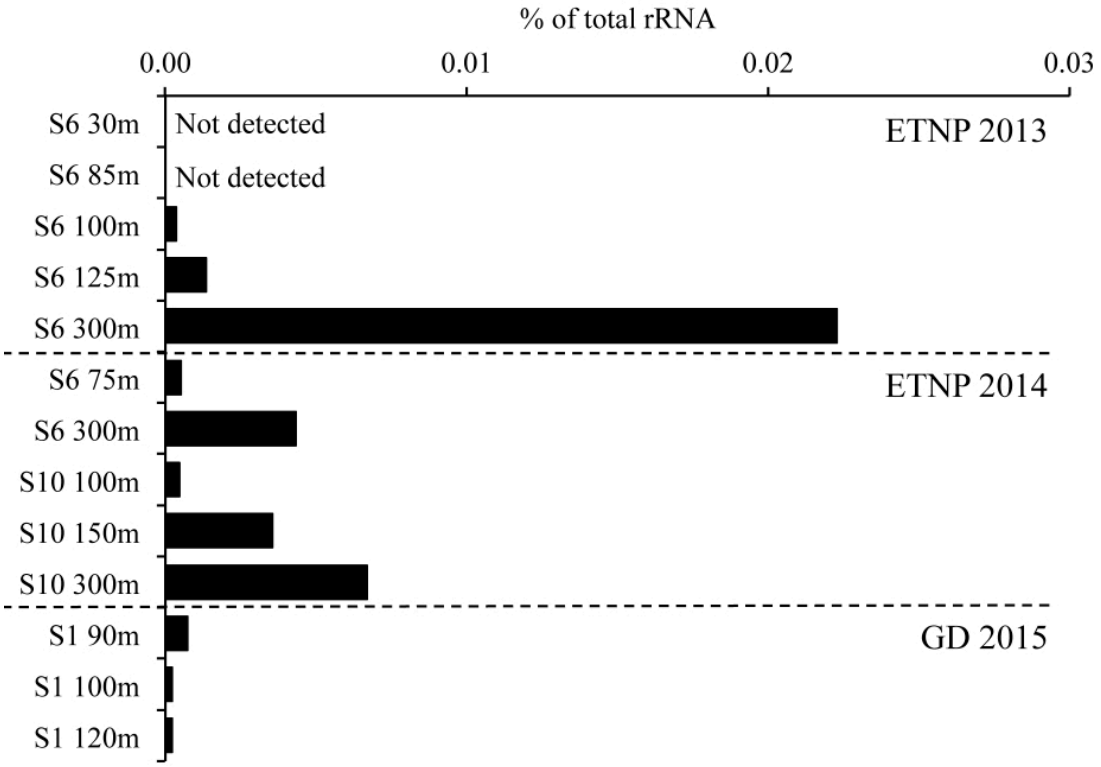

Figure C.3 Abundance of rRNA transcripts matching NC10 bacteria. Abundances are expressed as a percentage of total rRNA transcripts recovered in OMZ metatranscriptomes, with classification based on open reference picking of rRNA fragments (identified using riboPicker) against the comprehensive non-redundant rRNA database in QIIME.

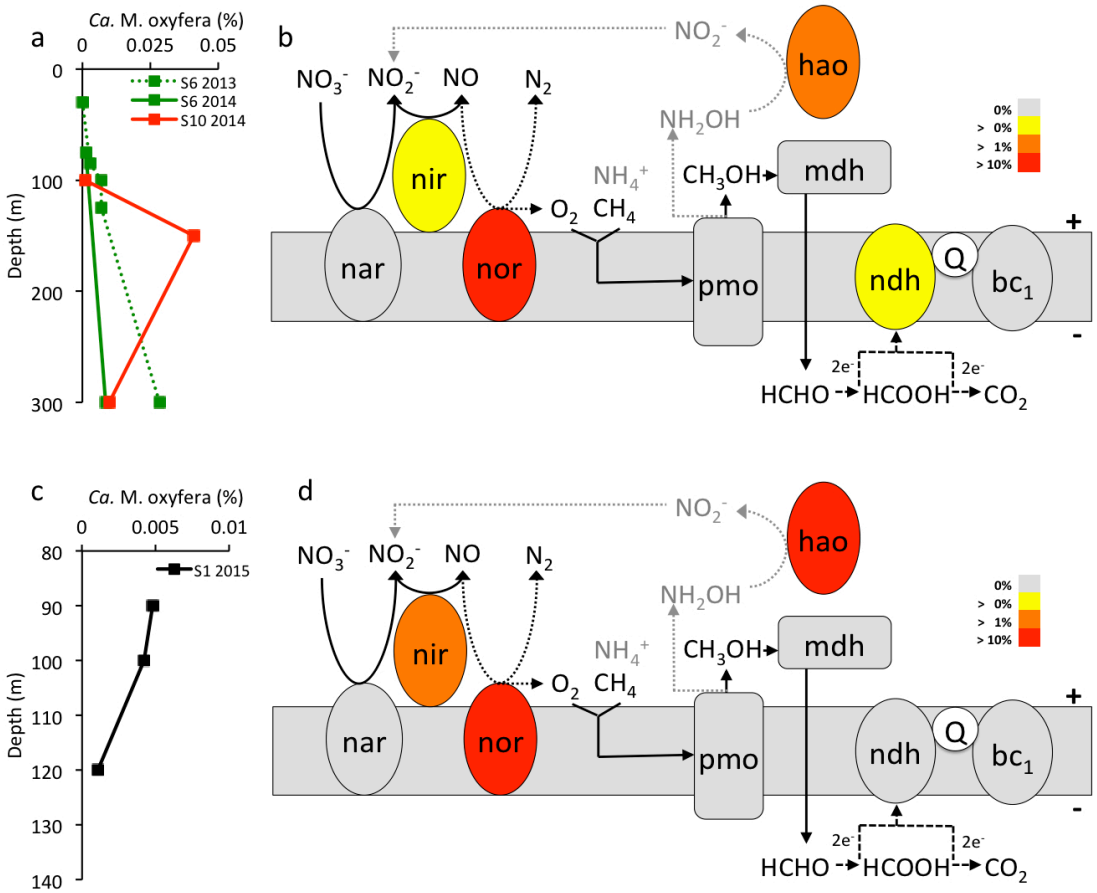

Figure C.4 Transcription of n-damo genes in the ETNP (a,b) and GD (c,d) identified by LCA analysis in MEGAN5. a,c Abundances of transcripts assigned to Phylum NC10 using lowest common ancestor binning of BLASTX results in MEGAN5, as a % of the total number of MEGAN5-classified mRNA transcripts in each sample. **b,d** % abundances of NC10-like transcripts matching genes of the proposed pathway for denitrification-dependent AOM (diagram modified from Wu et al., 2011; Wu et al., 2012). Data in **c** and **d** were binned over all samples shown in **a** and **c**, respectively, with abundance colored as a percentage of the total mRNA transcripts assigned to NC10 in MEGAN. nar = nitrate reductase, nir = nitrite reductase, nor = nitric oxide reductase, mdh = methanol dehydrogenase, pmo = particulate methane monooxygenase, bc1 = cytochrome bc1 complex, ndh = NAD(P)H dehydrogenase complex, Q = coenzyme Q, hao = hydroxylamine oxidoreductase. Light gray shows potential non-specific oxidation of ammonium by pMMO, followed by detoxification of hydroxylamine to nitrite by hao. Counts reflect matches to all subunits of each enzyme.

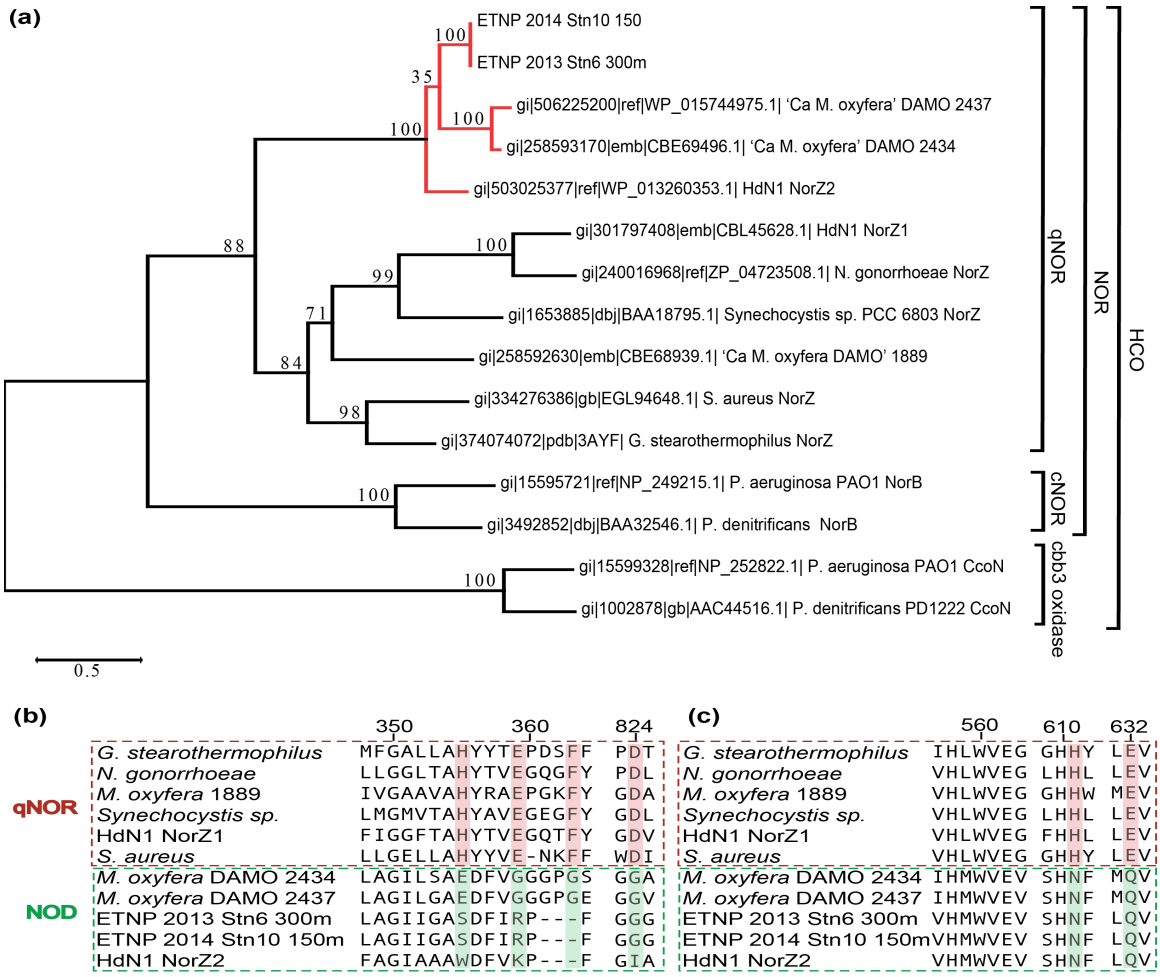

Figure C.5 Phylogeny and motif structure of NC10-like qNor transcripts in the ETNP OMZ. a, Molecular Phylogenetic analysis by Maximum Likelihood method, with putative nitric oxide dismutases (NODs) shown in red, including the two full length sequences (labeled ETNP) assembled from NC10-like transcript fragments. The sequences used for assembly were those with top matches (bit score > 50) to 'M. oxyfera' via BLASTX against the NCBI nr database. Canonical qNOR sequences are those used in Ettwig et al.[12] The evolutionary history was inferred by using the Maximum Likelihood method based on the Le and Gascuel_2008 model. The tree is drawn to scale, with branch lengths measured in the number of substitutions per site. Evolutionary analyses were conducted in MEGA6[51]. **b,c** Alignment of the qNor quinol binding (**b**) and catalytic (**c**) sites showing putative NOD (dashed boxes) compared to canonical qNor sequences. Catalytic site residues are conserved across all putative NODs.

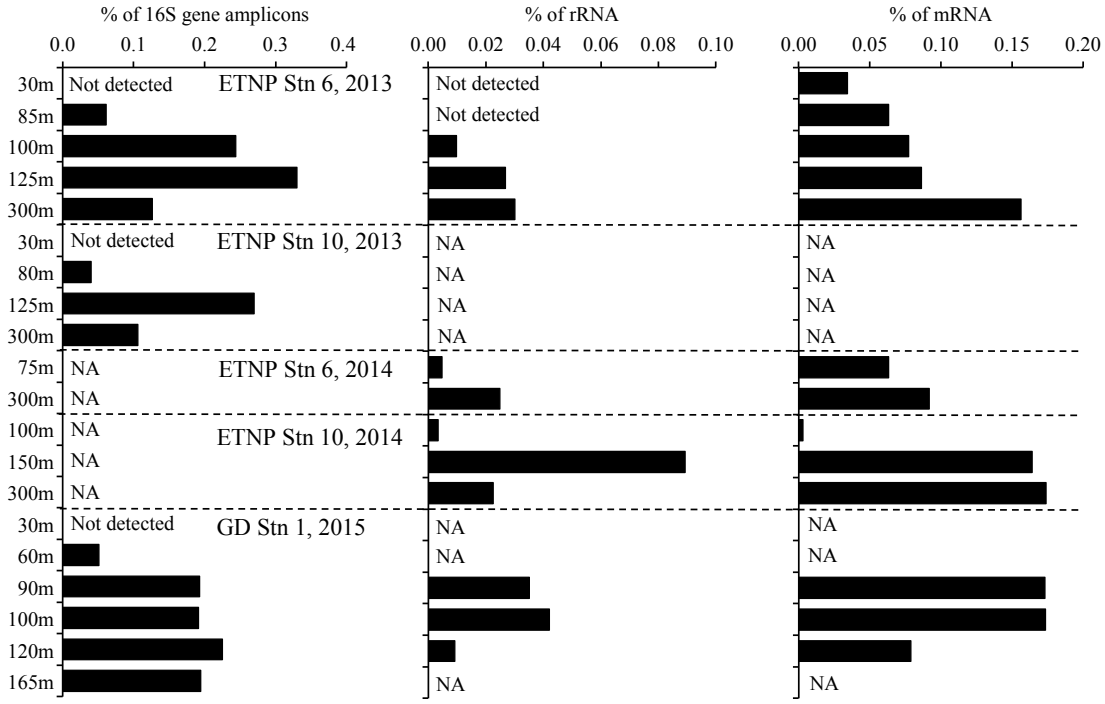

Figure C.6 Methanogen abundance in the ETNP OMZ. a-c, Percentage abundance of sequences affiliated with methanogenic Euryarchaeota in 16S rRNA gene amplicon (**a**), community rRNA transcript (**b**), and community mRNA transcript (**c**) datasets. The vast majority (>95%) of all methanogen 16S rRNA genes affiliated with the Class Methanobacteria. The remainder matched the Class Methanomicrobia

APPENDIX D.

SUPPLEMENTAL DATA FOR CHAPTER 4 METAGENOMIC BINNING RECOVERS A TRANSCRIPTIONALLY ACTIVE GAMMAPROTEOBACTRIUM LINKING METHANOTROPHY TO PARTIAL DENITRIFICATION IN AN ANOXIC OXYGEN MINIMUM ZONE

D.1 Supplemental figures

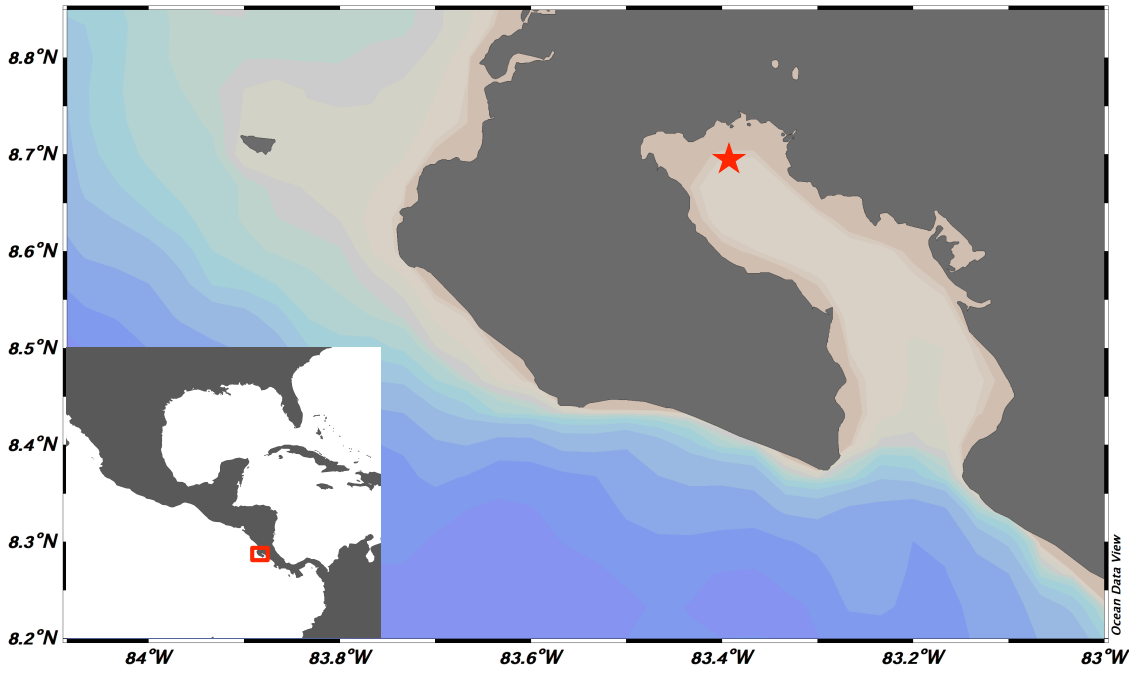

Figure D.1 Sample site (star) in Golfo Dulce, Costa Rica.

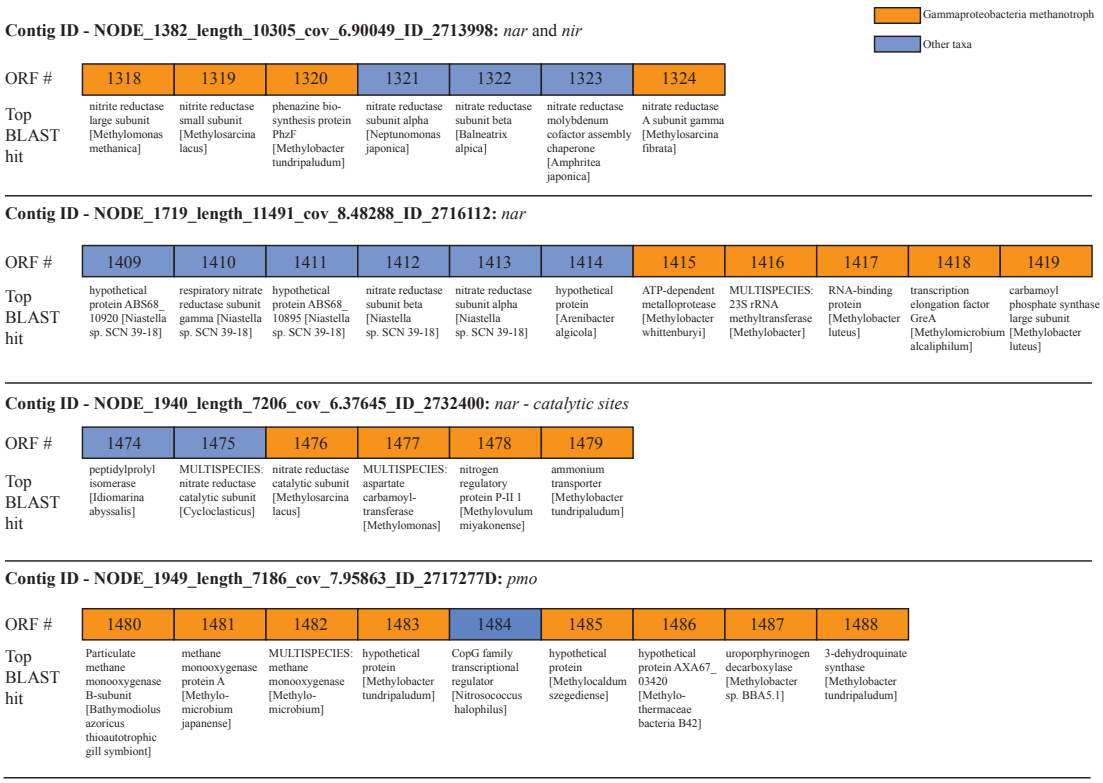

Figure D.2 Gene organization of bin 010 (GD_7). Contigs displayed contain genes encoding nitrate (nar) and nitrite (nir) reductases subunits, and particulate methane monooxygenase (pmo) subunits. The program Prodigal was used to predict open reading frames (ORFs), with predicted ORFs then queried bia BLASTP against the NCBI-nr database (April 2016). Top BLASTP matches and their associated taxonomic affiliation are shown. Colors represent taxonomic affiliation, with orange denoting gammaproteobacterial methanotrophs and blue denoting other taxa.

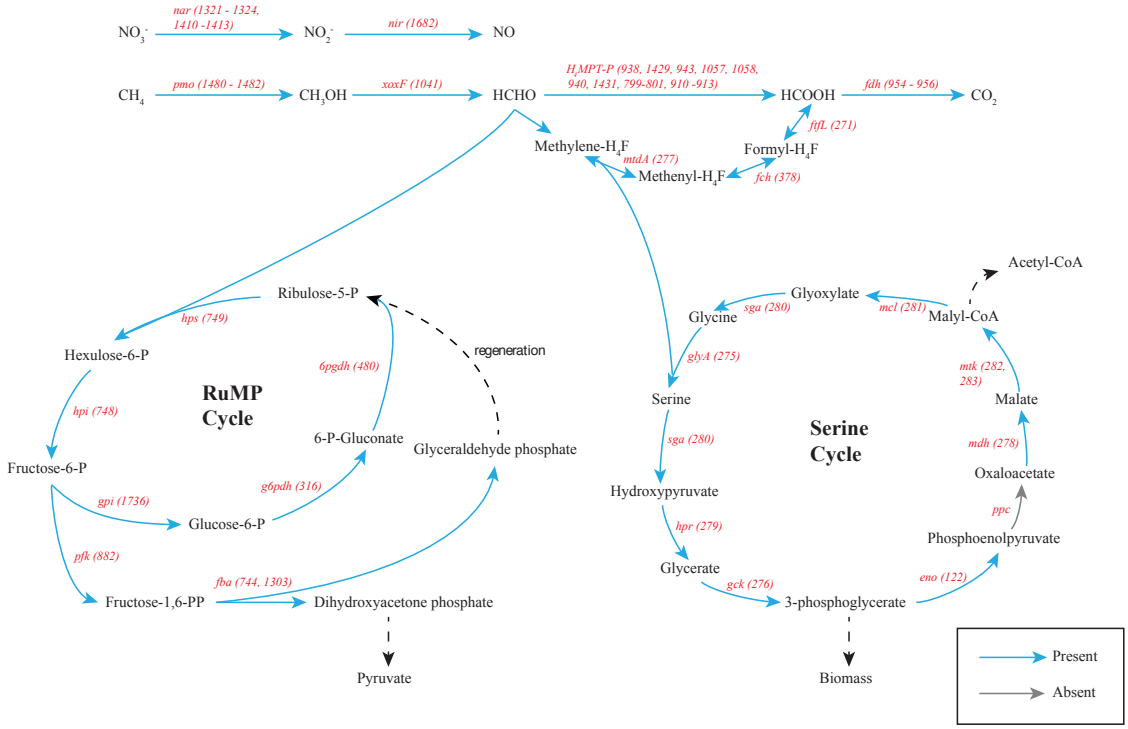

Figure D.3 Transcription of partial denitrification, methane oxidation, RuMP, and partial serine pathways in the GD_7 bin. This figure is based on pathways validated in other methanotrophs and provides a model for suspected metabolic transformations in GD_7. Transcripts originate from the 90 m sample from which rRNA was removed prior to sequencing. Recruitment of transcripts to the bin is based on BLASTX with the following criteria: bit score ≥ 50, amino acid ID ≥ 90%, alignment length ≥ 60% of the gene. Arrow color denotes presence or absence of a GD_7 gene in the metatranscriptome. Inferred reactions (dashed lines) are included to complete the cycles. All genes were assigned via MEGAN based on the KEGG database. Gene abbreviations (red): *6pgdh* - 6-phosphogluconate dehydrogenase, *eno* – enolase, *fba* - fructose bisphosphate aldolase, *fch* - methenyl-H4F cyclohydrolase, *fdh* – formate dehydrogenase, *ftfL* - formyl-H4F ligase, *g6pdh* - glucose-6-phosphate dehydrogenase, *gck* - glycerate kinase, *glyA* – serine hydroxymethltransferase, *gpi* - glucose-6-phosphate isomerase, *H4MPT-P* - methylene tetrahydromethanopterin pathway, *hpi* - 6-phospho-3-hexuloisomerase, *hpr* – hydroxypyruvate reductase, *hps* - 3-hexulose-6-phosphate synthetase, *mcl*– malyl-CoA/methyl malyl-CoA lyase, *mdh* – malate dehydrogenase, *mtdA*- methylene-H4/methylene-H4MPT dehydrogenase, *mtk*– malate thiokinase, *nar* – nitrate reductase, *nir* – nitrite reductase, *pfk* – phosphofructokinase, *pmo* – particulate methane monooxygenase, *ppc* - phosphoenolpyruvate carboxylase, *sga* - serine-glyoxylate aminotransferase, *xoxF* – methanol dehydrogenase.

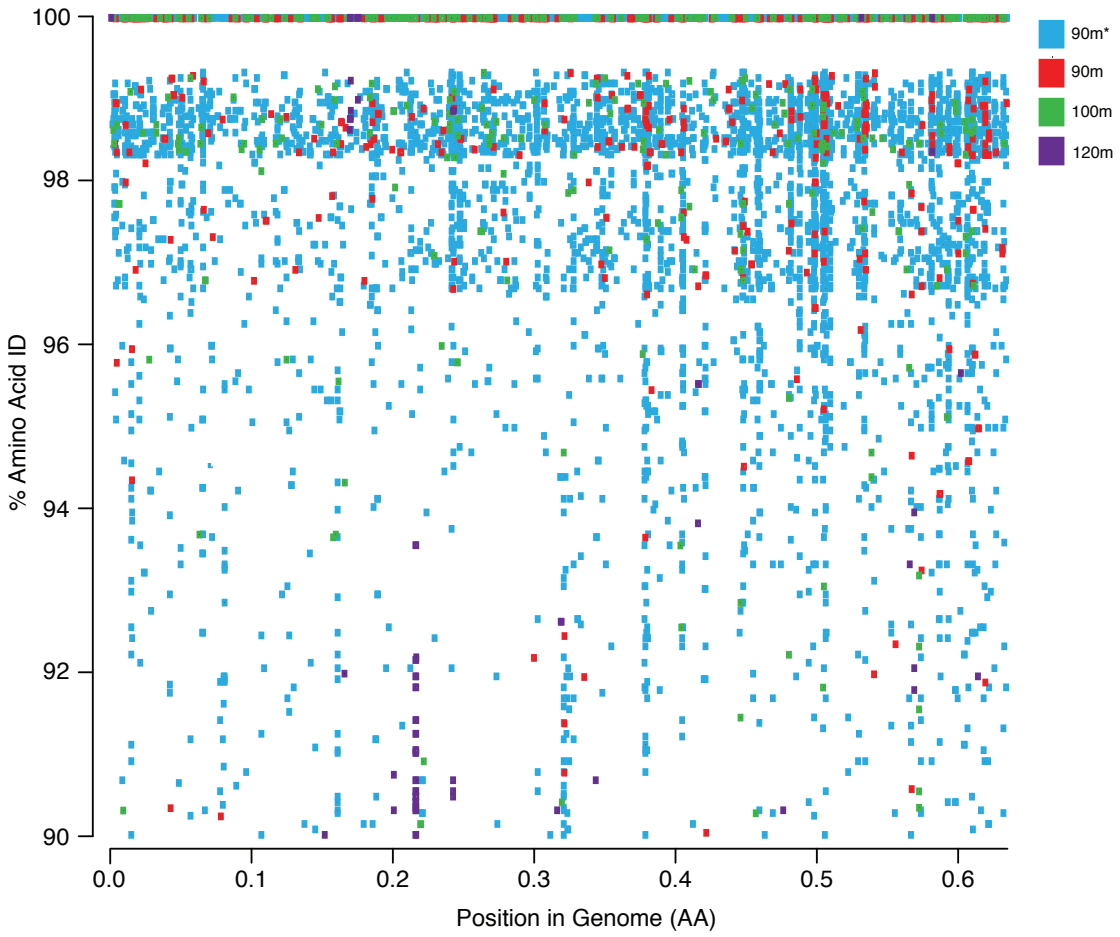

Figure D.4 Recruitment of transcriptome to the GD_7 bin. Samples are color-coded. Recruitment is based on BLASTX with the folloing criteria: bit score ≥ 50, amino acid ID ≥ 90%, alignment length ≥ 60% of the gene.

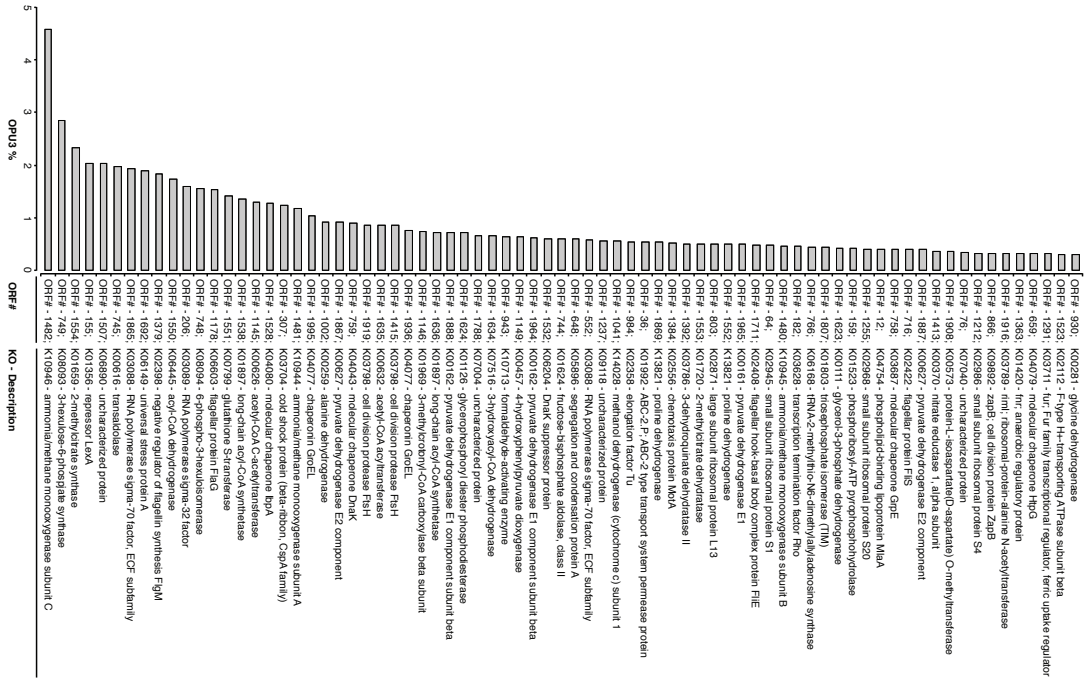

Figure D.5 Rank abundance plot of the top transcribed GD_7 open reading frames (ORFs) represented in the 90 m metatranscriptome. ORF numbers correspond to those listed in Supplementary Table 4. KEGG Orthology (KO) numbers and annotations are displayed for each ORF. Transcript mapping to GD_7 is based on BLASTX with the following criteria: bit score ≥ 50, amino acid ID ≥ 90%, alignment length ≥ 60% of the ORF.

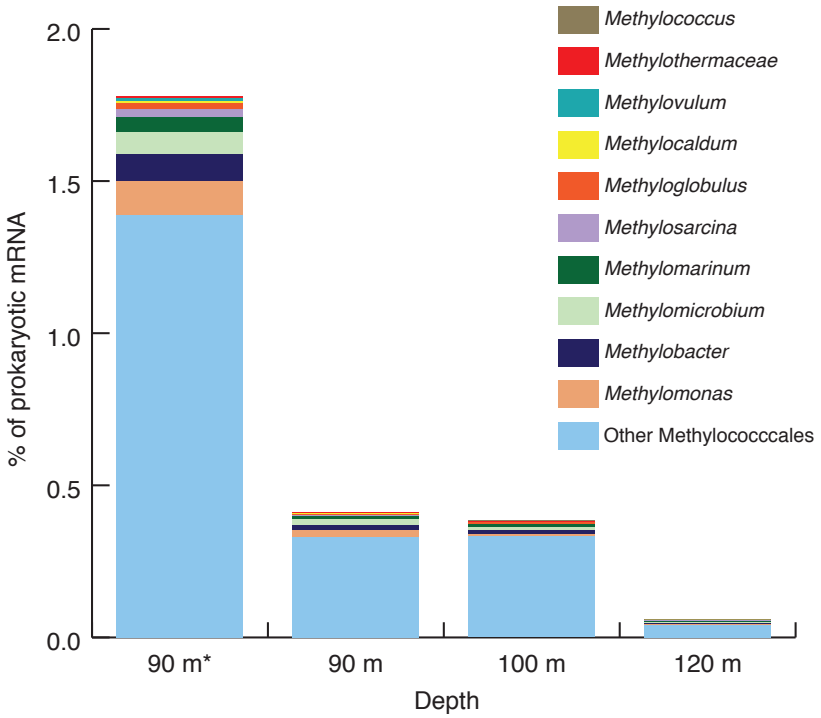

Figure D.6 Taxonomic classification and abundance of Methylococcales mRNA. Values reflect transcripts assigned to the Methylococcales using the LCA algorithm in MEGAN5. The input sequences for MEGAN5 analysis were those identified via DIAMOND queries against the NCBI-nr database. Abundance is shown as a percentage of all prokaryotic (Bacteria + Archaea) mRNA reads in each sample. The 90 m* sample reflects the dataset generated after rRNA removal using the Ribo-ZeroTM rRNA Removal Kit for bacteria (Epicentre).

APPENDIX E

ATTEMPTS AT ENRICHING DENITRIFICATION-DEPENDENT METHANOTROPHS FROM THE EASTERN TROPICAL NORTH PACIFIC

E.1 Introduction

To date there are no cultured representatives of oceanic methanotrophs from the water column. This is an important knowledge gap in understanding how these pelagic methanotrophs function. As such, the full extent of their metabolic and genomic potential remains unknown. Most of the cultured methanotrophs have been isolated from sediments or from aquifer sludge. Marine oxygen minimum zones (OMZs) offer a unique niche for denitrification-methanotrophic bacteria. OMZs are replete in both CH_4 and NO_2^- which are crucial substrates for NC10 N-DAMO and the aerobic methanotrophy supported by partial denitrification processes. Indeed, organisms utilizing both metabolic strategies are enriched in the anoxic core of OMZs (Chapters III and IV).

OMZs could be a potential site from which to enrich and subsequently isolate these pelagic microbes due the elevated abundance of denitrification-dependent methanotrophs in these systems. We attempted to enrich denitrification-dependent methanotrophs from the Eastern Tropical North Pacific (ETNP) in May of 2014. We used a combination of chemical measurements and 16S rRNA sequencing to determine microbial activity and community shifts during a 1-month incubation.

E.2 Methods

E.2.1 Water collection and enrichment set up

Seawater was collected from the ETNP in May 2014 at two stations, station 6 (18 54.0° N, 104 54.0° W) and station 8 (18 12.0° N, 104 54.0° W). A CTD rosette was used to collect seawater from the OMZ core, 300 m, where O_2 concentrations were below the detection limit of STOX sensors (~20 nM). The Niskin bottles were drained into 20 L polycarbonate containers and brought to a cold room (~10° C). Enrichments were set up into two main treatments: whole seawater (WSW) and concentrated cells (CC). In addition, 2L of seawater was filtered onto a 0.2 μm Sterivex filter, preserved in lysis buffer, and stored at -20° C to serve as a sample of the initial community.

For the WSW enrichments, 100 mL was pipetted directly into a 180 mL autoclaved serum vial. To prepare CC enrichments, 2 L of seawater was pumped using a peristaltic pump through a 47 mm diameter, 0.2 μm Isopore filter to collect suspended biomass. The filters were then placed in a 50 mL falcon tube containing 25 mL of filtered seawater. The collected cells were re-suspended by vortexing the filters with 25 mL of filtered seawater. The 25 mL cell slurry was pipetted into a 180 mL autoclaved serum vial. The final volume was brought to 100 mL using ambient seawater. Serum vials were immediately sealed with 20 mm red butyl stoppers (that had been boiled three times in a 10 mM NaOH solution) to minimize O_2 contamination.

Enrichments were amended with NO_2^- or NO_3^- treatments. The stoppers were briefly removed in order to add NO_2^- or NO_3^- in the following treatments: ambient conditions (no N addition), 10 μM, 100 μM, and 1000 μM of added substrate (NO_2^- or NO_3^-). The enrichments were also given separate headspace treatments, half with dinitrogen gas (N_2), the other half with CH_4. The headspace was achieved by bubbling gas directly into the enrichment media for 10 min using a cannula. The stopper was replaced as the cannula was being removed. The serum vials were then capped with 20 mm aluminum crimp tops. The treatment setup can be viewed in Table 1.

The enrichment samples were stored at 10° C for the duration of the oceanographic cruise. Upon reaching the lab the samples were incubated at 4° C. Enrichments were sampled on three separate occasions starting on October 4, 2014, then again 12 days later and 30 days later. Sampling information is presented in Table 2.

Table E.1. Enrichment treatment conditions. Whole seawater (WSW) and concentrated cells (CC) had both nitrogen (N_2) and methane (CH_4) headspace treatments. Nitrate and nitrite amendments are listed in μM

Cell Density	Headspace Gas	Nitrate (μM)	Nitrite (μM)
WSW	N	Ambient	
		10	
		100	
		1000	
			Ambient
			10
			100
			1000
	CH_4	Ambient	
		10	
		100	
		1000	
			Ambient
			10
			100
			1000
CC	N	Ambient	
		10	
		100	
		1000	
			Ambient
			10
			100
			1000
	CH_4	Ambient	
		10	
		100	
		1000	
			Ambient
			10
			100
			1000

Table E.2. Sampling information for the CC samples over a 1-month period.

Sample	N addition	Gas	Time point	Date collected	Day #	Volume (mLs)
18	NO_2^-	CH_4	1	10/4/14	1	9.8
18	NO_2^-	CH_4	2	10/18/14	12	9.9
18	NO_2^-	CH_4	3	11/5/14	30	10.25
22	NO_3^-	CH_4	1	10/4/14	1	10.1
22	NO_3^-	CH_4	2	10/18/14	12	9.9
22	NO_3^-	CH_4	3	11/5/14	30	10.3
26	NO_2^-	N_2	1	10/4/14	1	10
26	NO_2^-	N_2	2	10/18/14	12	10.3
26	NO_2^-	N_2	3	11/5/14	30	10.1
29	NO_3^-	N_2	1	10/4/14	1	10
29	NO_3^-	N_2	2	10/18/14	12	10
29	NO_3^-	N_2	3	11/5/14	30	9.9

E.2.2 Nitrate and nitrite measurement

All sampling occurred in an anaerobic chamber. Post sampling, the headspaces in all vials were flushed with 3x headspace volume with the corresponding gas. NO_2^- concentrations were obtained via NED colorimetric method. NO_3^- concentrations were measured utilizing vanadium (III) chloride reduction followed by a NED colorimetric measurement.

E.2.3 16S amplicon sequencing and analysis

Enrichments were sampled for nucleic acids at the same time as the NO_2^- and NO_3^- measurements. Roughly 10 mL of enrichment media was vacuum-filtered through a 0.2 μm, 25mm disc filter, preserved in lysis buffer, and frozen at -20° C. Samples were selected for DNA extraction and 16S rRNA gene amplicon sequencing based on NO_2^- and NO_3^- drawdown observed over the 1-month incubation period. The highest drawdown was observed in CC samples that were supplemented with 10 μM NO_2^- and NO_3^- (Table 2). DNA was extracted using a phenol:chloroform protocol. Cells were lysed by adding lysozyme (2 mg in 40 μl of lysis buffer per filter) directly to the filter and incubating for 45 min at 37°C. Proteinase K (1 mg in 100 μl lysis buffer, with 100 μl 20% SDS) was added, and incubated for 2 h at 55°C. The lysate was removed, and DNA was extracted once with Phenol:Chloroform:Isoamyl Alcohol (25:24:1) and once with Chloroform:Isoamyl Alcohol (24:1) and then concentrated by spin dialysis using Ultra-4 (100 kDa, Amicon) centrifugal filters.

High-throughput sequencing of dual-indexed PCR amplicons encompassing the V4 region of the 16S rRNA gene was used to assess microbial community composition as in Chapters 2,3, and 4. Amplicons were analyzed using QIIME following standard protocols. Barcoded sequences were de-multiplexed and trimmed (length cutoff 100 bp) and filtered to remove low quality reads (average Phred score <25) as in Chapters 2, and 3. Operational Taxonomic Units (OTUs) at 97% sequence similarity were generated by using the open-reference picking with the UCLUST algorithm in QIIME. Taxonomy was assigned to representative OTUs from each cluster using the Greengenes database. OTU counts were rarefied (10 iterations) to a uniform sequence depth (70,000 sequences). Taxon (Family level) abundances were used to assess changes in taxa over time. Families with abundance >1%, averaged across all samples, were used to track these differences over time.

OTUs affiliated with methanotrophs and methylotrophs were chosen for phylogenetic analysis. Taxonomic classification of these OTUs was confirmed by BLASTN against the NCBI-nr database. The top 10 OTUs (>50 counts, averaged across all samples) were then used for phylogenetic analysis. Reference sequences for the phylogeny were collected by using the top sequence match from the RDP and the top BLASTN hit against NCBI for each OTU. All sequences (enrichment OTUs, RDP matches, and top BLASTN hits) were aligned using MUSCLE. A model test selected the Kimura-2 model based on the resulting alignment. A maximum likelihood tree was generated in MEGA7 using the Kimura-2 model and iterated 1000 times. The resulting phylogeny was visualized and edited with FigTree.

E.3 Results

Enrichment samples that showed the strongest NO_2^- and NO_3^- drawdown were the 10 μM additions with CH_4 gas collected from station 6 (Table 2). For comparison the negative controls (N_2 gas headspace) were sequenced as well. In all, 12 samples were sequenced for 16S rRNA. At the Family level there were clear shifts in taxonomic composition, particularly between the sample at day 1 compared to the day 12 and 30 samples (Figure 1).

Screening of OTUs revealed 10 sequences that made up the majority of methanotrophic and methylotrophic diversity (Figure 2). Sequences affiliated with Methylophaga and closely related Gammaproteobacteria made up 5 of the 10 OTUs. A single OTU from the Methylococcales Order was detected and clustered closest to an uncultured *Methylomicrobium* recovered from hot spring sediments. The rest of the OTUs clustered with the Alphaproteobacterial methanotrophs. Three OTUs were particularly abundant in the enrichment samples, consisting of up to ~25% of the total 16S rRNA gene sequences recovered. These abundant methano/methylo OTUs were OTU6750 from the Thiotrichales Order, OTU10637 related to *Methylophaga* sp. DG1507, and finally OTU9658 a member of the *Methylophilales* Genus (Figure 2A).

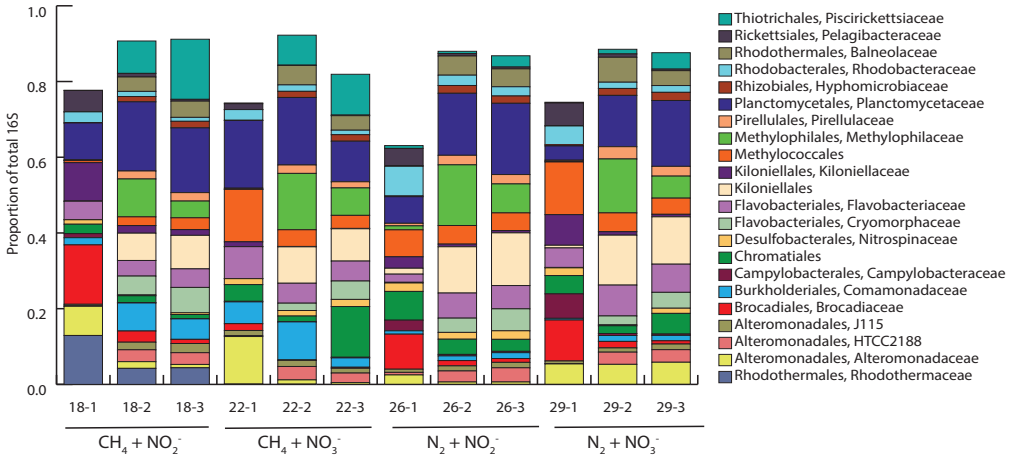

Figure E.1. Taxon abundance at the Family level presented as a proportion of total 16S rRNA gene sequences. Families with abundance >1% are shown.

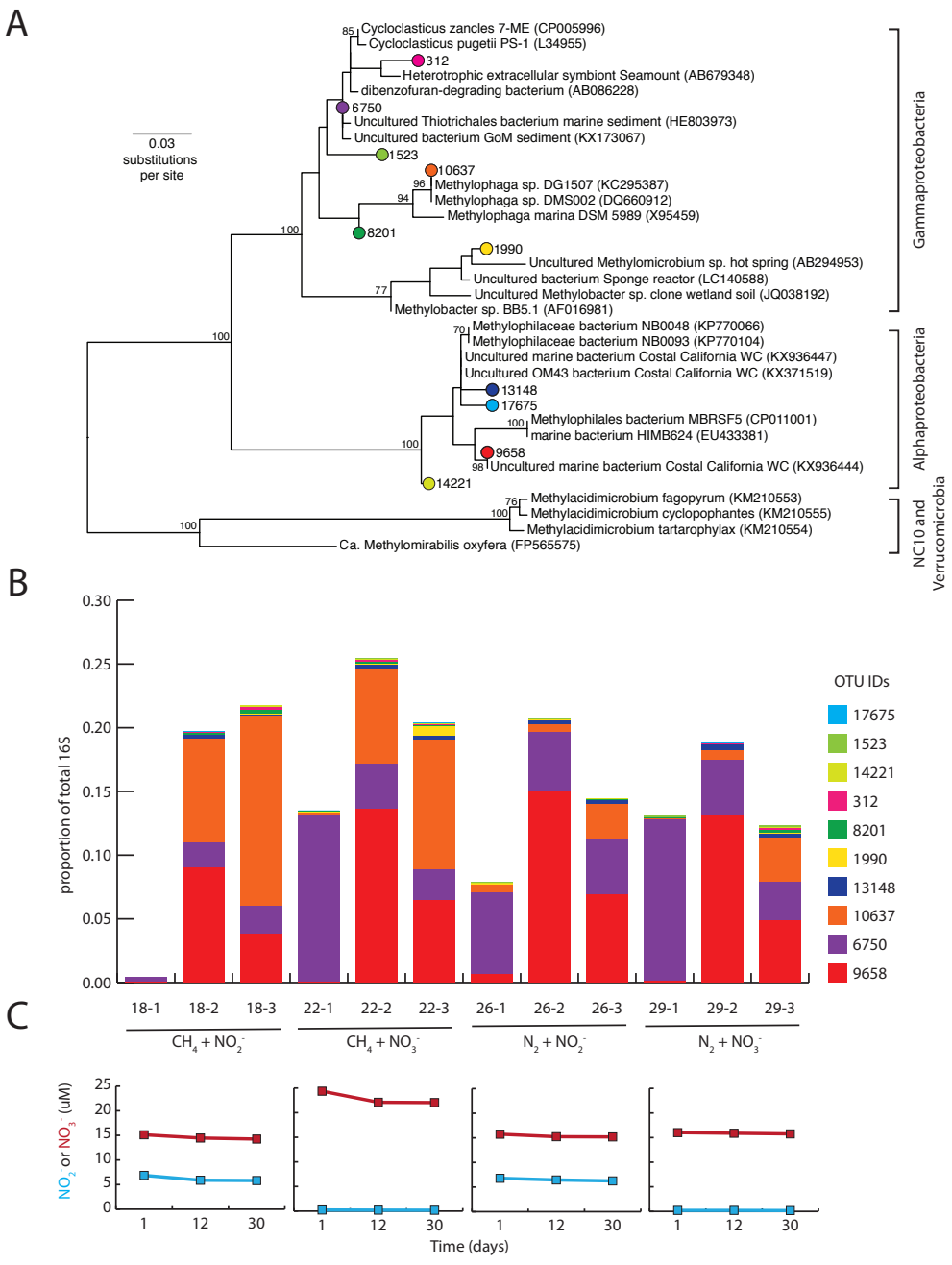

Figure E.2. Methanotroph and methylotroph OTUs and N dynamics in CC - 10 µM enrichments. (**A**) Maximum likelihood 16S rRNA gene phylogeny of the top 10 methanotrophic and methylotrophic OTUs, using the Kimura-2 model iterated 1000 times. Scale bar represents nucleic acid substitutions per site. (**B**) OTU abundance presented as a proportion of total 16S sequences. Colors match nodes in **A**. (**C**) Nitrite (blue) and nitrate (red) concentrations taken at the time of DNA sampling. Values were measured using the NED colorimetric method.

In these samples, CH_4 treatments displayed a largest drawdown of NO_2^- and NO_3^- than their corresponding N_2 controls (Figure 2C). The CH_4 enrichments displayed differences in methano/methylotroph diversity (Figure 2B). At the start of the incubation OTU6750 (Thiotrichales) was the most dominant OTU in all enrichments. In the CH_4 treatments OTU10637 and OTU9658 were both enriched, while in the N_2 treatments OTU9658 exhibited a pronounced increase in abundance (Figure 2B). It appears that the CH_4 treatment enriched for the *Methylophaga*-like OTU compared to the N_2 control.

E.4 Discussion

It appears N-DAMO processes affiliated with NC10 bacteria were not enriched by this technique. NC10-like 16S rRNA gene sequences were not recovered using this method. However this is not surprising, as the 16S amplicon analysis described in Chapter 3 did not detect any NC10 16S amplicons. Aerobic methanotrophs affiliated with the Methylophilaceae Family and methylotrophs from the *Methylophaga* genus were enriched during this experiment. These OTUs were either not present or a very low abundance at the beginning of the incubation but were enriched to up to 20% of the amplicons over the course of the incubations. The presence and enrichment of these OTUs may indicate an active CH_4 cycle in the samples. There is no clear indication as to what may be the mechanism for NO_2^- or NO_3^- drawdown based on these OTUs. This, however, does not rule out denitrification. As seen in Chapter 4, methanotrophs classified as aerobic Methylococcales encoded and transcribed a partial denitrification pathway.

This would have been overlooked as a route of denitrification if the analysis had just depended on 16S rRNA amplicon sequencing.

We cannot rule out the potential that O_2 contaminated the enrichments. The method used to collect the seawater and concentrate cells was not done in an anaerobic chamber. Moreover, the water samples had significant contact with the atmosphere during the enrichment set up. This work could probably benefit from a sample collection method that focuses on preserving the anoxic conditions in the OMZ. The stopper material may also play a key role in either O_2 permeability or microbial selection. It has been shown that stoppers can play a key role in these types of enrichments. With this experimental setup and analyses, we cannot rule out either O_2 or stoppers as a key driver of the OTU enrichment observed here.

Attempts to enrich OMZ taxa and methanotrophs using a variety of methods should remain a key goal of future work. Different methods such as dilution to extinction experiments, preserving cells in glycerol, or a modified version of the method presented here may provide more robust results.

VITA
CORY CRUZ PADILLA

Orginally from Pacifica, CA, Cory earned his Bachelor's degree in Marine Biology from the University of California at Santa Cruz (UCSC), completing a senior thesis in the laboratory of Dr. Jonathan Zehr. Prior to comsencing his Ph.D, his interests in oceanography lead to an array of research positions at UCSC with Dr. Rachel Foster, University of Hawaii at Manoa with Dr. David Karl, and at Woods Hole Oceanographic Institute with Dr. Daniel Repeta. Following his passions and the advice of his colleagues he pursued a Ph.D. in Molecular Biology at Georgia Institute of Technology in the lab of Dr. Frank Stewart.

Below is a list of all Cory's publications as of November 1, 2017:

Padilla CC, Bertagnolli AD, Bristow LA, Sarode N, Glass JB, Thamdrup B, Stewart FJ. 2016. Metagenomic binning recovers a transcriptionally active Gammaproteobacterium linking methanotrophy to partial denitrification in an anoxic oxygen minimum zone. 2017. *Frontiers in Marine Science. 4:23. doi: 10.3389/fmars.2017.0023.*

Padilla CC, Bristow LA, Sarode N, Garcia-Robledo E, Gomez Ramirez E, Benson CR, Bourbonnais A, Altabet MA, Girguis PR, Thamdrup B, Stewart FJ. 2016. NC10 bacteria in oxygen minimum zones. *ISMEJ*. doi: 10.1038/ismej.2015.262.

Padilla CC, Ganesh S, Gantt S, Huhman A, Parris DJ, Sarode N, Stewart FJ. 2015. Standard filtration practices may significantly distort planktonic microbial diversity estimates. *Frontiers in Microbiology*. 6:547. doi: 10.3389/fmicb.2015.00547.

Tsementzi D, Wu J, Deutsch S, Nath N, Rodriguez-R LM, Burns AS, Ranjan P, Sarode N, Malmstrom RR, **Padilla CC**, Stone BK, Bristow LA, Larsen, Glass JB, Thamdrup B, Woyke T, Konstantinidis KT, Stewart FJ. 2016. SAR11 bacteria linked to ocean anoxia and nitrogen loss. *Nature*. 536:179-183. doi:10.1038/nature19068.

Bertagnolli A, **Padilla CC**, Glass JB, Thamdrup B, Stewart FJ. Metabolic potential and in situ activity of Marine Group A-SAR406 in an anoxic water column. *Environmental Microbiology*. In press.

Garcia-Robledo E, **Padilla CC**, Aldunate M, Paulmier A, Stewart FJ, Ulloa O, Revsbesh NP. Cryptic oxygen cycle in the minimum zone: the role of the secondary chlorophyll maximum. *Proceeding of the National Academy of Sciences of the USA. doi: 10.1073/pnas.1619844114.*

Mandric I, Knyazev S, **Padilla CC**, Stewart FJ, Māndoiu I, Zelikovsky A. Metabolic analysis of metranscriptomic data from planktonic communities. 2017. *Internal Symposium on Bioinformatics and Applications*. 7:41. Doi: 10.1007/978-3-319-59575_41.

Vik DR, Roux S, Brum JR, Bolduc B, Emerson JB, **Padilla CC**, Stewart FJ, Sullivan MB. Putative Archaeal viruses from the mesopelagic environment. *PeerJ*. Doi: 10.7717/peerj.3428.

Stenegren M, Berg C, **Padilla CC**, David S, Montoya JP, Yager PL, Foster RA. 2017. Piecewise Structural Model (SEM) disentangles the environmental conditions favoring Diaton Diazotroph Associations (DDAs in the Western Tropical North Atlantic (WTNA). 2017. *Frontiers in Microbiology*. 8:810. doi: 10.3389/fmicb.2017.00810.